UNIVERSITY OF CAPE COAST

RIVER SEDIMENT DISCHARGE INFLUENCE ON SHORT-TERM

SHORELINE CHANGE OF ANLO BEACH, WESTERN REGION,
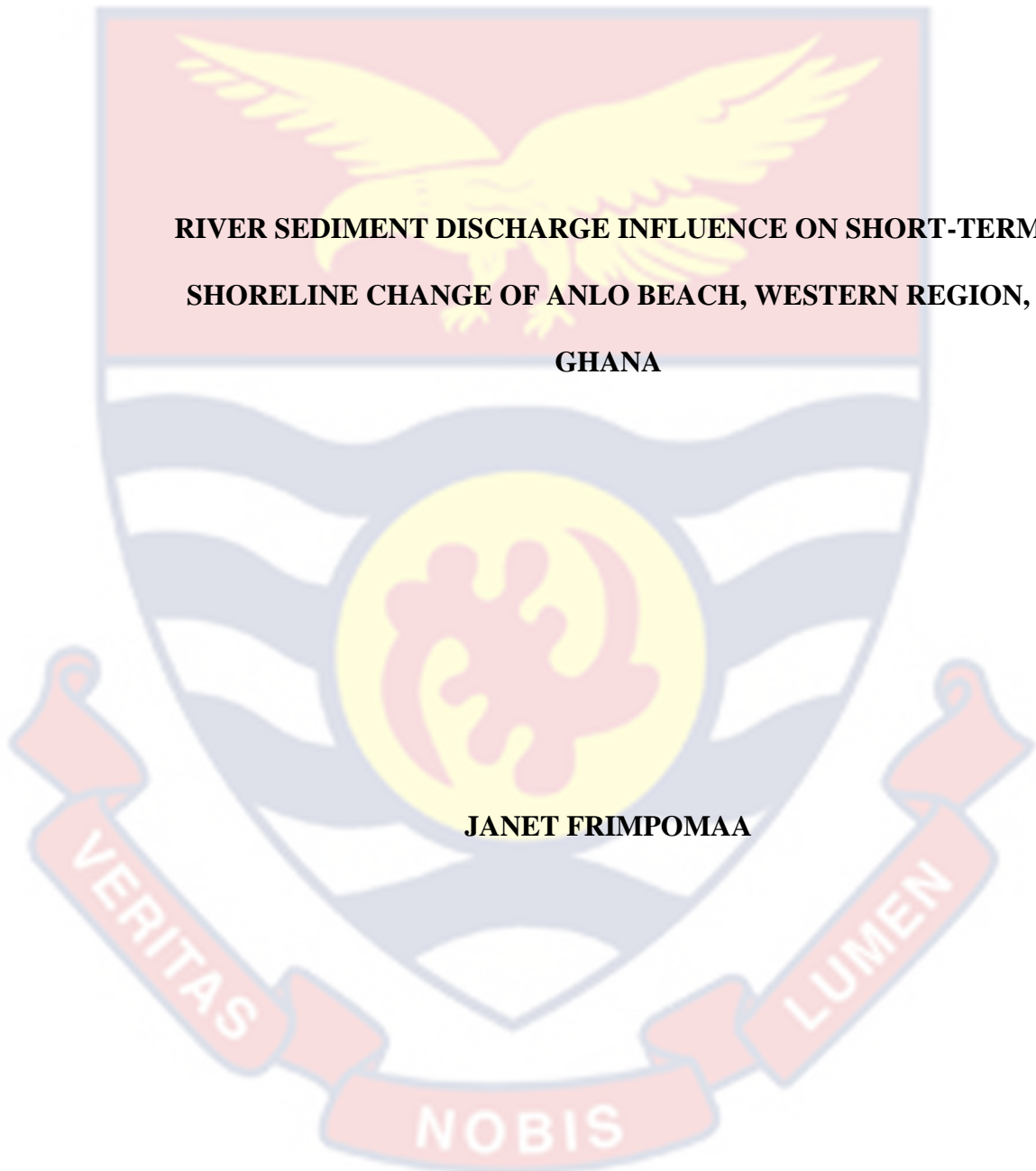
GHANA

JANET FRIMPOMAA

2022

UNIVERSITY OF CAPE COAST

RIVER SEDIMENT DISCHARGE INFLUENCE ON SHORT-TERM

SHORELINE CHANGE OF ANLO BEACH, WESTERN REGION, GHANA

BY

JANET FRIMPOMAA

THESIS SUBMITTED TO THE DEPARTMENT OF FISHERIES AND

AQUATIC SCIENCES OF THE SCHOOL OF BIOLOGICAL SCIENCES,

COLLEGE OF AGRICULTURE AND NATURAL SCIENCES,

UNIVERSITY OF CAPE COAST, IN PARTIAL FULFILMENT OF THE

REQUIREMENT FOR THE AWARD OF MASTER OF PHILOSOPHY

DEGREE IN OCEANOGRAPHY AND LIMNOLOGY

DECEMBER 2022

DECLARATION

Candidate's Declaration

I hereby declare that this thesis is the result of my own original research and that no part of it has been presented for another degree in this university or elsewhere.

Candidate's Signature...…………………..   Date…….…………..

Name:

Supervisor's Declaration

We hereby declare that the preparation and presentation of this thesis were supervised in accordance with the guidelines on supervision of thesis laid down by the University of Cape Coast.

Principal Supervisor's Signature……………………Date…………………...

Name:

Co-Supervisor's Signature………………………….Date…….…………...

Name:

ii

ABSTRACT

Riverine systems are important due to sediment transport to the coast. However, this benefit is decreasing due to increasing rate of human influences that affect river flow pattern and sediment discharge to coastal areas, leading to coastal instability in many countries. This study assessed riverine sediment discharge contributions to the short-term evolution of the coastline of the Anlo Beach in Ghana. The Pra River catchment with focus on the coastal frontage (~3.5 km) and 1.6 km inland was studied, with field surveys for six months (May to October, 2022). River depths, sediment load, river velocities, and aerials photographs were collected for each survey, and subsequently processed and analysed with established protocols in ArcMap to produce shoreline changes, bathymetry maps, river sediment and water discharges and particle size distribution. Results from the study suggest a decreasing trend of average daily river discharges, sediment load and particle sizes. These results were however larger than what was reported in other rivers in and outside Ghana. Beach sediment and shoreline are also eroding at a rate of -105,695.72 m^3 and -8.22 m for the six months period. The dynamics of the beach is associated with illegal small-scale mining that supplies smaller sediment particles to the beach, and reduction in longshore sediment transport by sea defence structures located to the west of this beach. Also, shallow bathymetry was observed at the Pra Estuary, which could lead to flooding during rainfall and high discharges.

ACKNOWLEDGEMENT

DEDICATION

To my mother, Mad. Selina Serwaa and my late father, Mr Samuel Asamoah

TABLE OF CONTENTS

LIST OF TABLES

LIST OF FIGURES

LIST OF ACRONYMS

DEM	Digital Elevation Model
DoD	DEM of Difference
DSAS	Digital Shoreline Analysis System
GCD	Geomorphic Change Detection
GCPs	Ground Control Points
IDW	Inverse Distance Weighting
IPCC	Inter-governmental Panel on Climate Change
LRR	Linear Regression Rate
NSM	Net Shoreline Movement
NTN	Natural Neighbor Interpolation
OK	Ordinary Kriging
PPM	Parts Per Million
QB	Bedload Discharge
RMSE	Root Mean Square Error
RTK DGPS	Real-Time Kinematic Differential Global Positioning System
SSC	Suspended Sediment Concentration
SSQ	Suspended Sediment Discharge
TIN	Triangulated Irregular Network
TSQ	Total Sediment Discharge

CHAPTER ONE

INTRODUCTION

1.1 Overview

Riverine systems and their processes such as sediment transport are important due to the numerous services they provide to human and coastal systems. However, the services are decreasing because studies have shown that the increasing rate of anthropogenic influences are affecting the natural river flow patterns and sediment discharges to the coastal area, leading to coastal instability in many countries. Consequently, coastal engineering solutions have been applied in areas with significantly degraded shoreline, yet they seem not to be lasting solutions. This chapter therefore provides background information pertaining to how river discharges and sediment transport to the sea influences the coastline. In addition, the problem of this research has been stated and justified and the objectives have been outlined, as well as how the thesis was organised.

1.2 Background to the Study

Historically, denudational processes like weathering and erosion of rock particles are known to be some of the natural processes, which are continuously enriching river catchments with sediment and nutrients in solid or dissolved form (Babiński, 2005; Bastia & Equeenuddin, 2016; Boakye et al., 2020; Chakrapani, 2005; Duru et al., 2017; Mouyen et al., 2018; Osadchiev & Korshenko, 2017). Rivers are large naturally flowing water bodies channelled directly or indirectly into the sea. It is widely known that rivers serve as a medium for transporting a quantum of land-derived sediments, which enter the

1

seas (Akrasi, 2011; Milliman & Farnsworth, 2011; Yang et al., 2006) and occasionally the deep seas over several time scales (Chen et al., 2018). It is estimated that rivers supply the highest quantity (that is, about 95%) of the total load of sediment that is deposited at the coast, thereby ensuring beach building and coastal stability (Abdul-Kareem et al., 2022; Cantalice et al., 2015; Syvitski, 2003; Walling, 2006). Beside their link to the coastal-ocean, rivers have played major roles regarding the history and habitation of humans, serving as a form of protection, means of transport and water provision to inhabitants of a catchment (Milliman & Farnsworth, 2011). In addition, the nutrient-rich nature of deposited sediment is able to support marine life and agricultural activities (Flores et al., 2020), especially in deltaic regions (Mouyen et al., 2018). Coastal processes such as alongshore and cross-shore sediment transport are made continually possible due to the daily discharge of river sediment to the coast (Boye et al., 2019; Nyarko et al., 2016). Currently, most rivers worldwide are having a rapidly declining water and sediment discharge due to excessive river damming, exacerbated by the changing climate (Amenuvor et al., 2020; Bastia & Equeenuddin, 2016; Das, 2019; Das et al., 2021; Dunn et al., 2018; Guo et al., 2018; Liu et al., 2021; Ly, 1980; Wu et al., 2019).

Over the past decades, the transport of sediment to coastal areas has been considered as a very delicate issue for society. Sand resources are needed at the coast, especially for buffering against extreme events like storm surges, flooding and eroding coastlines (Chakrapani, 2005). The construction of coastal defence structures has become popular worldwide and in Ghana due to coastline erosion (Alves et al., 2020; Angnuureng et al., 2013; Jonah et al., 2016; Xorse, 2013). Coastal defence structures, including both soft (like beach nourishment)

and hard engineering (like groynes, sea walls, offshore breakwaters) solutions have been used for buffering the shoreline against extreme storm surges, erosion, and flooding in West Africa (Alves et al., 2020). In Ghana, revetments, jetties and groynes have been constructed along some of the important coastal communities experiencing shoreline recession (Jonah et al., 2016). However, these structures have led to "knock-on effects" downdrift of the coast. For instance, the Keta Sea defence structure trapped sediment updrift, leading to sediment starvation downdrift of the beach (Alves et al., 2020; Angnuureng et al., 2013). As stated by Syvitski et al. (2005), the retreat of coastlines has a direct link with sediment supplied by rivers. Therefore, it is important to gain a comprehensive understanding of the roles river sediment discharges play in ensuring coastal stability.

1.3 Statement of the Problem

Sediment input from rivers to the coast of Ghana is declining and coastal erosion is escalating, making riverine sediment discharge to the coast very important. Activities like the regulation of water flow through the creation of dams and barrages on rivers reduce water and sediment discharged by rivers (Amenuvor et al., 2020; Roest, 2018). For instance, in Ghana, the central and eastern coastline eroded between 2 to 6 m/yr after the construction of the Akosombo Dam on the Volta River in the 1960's with about 99.5 % retention of sediment behind the dam (Ly, 1980). This problem worsened after the addition of the Kpong Dam, downstream of the Akosombo Dam in 1982 (Angnuureng et al., 2013). That is, the coastline recession rate increased from 3 to 17 m/yr (2001 - 2011) on the eastern coastline of Ghana (Angnuureng et al.,

3

2013). This is therefore a major indication that a continuous reduction in the discharge of riverine sediment would have a detrimental effect on the coastal and marine environment (Boateng et al., 2012).

Agricultural activities and heavy mining activities, especially the illegal small-scale mining (also known as Galamsey in Ghana) supply excessive fine sediment to rivers which usually stay in suspension, hence influencing the sediment discharge and eventually modifying the coastline. Although the government of Ghana has invested in the construction of several sea defence structures along the coastline of Ghana (Alves et al., 2020) to control erosion, the erosion is persistent on some known areas as well as new areas.

On the estuarine region of the Pra River and its adjacent beaches where the Anlo Beach community is located, it has been reported by some of the community members that there is a continual shoreline recession that has been observed for years. In addition to this, there is an increasing rate of storm surges and flooding, causing displacement of settlement (~50 % of the population), and causing the collapse of the only school in the community (Appiah, 2022). It is unclear what the cause of this problem is, because several authors (Boakye et al., 2021; Boye et al., 2019; Kusimi, 2014) have reported that the Pra River system forms part of the rivers with significant sediment yield in Ghana. Nonetheless, there is inadequate data (Akrasi, 2011; Amenuvor et al., 2020; Boakye et al., 2020), in addition to less studies conducted to investigate the impact of the Pra River's sediment discharge on the morphological evolution of the Anlo Beach coastline. It has also been noted that previous studies (Akrasi, 2011; Boye et al., 2019; Kusimi et al., 2014) have principally focused on either quantifying suspended sediment load delivered by the Pra River or investigating

4

shoreline change on a large scale (Boateng, 2012; Boye et al., 2019). Since beaches depend largely on inland rivers for offsetting sediment losses, this study addresses the gap linking sediment discharge from the Pra River to the morphological changes of the Anlo Beach.

This study will therefore employ the collection of river discharges, sediment loads, bathymetry, and water levels in the Pra Estuary as well as shoreline information to understand the short-term evolution of the shoreline adjacent the mouth of the Pra River (Figure 1.1).

Figure 1.1: A section of the Anlo Beach community

1.4 Purpose of the Study

The purpose of this study is to enhance the understanding of riverine sediment discharge impact on the evolution of Anlo Beach through the collection of riverine sediment loads, depths, velocities, water levels and shoreline information. Observations made would highlight information which could be useful in making policies for the management of riverine systems and the coastal areas to ensure an ensure a balance in coastal sediment budgets and

5

consequent coastal stability in Ghana. This would help improve the living conditions of the people of Anlo Beach and contribute to identifying other areas for further studies.

1.5 Main Aim and Specific Objectives

The main aim of this study is to assess the contribution of riverine sediment discharge to the short-term evolution of the Anlo Beach. The specific objectives are:

1. To assess the quantity of sediment discharge from the Pra River into the sea
2. To assess the short-term changes in the shoreline along the Anlo Beach
3. To investigate the bathymetric changes of the Pra Estuary

1.6 Research Questions

1. What quantity of sediment does the Pra River discharges into the sea?
2. Is the Anlo Beach eroding or accreting?
3. Is there an ongoing erosion or sedimentation in the Pra Estuary?

1.7 Justification of the Study

Riverine sediment discharged to the coastal areas is important due to the influence it has on beach dynamics (Boye et al., 2019; Cantalice et al., 2015; Selvan et al., 2014; Walling, 2006; Yang et al., 2006). In addition, coastal erosion is now a national issue and many investments are put into it (Alves et al., 2020), making it a necessity for understanding morphodynamics and investigating these areas. The study falls under the ACECoR thematic area:

6

Coastal Geomorphology and Engineering hence, will provide relevant data for addressing problems pertaining to riverine systems and coastal area management.

1.8 Delimitations

i. This study assessed the short-term influence of discharged sediment from the Pra River to coastal evolution of the Anlo Beach. The Pra River catchment with focus on the coastal frontage (~3.5 km alongshore) and 1.6 km inland of the estuarine region was studied.

ii. Samples were taken once bi-monthly from May to September 2022 for all variables, however the aerial photographs included one sample taken in October, 2022

iii. Variables sampled include river depths, water levels, suspended sediment load, bedload, river velocities, and aerials photographs

1.9 Limitations

i. Sampling approach: samples were taken once bi-monthly because of the cost involved in sampling at a higher frequency. This would exclude temporal variation which would occur between sampling periods. Also, point sampling of river depths, suspended sediment load, bedload and river velocities would not represent the entire area studied.

ii. Laboratory equipment: Sediment samples were manually sieved to analyse sediment particles sizes due to the faulty mechanical shaker found at the Department of Fisheries and Aquatic Sciences. This may

7

have affected the sediment particle size distribution obtained for the study.

iii. Although river sediments influence shoreline changes, other coastal processes like waves, storms, currents and longshore sediment transport affect shorelines but are not included in the study.

iv. Variables collected in the estuarine region are prone to influences of tidal fluctuations, although samples were as much as possible, taken at low tides.

1.10 Organisation of the Thesis

Chapter One of the thesis introduces the topic under discussion: which consists of the background to the study, statement of the problem, justification of the study, objectives, and organisation of the study. Chapter Two deals with the literature review, that is, climate, river processes, coastal processes and measurement techniques. Chapter Three describes the materials and methods for the study – study area; data collect, processing and analysis techniques. Chapter Four deals with the results obtained from the study. Chapter Five deals with the discussion of results obtained, while Chapter Six is made up of the conclusions and recommendations for the study.

1.11 Summary

This chapter has provided background information pertaining to how river discharges and sediment transport to the sea impacts on the coastline. It has been realised that rivers supply sediment to the coastal areas by means of weathering, erosion and transportation. These sediments are important for the

8

building up of beaches and facilitating coastal processes as well as agricultural support. However, human interventions like damming and land exploitation in river catchments in these times where climatic change is dominant affects the net sediment transported to the coastal area leading to coastal erosion in most cases. This has resulted in the use of hard-engineered sea defence structures along most eroding coastlines to trap sediment for beach build and avoid further erosion, particularly in Ghana, of which usually led to further erosion in adjacent coasts. The thesis has also been organised into six chapters.

9
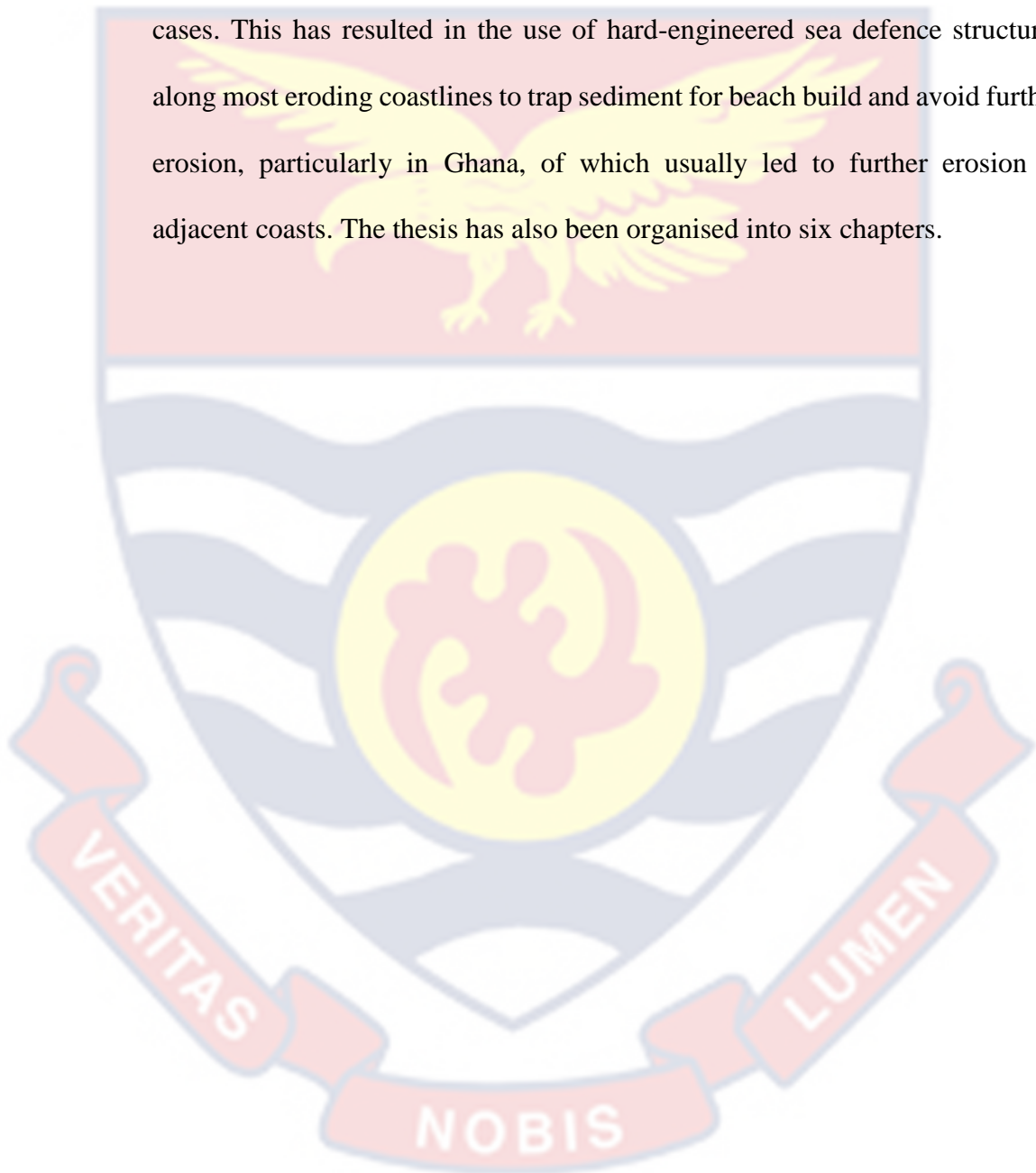
CHAPTER TWO

LITERATURE REVIEW

2.1 Overview

This chapter gives an account on various literature pertaining to rainfall and temperature climate of some river basins in Ghana and its implication to the Pra River system. It also explores river discharges, weathering and erosion in rivers, particle size distribution, sedimentation, anthropogenic factors affecting riverine sediment transport, their relationships and ultimate impact on riverine sediment discharged at the coastal side of the Pra River catchment. In addition, discussions on sediment dynamics, wave and longshore current impacts on beaches, tidal patterns, storm surges as well as the present coastal erosion management practices in Ghana and Anlo Beach for that matter have been highlighted. A further discussion on methods for quantifying the various processes occurring in rivers and the coastal area has been made below.

2.2 Conceptual Framework of the Research Work

This research work was guided by the conceptual framework (Figure 2.1), which employed the collection of river velocities, sediment discharges (bedload and suspended load), river depths and water levels from the Pra River to assess their contribution to the evolution of the Anlo Beach. The evolution of the beach was also assessed by the use of nearshore aerial photographs of Anlo Beach.

10
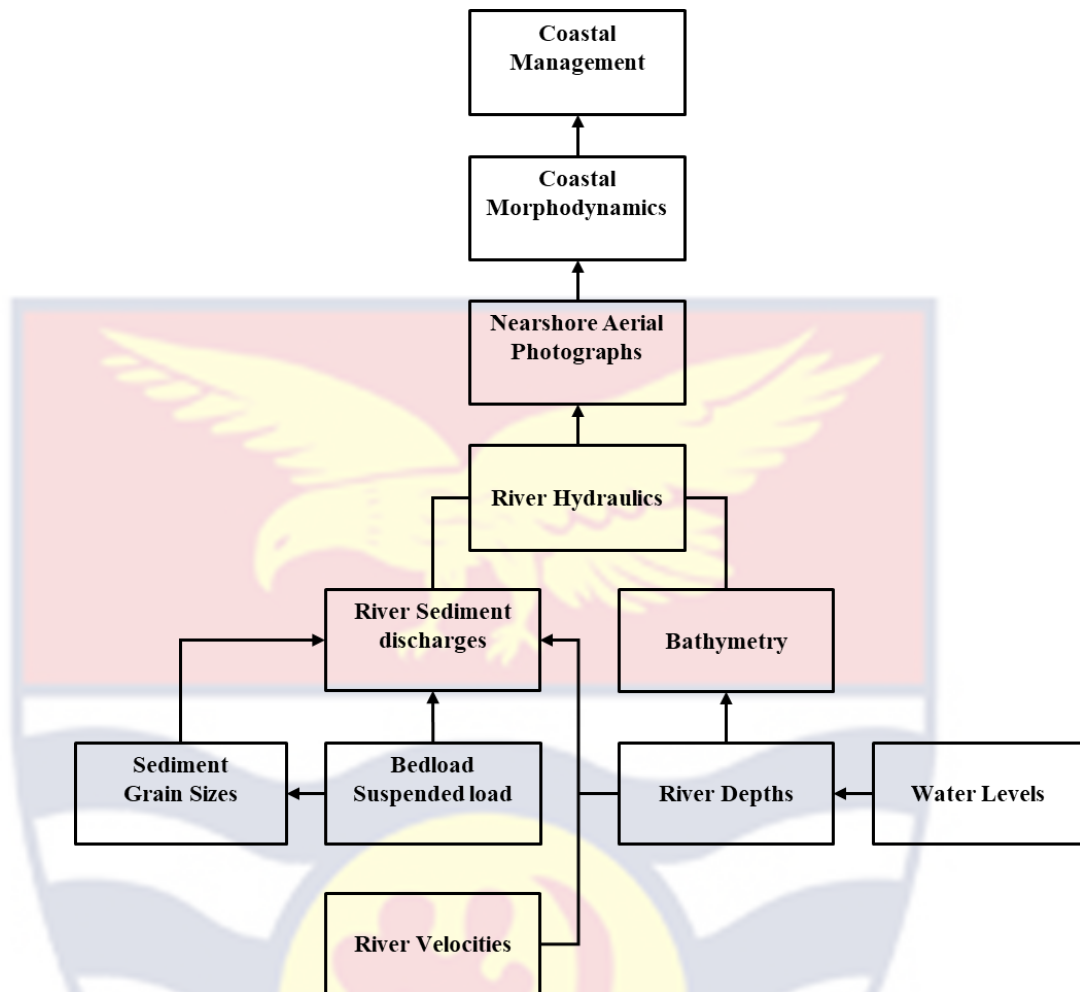
Figure 2.1: The conceptual framework of the research work

2.3 Climatic change indicators in the Pra River Catchment

Climatic change indicators represent the trends of specific environmental conditions over a time period of 30 years or more in a specific region (WorldAtlas, 2022). Examples of these indicators are the changes in temperature and precipitation, melting of sea ice, wildfires, among others (WorldAtlas, 2022). The focus of the review would be mainly the temperature and precipitation (particularly, rainfall) changes of river catchments in Ghana and their impacts on river flows and sediment transport.

2.3.1 Rainfall and temperature changes

Climatic factors like temperature and rainfall are important in determining a river catchment's discharge of water and sediment. Rainfall variability and other extreme weather events have been reported to have caused increased runoffs in the Densu River in Ghana as well as Shiyang and Tarim Rivers in China (Chen et al., 2006; Huo et al., 2008). A climatological study of the Pra River catchment from 1974 to 2003 by Kankam-Yeboah et al. (2013) indicated that the highest rainfall occurs in June, and temperatures were high in months with low rainfall (Figure 2.2, Figure 2.3). Obuobie et al. (2012) predicted a decline rainfall in the catchment of the Pra River. The study forecasted that rainfall would decrease at a rate of 17.8 % in 2020 and further decrease by 25.9 % in 2050. Kankam-Yeboah et al. (2013) also confirmed Obuobie et al. (2012) using the IPCC scenario A1F1, which indicated that there would be an increasing temperature with a decreasing rainfall for both the 2020s and 2050s in the Pra River Basin and the White Volta River Basin. In addition, Nsiah et al. (2022) also studied the climatic conditions of the Pra River catchment from 1950 to 2019 using trend and change-point analysis. Observation from this study has also indicated a general increasing trend of temperature against a decreasing precipitation level over the catchment. It was further revealed by Nsiah et al. (2020) that from 1950 to 2019, temperatures were generally low in the rainy season while dry seasons experienced increased temperatures. A study by Gyamfi et al. (2021) has also agreed with Kankam-Yeboah et al. (2013), Nsiah et al. (2020) and Obuobie et al. (2012), that currently, a general reduction in rainfall for the Pra River catchment is occurring. The dry season is noted to be getting drier at a rate of 0.17 mm per

year and in the rainy season, rainfall is decreasing at a rate of 0.05 mm per year. Although these studies are indications that the Pra River catchment is getting warmer, with reduced rainfall (Ampadu, 2021), these were not compared with river flow and sediment discharges, thereby paving way for studying this phenomenon.
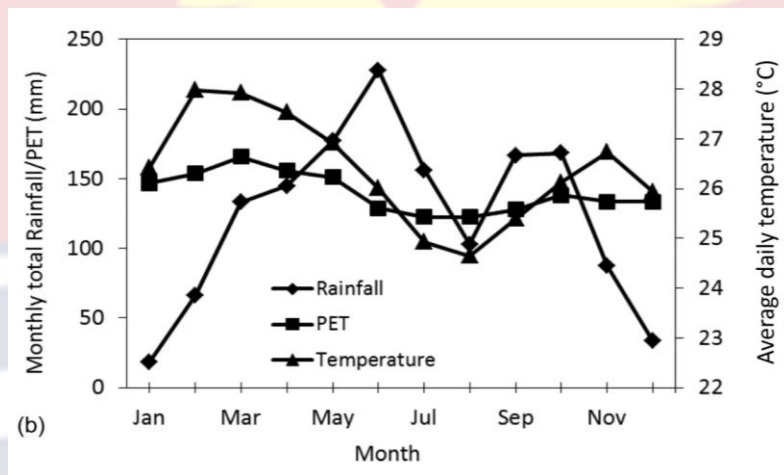
Figure 2.2: Climatology of the Pra Basin (1974–2003). Source: Kankam-Yeboah et al. (2013)
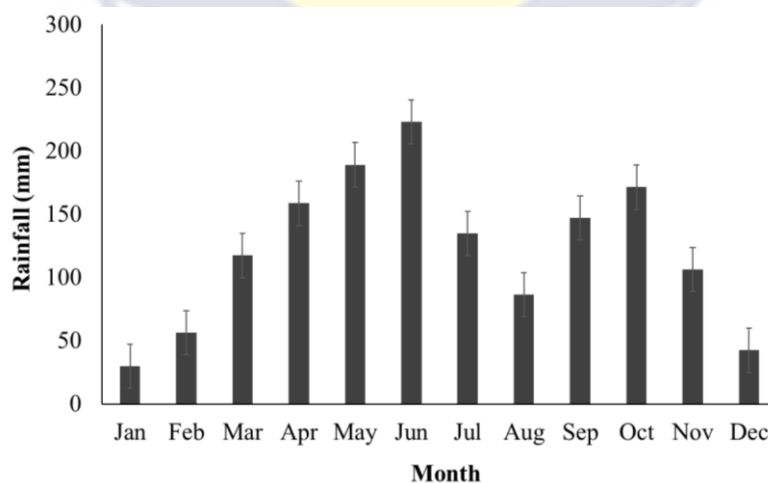
Figure 2.3: Mean monthly rainfall distribution at Twifo Praso (1986-2010), a town in the Pra River catchment. Source: Kusimi (2014)

13

2.4 River Processes

River processes are those processes through which erosion, transportation and deposition of sediment occur, and result in the changes in the river channel and the landscape on the course of the river (StudySmarter, 2022). Examples of these processes include tidal fluctuations, longshore currents, waves, storm surges, among others. These processes have been discussed, including their impacts on the coast of Ghana.

2.4.1 River discharges

A river catchment is a hydrological unit that collects water within a watershed and it is separated by a drainage divide. A river basin is formed when a smaller or relatively smaller tributary joins a lager river (Zeiringer et al., 2018). Water balance in a river's catchment is obtained through the computation of losses, gains, and storage of water in the basin. Loss of water in a river occurs through several means like evaporation, runoffs and evapotranspiration; it could also be gained mainly by precipitation and stored as ice, groundwater, or soil water (Zeiringer et al., 2018). To observe river discharge at a specific location, Zeiringer et al. (2018) identifies biogeophysical and meteorological factors as the main determinants. Biogeophysical factors that could determine river discharges include basin elevation, the drainage area, topography, shape of the basin and its drainage network patterns, vegetation cover; land use activities, type of soil as well as lakes, sink, barrages, ponds, and impoundments located in the catchment, which could interfere in downstream runoff. The meteorological factors include the precipitation type; the quantity, intensity, extent as well as how the rainfall is distributed over the entire catchment; soil

14

moisture that occurred due to previous rainfall, and meteorological factors affecting infiltration and evapotranspiration.

Studies conducted by Kankam-Yeboah et al. (2013) on the Pra River showed that from 1954 to 1997, the highest monthly mean daily discharge was approximately 380 m³/s occurring in July and a monthly average of ~215 m³/s. In this same area, Boakye et al. (2021) found that between the years, 2017 and 2018 the highest discharge recorded was ~1000 m³/s in July. However, it was observed that on the same day of data collection at Beposo (~60 km from Twifo Praso), the discharge was relatively lower (650 m³/s). At Beposo, Boakye et al. (2021) obtained an average monthly discharge of ~282 m³/s and recorded the highest daily discharge of 700 m³/s in October, with the second highest of 650 m³/s in July, 2017. In addition, it was noted from these studies that high river discharges occur predominantly in the rainy seasons, starting from May to November (Figure 2.4). Furthermore, Bekoe et al. (2012) observed that the Ayensu River, which forms part of the South-western River systems in Ghana also has a seasonal discharge pattern which is similar to the Pra River and may be as a result of the bi-modal rainfall pattern.
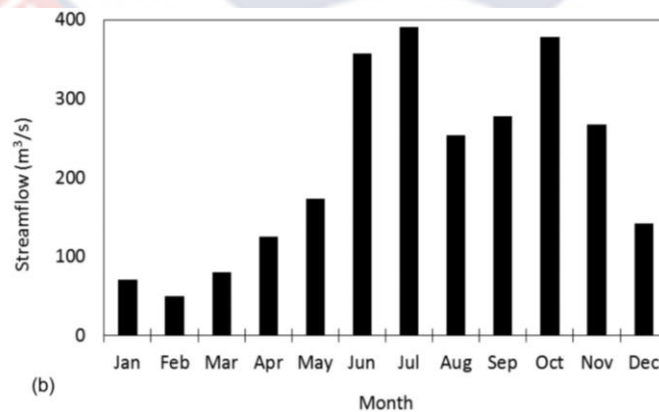
Figure 2.4: Mean daily discharge of the Pra River the Twifo Praso (1954 – 1997). Source: Kankam-Yeboah et al. (2013)

15

In other river catchments in Ghana like the White Volta (located in the northern part of Ghana), Kankam-Yeboah et al. (2013) observed that from 1963 to 2003, daily river discharges were relatively low in the months of December to May (< 100 m^3/s) and reaching peak in September with discharge of > 1700 m^3/s. The high peak discharges associated with the White Volta was primarily due to the catchment size and high rainfall that occurs during the rainfall season (unimodal). Mawuli and Amisigo (2016) observed that in the year 2013, the White Volta catchment recorded the highest discharge of ~ 1319.2 m^3/s in October. The above review gives a clear indication that rainfall patterns affect discharges of rivers in Ghana, with the Pra River basin usually having the highest discharges in July. This study is therefore undertaken in the rainfall season, which would help affirm whether high discharges occur in the month of July or not.

2.4.2 Weathering and erosion in rivers

Weathering and erosion in rivers are undoubtedly crucial factors contributing to sediment in rivers. How dissolved and particulate matter from inland redistribute through erosion has been identified as pivotal to geological sciences (Cantalice et al., 2015). Erosion encompasses the disintegration of rock and soil particles, which are transported and deposited under the influence of rainfall, winds and surface runoffs (Boakye et al., 2020). Riverine sediment consists of fragments of weathered inorganic materials originating partly from the river channel as well as the catchment area (World Meteorological Organisation, 1981). Sediments are eroded by two main processes: sheet erosion and channel erosion (Roehl, 1962). Sheet erosion is an upland source of

16

sediments while channel erosion results from gully erosion, valley trenching, stream bank and bed erosion (Kusimi, 2014). The volume as well as the kind of particles that are eroded and transported in rivers varies significantly by time and space (Alexandrov et al., 2008).

Eroded sediment in rivers is transported as suspended load or bedload (Milliman & Farnsworth, 2011). Cantalice et al. (2015) defined suspended load as particles which are kept in suspension for long periods by the vertical component of velocity in turbulent flow as they are transported by the horizontal aspect of velocity in the same flow. The velocity with which suspended sediment moves is almost the same as the velocity of the water body transporting it (Cantalice et al., 2015; World Meteorological Organisation, 1981). The suspended sediment load of a river primarily constitutes particles of silt and clay (< 0.062 mm) (Babiński, 2005) and the quantity discharged reflects activities occurring in the catchment. Babiński (2005) identifies two denudation processes which affect suspended sediment transport: (1) the source of the sediment (example, from bank erosion, mass wasting, surface and gully erosion; (2) the sediment supply rate, the vegetation cover density, catchment topography, magnitude of rainfall influx and the erodibility characteristics of soil in a catchment.

Bedload on the other hand is the component of fluvial sediment that are not able to stay in suspension but are transported by saltation or rolling (Gomez, 1991). It is a part of the sediment constituent, which has almost consistent contact with the bed of the river, and it is transported by means of hopping, sliding or rolling (World Meteorological Organisation, 1981). In this study, both

17

bedload and suspended load as well as river velocities are used in understanding the sediment discharges of the Pra River.

2.4.3 Sedimentation of rivers

It has been established by Walling (1983) that a small portion of eroded sediment in river basins from the upper and middle course reach the lower course, and consequently into the outlet. River sedimentation occur as temporal or permanent deposition (in the channel, swales, base of slope or floodplains) of sediment as they are transported to the basin outlet (Walling, 1983). The occurrence of river sedimentation is mainly due to several causative factors, usually the properties of the river basin – including its area, geology, and topography; climatic conditions and land use (Boakye et al., 2021). Hence, variations in these factors could lead to change in sediment deposited in rivers. For instance, studies by Nyarko et al. (2016) revealed that since the 15th century, the Pra Estuary experienced temporal variations in the rate of sedimentation mainly due to land-use like gold mining activities occurring in various areas of the Pra River catchment. The rate of river deposition is a fundamental function of the size of the river. Therefore, rivers with smaller area tend to deposit less sediment due to inadequate area for sediment storage while the larger rivers deposit more in their course of transport (Boye et al., 2019; Walling, 1983). This information would help to understand the bathymetry dynamics of the Pra Estuary.

18

2.4.4 Sediment particle size distribution in rivers

The distribution of sediment particle size is important in understanding the hydrodynamic characteristics of riverine system, including sediment transport as well as sedimentation processes (Wang et al., 2020). Studies have shown that suspended sediment in Ghanaian rivers is very fine with about 50 % being less than 63 μ (Boateng, 2012; Boye et al., 2019). Faseyi (2022) observed that 34 % of bed materials in the Pra and Ankobra Estuaries were silt (< 63 μ); over 65 % were sand (63 to 2000 μ) and 1 % gravel (> 2000 μ). Logah et al. (2017) also found the bed material of the Lower Volta River to be about 65 % sandy and less than 5 % gravel. These studies imply that most rivers in Ghana are characterised by sandy bed materials with very small proportion of gravels. However, the implications for erosion and accretion of the river bed were not accounted for in these studies, hence, the need for the present study to investigate this area.

2.4.5 Main anthropogenic factors influencing sediment transport in rivers

Many river systems have had their natural flow characteristics altered by human impact. A number of towns and some major cities originated along river banks worldwide, primarily to have easy accessibility to water resources and to exploit them for sustenance of their livelihoods and development of the inhabited area (Awotwi et al., 2019; Cantalice et al., 2015). This has led to the interference in the discharge of sediment due to the growing population and the demand for extra resources to meet the needs of the populace. The alteration of river flow regime through human activities changes the actual pattern of the natural hydrologic variation (Flores et al., 2020). It disrupts the dynamic balance

19

existing between the sediment and water movement in unaltered rivers (Flores et al., 2020; Zeiringer et al., 2018). Interventions made by man on rivers include but not limited to impoundments (dams/reservoirs), barrages, levees channelisation, groundwater pumping, and agricultural activities (Awotwi, 2019; Flores et al. 2020; Zeiringer et al., 2018).

Sediment delivered by many rivers to sea has reduced significantly in the last few decades (Ly, 1980; Syvitski et al., 2005). This has been associated with the numerous dams, reservoirs and barrages which are constructed on rivers (Amenuvor et al., 2020; Boye et al., 2019; Chen et al., 2018; Darby et al., 2020; Guo et al., 2018; Latrubesse et al., 2005; Tamene et al., 2006; Yang et al., 2006; Yang et al., 2007; Zeiringer et al., 2018). These structures alter most of the natural ecosystems in rivers due to dynamics in sediment and nutrients discharged. Large dams have high potential of trapping large quantities of sediment (Latrubesse et al., 2005) while smaller dams trap less sediment. In the Pra River catchment, Water Resources Commission (2012) reported that nine mini dams/reservoirs (example: Barekese Dam – Figure 2.5, Owabi Dam – Figure 2.6) have been constructed to supply water for domestic and industrial use. However, on the account of their abstraction rates (Table 2.1), these mini dams will result in less than 2 m^3/s water discharge reduction, which may be quite negligible. Yet, more bedload may be deposited behind these dams, which could lead to bed erosion at the lower reaches of the Pra River.

Figure 2.5: The Barekese Dam on a tributary of the Pra River
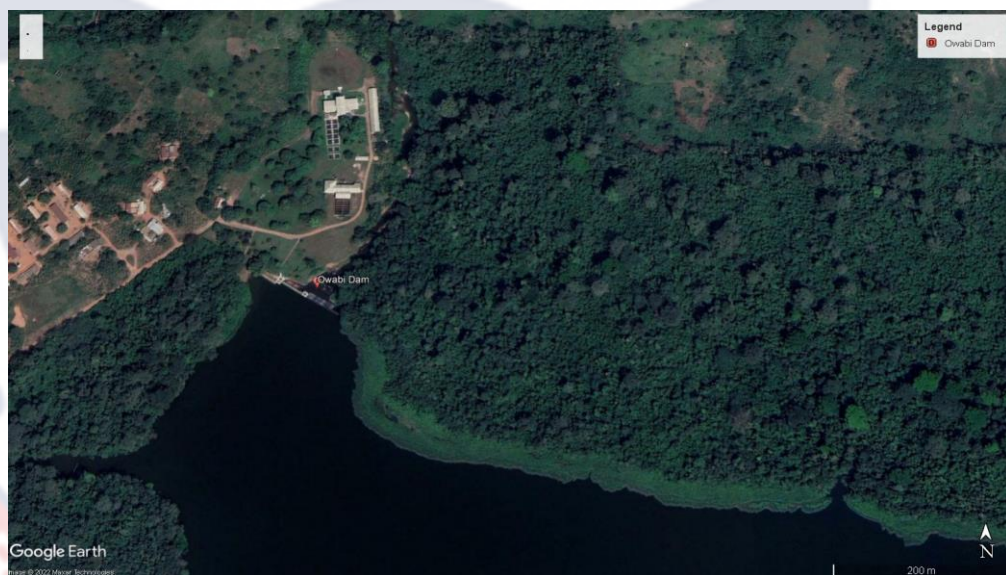
Figure 2.6: The Owabi Dam on a tributary of the Pra River

21

Table 2.1: Mini dams/reservoirs in the Pra River catchment

Location of Reservoir/ Mini Dam	Capacity (thousand of m³)	Annual Abstraction Rate (m³)
Barekese	89,588.52	29,862,840
Owabi	15,329.91	5,109,971
Daboase	29,880.36	9,960,120
Ofoase	236.52	78,840
Osenase	236.52	78,840
Kusi	236.52	78,840
Kibi	236.52	78,840
Osino	236.52	78,840
Bunso	998.64	332,880

Source: Water Resources Commission (2012)

Impoundments reduce the intensity and frequency of high river discharge, which results in fine sediment deposition, gravel sealing in river beds, stabilisation and narrowing of river channels. Furthermore, floodplain disconnection, as well as bank and river bed erosion will occur due to sealing and land drainage thereby increasing the intensity and frequency of large floods. Groundwater recharge also is minimised due to less soil infiltration. Channelisation and levees reduce overbank flows, which results in the floodplains deposition and restricted channel migration, hence the development of more tributaries. In addition, due to groundwater pumping, the water table becomes lower, inhibiting the growth of plants. Riverbanks then begin to erode due to the loss of vegetation (Zeiringer et al., 2018).

The removal of natural vegetative cover due to changes in land use could greatly increase the rate of erosion as well as sediment yield in a river catchment (Kusimi, 2014; Milliman & Farnsworth, 2011). Flores et al. (2020), Liu et al.

22

(2021) and Milliman and Farnsworth (2011) pointed out that deforestation (logging and clearing of lands) for farming, mining, development of infrastructure could lead to a general increase in soil erosion in catchments and consequential increase in sediment loads in greater magnitude compared with forested areas.

Some effects have been associated with mining, and these are often negative to rivers due to increasing suspended sediment concentration in rivers (Milliman & Farnsworth, 2011). Akrasi (2011) suggests that sediment yield of river catchments is mainly associated with land-use like farming, over exploitation of timber trees (logging) and urbanisation which leads to the erosion of top soils. Galley et al. (2018) reported that the intensive mining of gold for over 15 years in the Maroni River basin in French Guinea resulted in significant increase in suspended sediment loads in the basin. Galley et al. (2018) however noted contrasting findings. That is, although the Oyapock River Basin (close to the Maroni River Basin) also experienced similar mining impacts, there were no significant changes in suspended sediment yield. This was attributed to high sedimentation rate on the bed of the Oyapock River as well as dilution by other adjoining tributaries that do not experience gold mining activities.

In Ghana, Awotwi et al. (2017) reported that, since the early 21st century, anthropogenic impact on the Pra River has risen significantly as most perennial crop farmlands have been converted to lands for gold mining. After the mineral bearing potential has been lost in a land, no reclamation is done although it is required to engage in land reclamation to at least 75 % of the

23

original state (Awotwi et al., 2017). Since lands are not reclaimed, new forest areas are cleared for farming.

Several authors (Boakye et al., 2021; Boye et al., 2019; Kusimi et al., 2014) have reported that in the last few decades, the whole Pra River catchment is beleaguered with severe illegal small-scale mining (Galamsey) activities in the river channels and along their banks (Figure 2.7). In addition, there is indiscriminate waste disposal, uncontrollable agricultural practices and urbanisation along the Pra River catchment, which has led to excessive sediment discharge (Boye et al., 2019).

Considering Boakye et al. (2020), the Lower Offin sub-basin in the Pra catchment experiences an average of 59.88 tons/ha/year loss of sediment particularly from alluvial gold mining (Figure 2.7). Awotwi et al. (2018) observed 10 % increase in surface mining areas in the Pra River catchment within a period of four years (2013 – 2016). Yet, between 2014 and 2018, studies conducted by Boakye et al. (2021) and Kusimi et al. (2014) showed that suspended sediment yield obtained in various sub-basins of the Pra catchment had declined between 7.9 and 29.9 % aside one area with 6.7 % increase (Table 2.2) The decline was primarily due to "Anti-Galamsey" operations imposed by the government of Ghana in 2017. This this study does not cover the anthropogenic impacts on sediment delivery to the lower reaches of the Pra River. However, the literature above demonstrates that sediment discharges in the Pra River catchment is mainly influenced by the alluvial gold mining activities along the various tributaries, which could have impacts on the coastal, especially, the areas adjacent the river mouth. A summary of land-use impact

on riverine sediment delivery in the Pra River catchment has been provided in

Table 2.3.
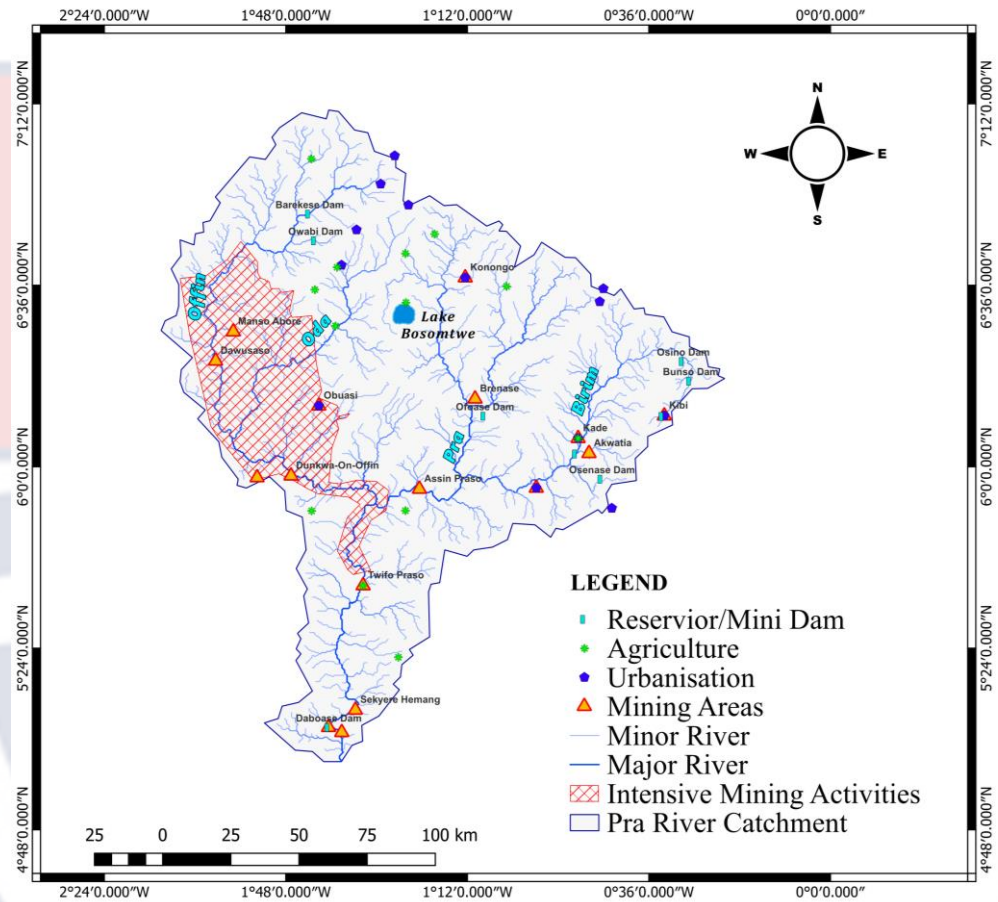
Figure 2.7: Major anthropogenic activities affecting sediment yield in the Pra
River catchment. Sources: Google Earth (2022); Kusimi (2014); Boakye et al.
(2021)

25

Table 2.2: Variations in annual suspended sediment discharge at various sub-basins in the Pra catchment before and after Anti-Galamsey operation in Ghana

Sampling Station	Annual suspended sediment yield (tons/year)		Percentage Change
	Kusimi et al. (2014)	Boakye et al. (2021)	
Anwiankwanta	6.6094×10^4	6.0892×10^4	-7.9
Adiembra	11.5372×10^4	7.6054×10^4	-34.1
Brenase	15.0455×10^4	5.7834×10^4	-61.6
Assin Praso	22.0907×10^4	15.4767×10^4	-29.9

Table 2.3: Summary of land-use impact on riverine sediment delivery in the Pra River catchment

SN	ITEM	IMPACT	SEVERITY
1	Dam/Reservoir	Traps sediments	Low
2	Urbanisation (creation of buildings and hard surfaces)	Increase runoff and erosion	Moderate to high
3	Agriculture (plant cultivation)	Induce soil erosion	Low to moderate
4	Logging	Induce erosion	High
5	Mining	Increase erosion and sediment runoffs	Very high

26

2.4.6 Sediment yield in rivers

Sediment yield of a river is the quantity of sediment passing the outlet of a river basin within a specified period, which is due to erosional and depositional processes occurring within the catchment/basin (Boakye et al., 2018; Kusimi, 2014). The magnitude of sediment yield is as a result of the interplay between physical (rainfall, basin size, and topography) and anthropogenic (logging, mining, farming, damming, construction, etc.). Sediment yield of a river catchment include both suspended load and bedload. In Ghana, studies on sediment yield in rivers have mainly been focused on suspended load (Akrasi, 2011; Boakye et al., 2021; Boateng, 2012; Boye et al., 2019; Kusimi, 2014; Kusimi et al., 2014), with little information regarding the bedload. Usually, bedload is assumed to be 10 % of suspended sediment according studies by Walling (1984) and this has been adopted by several researchers who are not able to do in situ bedload measurements (Boateng, 2012; Boye et al., 2019). However, studies from Boateng (2012) revealed that percentage of bedload discharged by rivers in Ghana ranged between 10 and 56 % of the suspended sediment. Kusimi (2014) indicated that the grain size of bedload and the velocity of the river affect the ratio of bedload to suspended load discharged. Babiński (2005) suggests that the actual ratio of bedload to suspended load of a river is dependent upon the river's transport power, the hydrological regime, catchment geology as well as anthropogenic activities, hence no single factor could explain the ratio of bedload to suspended load.

Sediment yield studies on the Pra River has given an indication that the river has high sediment load, especially the suspended component. Boye et al. (2019) used existing river discharge measurements from 1974 to 2005 to

27

estimate sediment discharged by rivers in the Western Region of Ghana to the sea. It was revealed that the Pra River discharged suspended sediment (SSQ) of 249,459.2 tons/day and total sediment discharge of 274,405 tons/day. These values are extremely high and likely to be overestimation, comparing to recent trends in sediment discharged by the Pra River (Table 2.4). Akrasi (2011) used daily suspended sediment obtained through dip sampling to predict sediment discharged by the Pra River catchment. The suspended sediment discharge (SSQ) obtained was 1025253.9 tons/year and added 10 % correction factor as bedload to get a total sediment discharge of 1,139,171 tons/year. Kusimi (2014) found the Pra River to discharge 9,936,857.33 tons/year of suspended sediment at Sekyere Hemang (in 2012), an area which is close to the mouth of the river. Boakye et al. (2021) also observed 6,074,457.75 tons/year of suspended sediment at Beposo, approximately 13 km downstream of Sekyere Hemang in 2018, indicating a significant reduction in sediment yield. This was associated with the imposed ban on illegal gold mining activities in Ghana in 2017. Sediment discharges of the Pra River in various studies is summarised in Table 2.4.

Table 2.4: The average annual sediment discharge of the Pra River

Source	SSQ (tons/day)	SSQ (tons/year)	Average total discharge (tons/year)
Boye et al. (2019)	249,459.2	91,052,608.00	100,157,825.00 (SSQ + 10 %)
Akrasi and Ansa-Asare (2008)	2,931.96	1,070,164.20	–
Akrasi (2011)	2,808.91	1,025,253.90	1,139,171.00 (SSQ + 10 %)
Milliman and Farnsworth (2011)	6,579.73	2,401,600.00	–
Kusimi (2014)	27,224.27	9,936,857.33	8,238,219.11
Boakye et al. (2021)	16,642.35	6,074,457.75	-

Increasing river discharges has been associated with increasing rainfall and consequential increase in sediment discharged, especially the suspended sediment (Kusimi, 2014). Measurements of suspended sediment in the Pra River by Kusimi (2014) showed a positive relationship with the rainfall pattern in the catchment. Also, Ofori et al. (2016) studied the influence of rainfall pattern on river flow and sediment discharges in the Weija reservoir situated on the Densu River in Ghana. The study suggested that river flow and sediment discharges in the river was directly linked with rainfall pattern in the area. This implies that, extreme rainfall (rainstorms) could have severe impact on sediment discharged by rivers.

29

Riverine sediment impact on beach building is said to be dependent on particle size of sediment discharged. Boateng (2012) and Boye et al. (2019) referred to Ayibotele and Tuffour-Darko (1979) and used 50 % as portion of suspended sediment that is relevant for beach building. This is because, Ayibotele and Tuffour-Darko (1979) found 50 % of suspended sediment in Ghanaian rivers to be very fine, and would be disturbed by the slightest turbulence, hence would not stay on the beaches. Based on Faseyi (2022), about 34 % of bedload in the Pra and Ankobra Rivers are finer than 63 µ. This implies that only 66 % of bed sediment would be relevant for beach building and reduction of coastal erosion. Other studies like Haider et al. (2021), Jayson-Quashigah et al. (2019) and Nguyen et al. (2016) are also of the view that sediments finer than 150 µ would not be relevant for beach building and coastal stability. This study will therefore adopt Ayibotele and Tuffour-Darko (1979) to determine the quantity of sediment which would be relevant for beach building.

2.5 Coastal Processes

Coastal processes are means through which sediment are transported in and deposited in the coastal system to cause modifications at the coastal area (Geography Revision, 2022). Examples of these processes include tidal fluctuations, longshore currents, waves, storm surges, among others. These processes have been discussed, including their impacts on the coast of Ghana.

2.5.1 Beach sediment dynamics

Beaches are in a delicate equilibrium between forces of erosion and sediment supply. This delicate balance is primarily affected by both natural (waves, storms, tides, currents) and human induced factors such as sand mining and artificial structures construction with direct impact of sediment transport (Frihy, 2001; Jonah et al., 2015). Hence, some studies have estimated sediment volume changes on beaches in relation to anthropogenic and naturally induced sediment volume changes. For instance, Brempong et al. (2021) observed a higher quantity of sediment loss than sediment gained on the Dzita Beach (on the Eastern coast of Ghana) throughout a study period of 20 months. The sediment loss was mainly attributed to littoral drift of large quantities of sediment to downdrift coasts. Other factors such as the mining of beach sand and gravels as well as the interception of sediment behind the Ada sea defence system were identified as human-induced factors of sediment loss on the Dzita Beach. It is however noted that periodic accretion occurred on this coast and was attributed to this beach being situated between two coastal defence systems. Angnuureng et al. (2019) suggests that erosion on the Dzita Beach may be caused by inadequate sediment discharge from the Volta River due to sediment interception by the Kpong and Akosombo dams (Ly, 1980). Similar trend of sediment losses and gains on the Volta Delta was identified by Jayson-Quashigah et al. (2019), with sediment loss and gains mainly attributed to the presence of artificial infrastructure in the delta region and strong longshore currents and swells.

On the central coast of Ghana, Angnuureng et al. (2022b) observed a loss of sediment on the beach of Elmina. Although the main factor causing the

<div align="center">31</div>

sediment loss was not clear, wave conditions in the region was speculated to be the major cause. Other reasons were attributed to beach sand mining (Jonah, 2015) as well as jetties intercepting most of the sediment from the west direction. It could therefore be deduced that both anthropogenic and natural factors intertwine to determine the dynamics of beach sediment volume on beaches in Ghana, hence could be similar to the Anlo Beach.

2.5.2 Impact of waves and longshore currents on the coast

Waves are important regarding the reshaping of coastlines (Boye, 2015; Rajab & Thiruvenkatasamy, 2017). Waves destabilise sediment, putting them in suspension and influence the circulation of currents as they break on the coastline. Wave height, direction and offshore bathymetry are significant in determining the impact of waves breaking at the coast. Sandbar located farther from the beach causes wave energy to dissipate before reaching the coastline, making the coast less prone to erosion and vice versa (Abdul-Kareem et al., 2022; Angnuureng et al., 2017; Boye, 2015). For instance, studies by Appeaning Addo et al. (2011) revealed that erosion of the Keta coastline is partly because of the deep bathymetry and the large number of canyons, which are present from the continental shelf to the open ocean. Due to the deep bathymetry, waves are able to travel over a long fetch (distance covered from the place of origin) without interference by landmasses to cause energy dissipation. Hence, in most instances, a large portion of the wave energy propagates to the shore, causing erosion (Roest, 2018). Angnuureng et al. (2019) indicated that offshore bathymetry could be responsible for variation of waves impact on the Dzita Beach located on the east coast of Ghana. Furthermore, it has been pointed out

32

by Orme (2005) that the West Africa coastline has a narrow continental shelf, hence most strong waves (swells) are able to reach the shore faster to cause erosion (Xorse, 2013).

Two types of waves (swells and seas) with distinct origins approach the West Africa coastline (Appeaning Addo, 2010; Xorse, 2013). The seas are relatively weak waves formed from locally generated winds. The seas have a height and period not more than 1.25 m and 3 – 4 s, respectively (Allersma & Tilmans, 1993). The swells on the other hand are highly energetic waves with long period (over 10 s), which are generated over long fetches (Gooley, 2016). On the coast of Ghana, swells approaching the shores originate from the south of the Atlantic Ocean (Boye, 2015; Hopsch et al., 2007; Xorse, 2013). However, upon reaching the coastal areas, they are mixed up with the seas (generated by weak local monsoon – south-easterly winds), thereby making them calmer (Appeaning Addo, 2010). Currently, a study by Angnuureng et al. (2022b) on the coast of Elmina (~ 33 km to the Shama - Anlo Beach coast) indicated that the mean significant wave height (Hs) of the area ranges between 0.5 m and 2.2 m, although individual heights could reach about 3 m. These two areas (Elmina and Shama – Anlo Beach coast) have similar orientation to the sea, suggesting that they may experience similar wave climate. The daily Hs therefore gives a clear indication that both seas and swells mix up to hit the coast of Anlo Beach to cause rapid erosion of the coastline.

Longshore currents are those currents that move parallel to the coastline, thereby forming oblique wave incidence (Meng, 2013). That is, where oncoming waves from offshore approach the coastline at an angle, some of the energy flux is redirected alongshore, leading to longshore current generation,

which usually have a speed of 0.2 to 1.0 m/s (Davidson-Arnott, 2010). In Ghana however, the average longshore current is ~1.0 m/s and fluctuate between 0.5 and 1.5 m/s. These parallel moving currents work together with the waves, tides and prevailing winds (Appeaning Addo, 2010). Processes such as swash and backwash with the help of gravity move sediment along the beach as waves hit the coastline at an angle. The resultant movement of sediment slowly along the coastline leads to accretion or erosion, which is the longshore sediment transport (Figure 2.8) (Dean & Dalrymple, 2004; Xorse, 2013).

The rate of longshore sediment transport is dependent on the energy or waves approaching the shore as well as the angle (45° as the most effective) with which it hits the coastline (Xorse, 2013). Longshore sediment transport is very important, however, its significance on the entire coastline is dependent on whether its transport is not blocked by natural (headlands) or artificial structures such as hard-engineered coastal defence systems (Abdul-Kareem et al., 2022; Dean & Dalrymple, 2004; Frihy, 2001).
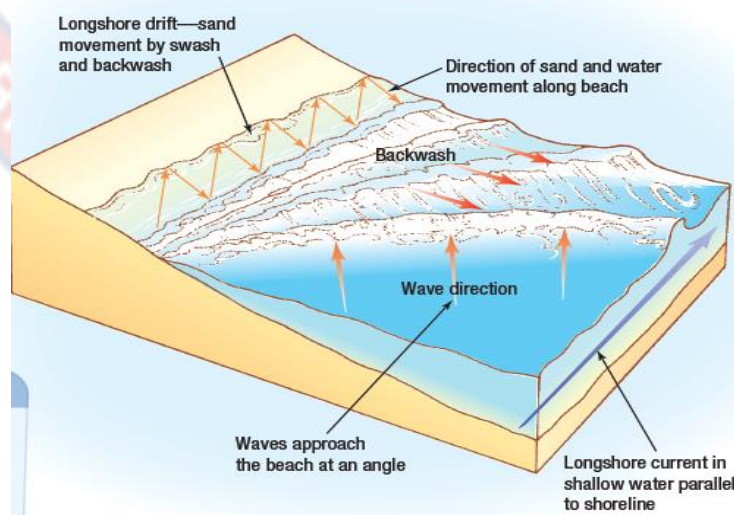
Figure 2.8: Longshore drift. Source: Croslinig (2011)

Along the surf zone of Accra, the longshore current is very strong (1 m/s and varies between 0.5 m/s and 1.5 m/s), making longshore sediment transport very significant to the coast (Appeaning Addo, 2010; 2015). It has been identified that longshore drift on the coast of Ghana is from West to East predominantly with an estimated 764554.9 m^3 of sediment transported annually due to large waves exposed to the coast (Angnuureng et al., 2020a; Wellens-Mensah et al., 2002; Xorse, 2013). A study by Angnuureng et al. (2019) indicated that the Dzita Beach has a total average longshore drift of 2227 m^3 with the direction being similar to that of the coast of Ghana. It was however noted that 45 % of the sediment drifted from the east to west, indicating a localised deviation from the general longshore transport. Anlo Beach may have a similar trend of longshore drift, however since no work has been done on it, it would be represented by that for the whole coast of Ghana.

2.5.3 Tidal patterns and the occurrence of storm surges

A coastal area experiences storm surges when ocean water is blown up against the coastline by winds. The destructive intensity of storm surges is determined by the wind-driven waves associated with it; the duration/extent; pressure as well as their coincidental occurrence with astronomical tides (Davidson-Arnott, 2010; Dean & Dalrymple, 2004). Storm surges are generally destructive and erosive (Boye, 2015). During high storm event, beach sand is transported offshore due to the disequilibrium in the beach profile during that period (Dadson, 2015). This leads to short-term shoreline change, which is a rapid erosion of the beach. However, recovery is slow and dependent on how distant the sediment was transported offshore (Angnuureng et al., 2017).

Shallow offshore bathymetry in addition to low-lying coastal areas has also been documented as factors which could trigger extreme storm surges and flooding (Davidson-Arnott, 2010; Dean & Dalrymple, 2004). Davidson-Arnott (2010) explained that the greatest storm surges occur on coasts with shallow gentle slope beaches as well as estuaries and partially-enclosed bays where coastal wind set-up has been superimposed by the local winds.

Tides are pivotal in the magnitude of storm surge occurrence, hence extreme high tides could trigger less destructive surges to become dangerous (Xorse, 2013). On the coast of Ghana, tides are semi-diurnal, with the mean tidal range for the western (0.9 m), central (0.96 m) and eastern (1.0 m) coasts being relatively low (Boateng, 2012). This makes storm surge a rare phenomenon on the coast of Ghana (Appeaning Addo, 2010). Furthermore, Appeaning Addo (2010), added that along the coastline of Accra, which falls within the central coastline of Ghana, storm surges are uncommon and could be associated with the significant differences in the speed of prevailing winds approaching the coastline. It has however been noted by Xorse (2013) that some cases of storm surges have been reported to have occurred along the west and east coasts of Ghana, which could be attributed to the continual rising of sea level. Sea level rise would create large storms which induce faster erosion of beaches, destruction of coastal settlements and infrastructure, and this could be similar to those which occur on the Anlo Beach (Dadson, 2015; Dasgupta et al., 2011).

2.5.4 Coastal erosion management practices in Ghana

For the past few decades, more coastal communities have and are being threatened by floods, erosion and storm surges. To safeguard prominent infrastructure along the coast, a number of coastal defence projects have been carried out to mitigate these challenges in some of the affected communities (Amlalo, 2005; Jonah et al., 2016). Some small-scale projects have also been undertaken by owners of infrastructure along beaches to ensure the protection of their assets. Jonah et al. (2016) stated that, "coastal management is regarded as a matter of protecting each individual's properties and does not require the acquisition of special permits from municipal authorities". Furthermore, Appeaning Addo and Appeaning Addo (2016), Boateng (2006) and Jonah et al. (2016) agree with Amlalo (2005) that there is no holistic approach/policy/ integrated plan existing for the management of flooding and coastal erosion in Ghana. The National Environmental Policy made in 2014 has no instituted action plan, even though it emphasises the need for management of the coastal zone and the marine environment (Jonah et al., 2016). This situation suggests that there is the lack of sufficient policy and enforcement in Ghana.

Although there are soft and hard engineering as well as nature-based approaches for mitigating highly eroding coastlines, hard engineering structures which are often constructed with boulders (Figure 2.9) are commonly used in Ghana. Some examples of these hard structures are groynes, revetment, jetties and breakwaters (Figure 2.10). Some notable communities along the coast of Ghana with hard engineering structures include Keta, Ada, Elmina, Cape Coast among others (Table 2.5) (Alves et al., 2020). From Alves et al. (2020) there

37

are no documentations as evidence of adopting nature-based solutions for management of the coastal areas in West Africa.

Figure 2.9: Materials used for hard-engineered sea defence structures along the coast of Ghana. Source: Author (2022)

Figure 2.10: Examples of sea defence structures used on the coast of Ghana and towns in which they are located. Source: Google Earth Pro (2022)

Table 2.5: Some communities along the coast of Ghana with hard engineering coastal defence structures

S/N	Community	Hard Engineering Type
1.	Komenda	Groyne
2.	Elmina	Groyne, revetment, jetty
3.	Cape Coast	Jetty, revetment
4.	Takoradi	Revetment, breakwater
5.	Aboadze	Revetment, jetty
6.	Anomabo	Groyne, revetment
7.	Dansoman	Groyne, revetment
8.	Jamestown	Groyne, revetment, jetty
9.	New Ningo	Groyne, revetment
10.	Old Ningo	Groyne
11.	Ada	Groyne
12.	Keta	Groyne, seawall, revetment, breakwater
13.	Atorkor	Revetment, groyne
14.	Sekondi	Revetment, breakwater
15.	Funko-New Amanful	Breakwater
16.	Tema	Revetment, breakwater

Sources: Alves et al. (2020); Angnuureng et al. (2013); Angnuureng et al. (2020a); Boateng (2009); Google Earth Pro (2022); Jayson-Quashigah et al. (2019); Jonah et al. (2016); Mohanty et al. (2012); Roest (2018)

Sea defence structures are by nature "non-comprehensive ad hoc, reactive, site-specific and hard engineered" (Appeaning-Addo, 2015). Usually, the concerns of most engineers are the residential area/built-up structures, their distinct function as well as the design. However, less attention is given to the important aspects like the geomorphology, ecology and recreational value of the beaches (Jonah et al., 2016). Therefore, due to the less comprehensive nature of

39

interventions adopted to mitigate coastal erosion, the impact of these structures is in the form of severe erosion at adjacent downdrift coasts (Alves et al., 2020; Angnuureng et al., 2013; Boateng, 2012; Frihy, 2001; Jayson-Quashigah et al., 2019). The aforementioned shows that there is a lot of room for improvement to integrated coastal zone management in Ghana.

2.6 Monitoring Techniques

Monitoring techniques are those approaches or methods used in the measurement of research variables. The review below is based on methods, which have been used in already existing studies for monitoring river and coastal processes.

2.6.1 River discharge measurement

Managing of water resources, especially riverine systems are a global concern due to the growing population and its impacts. River geomorphology depends not only on sediment load but water discharge is also a very significant factor (Das, 2019). Geomorphic characteristics of rivers become affected due to fluctuations in riverine discharges. Hence, several approaches have been used to estimate the flow rate of rivers worldwide. These approaches are in various forms such as the use of discharge data obtained from gauge stations (Bastia & Equeenuddin, 2016; Bini et al., 2021; Das & Banerjee, 2021; Das et al., 2021; Dey, 2016; Gallay et al., 2019; Guo, 2018; Joshi & Xu, 2017; Logah et al., 2014; Yang et al., 2007).

River discharges are also measured directly using underwater acoustics like the ADCP (Gallay et al., 2018; Okada et al., 2017; Yang et al., 2017).

Satellite imagery is also explored as means to measure discharges in rivers. It has been observed that despite the importance of these measurements, river discharges monitoring is declining in some parts of the world, including Ghana. This has been attributed to the high maintenance cost. Therefore, researchers engage in direct field monitoring as and when it is needed.

Although more comprehensive methods are available, the conventional methods like the use of current meters for velocity measurements, wading rods (Ofori et al., 2016), floats (Kusimi et al., 2014), are quite flexible in usage and budget-friendly but labour-intensive and mostly unsuitable for use in deep waters. The use of current meter involves dividing the river into several cross-sections and sampling the velocities from the midpoint of each cross-section as a station (Cantalice et al., 2015; Kusimi et al., 2014; Yang et al., 2017). The velocities (m/s) are taken concurrently with depths of the sampling points and the width (mostly prior determined). The river discharge measured in m^3/s is then computed as a function of the cross-sectional area and the velocities (Cantalice et al., 2015). In this study, the conventional method is applied in the measurement of river velocities and subsequent computation of sediment discharges for the Pra River.

2.6.2 Suspended sediment discharge

A number of techniques exist to obtain suspended sediment load of rivers and researchers adopt these techniques based on the available resources, data/sample requirement as well as the river discharge and sediment dynamics (Perks, 2014). Babiński (2005) identified three approaches for obtaining suspended sediment load, which include: (1) Collecting samples of water with

41

various samplers to determine the concentration of solids using optical methods or by gravimetry. (2) The measurement of quantity of materials discharged by the river as a result of erosion. (3) The measurement of sedimentation rates of rivers at dams/reservoir sites, estuaries, deltas, and the coastal areas (Tamene et al., 2006). The suspended load is then calculated as the concentration of sediment or turbidity, which is expressed as the weight density of the suspension (mg/l), or kg/m^3 (Babiński, 2005; Esteves et al., 2019; Galley et al., 2018; Mawuli & Amisigo, 2017; Minella et al., 2008).

Remotely sensed data (satellite imagery) and gauging stations are also set up to monitor long-term sediment discharge in rivers (Al-Ansari, 2015; Bini et al., 2021; Flores et al., 2020; Wu et al., 2019). Flores et al. (2020) and Gallay et al. (2019) used satellite images to estimate suspended sediment discharge using surface reflectance. Mouyen et al. (2018) also used satellite gravimetry to obtain suspended sediment discharge of major world rivers to the ocean.

Conventional methods such as taking water samples to analyse for suspended sediment concentration and converted to suspended sediment discharge using river flow rate has been used by several researchers worldwide (Akrasi & Ansa-Asare, 2008; Akrasi, 2011; Boakye et al., 2021; Galley et al., 2018; Joshi & Xu, 2017; Kusimi et al., 2014; Leeks, 2005; Mawuli & Amisigo, 2016; Ofori et al., 2016; Sulaiman et al., 2021). The conventional approach involves the use of manual (depth-integrated samplers – Dingman, 2009; Hicks, 1997) and automated samplers (point-integrated samplers) (Perks, 2014). Some examples of the depth-integrated samplers are US D-77, USDH-48; US DH-81. Some point-integrated samplers include US P-46, US P-61, US P-72 and these are best used in deep rivers. The automated samplers are calibrated to work

without the need of field operators (Alexandrov et al., 2009). Examples include time-integrating, passive, and the more advanced pump samplers (Alexandrov et al., 2009). In-depth description of their setup, advantages and disadvantages of these sampling approaches are discussed in Diplas et al. (2008).

In Ghana, Boakye et al. (2018) grouped suspended sediment discharge measurement into two forms: field measurements and the use of numerical modelling (example: Akrasi, 2005; Akrasi, 2011; Akrasi & Ansa-Asare, 2008; Boye et al., 2019). The field measurements were also classified by Boakye et al. (2018) into two forms: (1) The use of sampling equipment (example, depth-integrated samplers – which has been employed in the present study and dip-samplers) to obtain suspended sediment concentrations of rivers (Achite & Ouillon, 2007; Akrasi, 2011; Akrasi & Ansa-Asare, 2008; Boakye et al., 2021; Kusimi, 2014; Kusimi et al., 2014; Ofori et al., 2016). (2) Measuring of total erosion and sedimentation rates of small river catchments as well as in reservoirs, lakes and ponds (Amegashie et al., 2011; Ayadi, 2010).

New methods for measuring suspended sediment concentrations are laser diffraction devices such as the Sequioa LISST – SL (Gitto et al., 2017) and LISST-SL2 – measures real-time sediment concentration, particle size distribution, temperature, velocity, depth as well as other auxiliary parameters (Sequoia, 2017) hence, giving a comprehensive data for obtaining suspended sediment discharges.

2.6.3 Bedload discharges

Knowledge of bedload transport rate is very important for a number of reasons. First, it forms a part of the total load of sediment, which indicates net

43

erosion of the upstream section of a river catchment. Bedload may cause filling up of channels, impeding navigation as well as increasing the flooding potential (Kuhnle, 2008). It is however noted that the diverse nature of mechanisms involved in bedload transport (sliding rolling or saltation, and sometimes may be moved into suspension during turbulent discharges – Babiński, 2005; Cantalice et al., 2015) makes it difficult to quantify and often associated with a number of uncertainties (Babinski, 2005). In addition, most equipment for measuring bedload are often complicated, requiring much experience to use. A report by Gray et al. (2010) suggests that bedload measurements are not undertaken in many studies. This trend is the similar to studies done in Ghana.

Babinski (2005) and Habersack et al. (2010) identified several methods used in measuring bedload. They include: (1) traps and baskets which are often installed temporarily or permanently across small rivers or selected portions of the riverbed (Bunte et al., 2008). (2) Directly measured particle movement with markers or tracers such as magnetic detectors, radioactive material, fluorescent sand as well as painted stones and many others (Ergenzinger, 1992). (3) Magnetic and acoustic devices like geophones, sonar. (4) Directly measuring the quantity of sediment transport (Cantalice et al., 2015; Kuhnle, 2008). (5) Monitoring the rate of sedimentation in lakes and deltas. (6) Bedforms like dunes and ripples monitoring. Habersack et al. (2010), Gomez (1991) and Kuhnle (2008) stated that none of these methods are known to be suitable for diverse applicability due to spatio-temporal changes in the magnitude and rate of transport, hence, field calibration is needed for any method usage.

Direct measurement of bedload in rivers has been achieved by the use of portable basket samplers such as the US BL Helley-Smith sampler (Bunte et

44

al., 2008), Delft-Nile sampler, FISP BLH-84 sampler and US BL-84 sampler, with various sizes and weight for measurement either in deep or shallow waters (Dingman, 2009; Kuhnle, 2008). Other means of manual bedload discharge measurement is through the use of the vortex tube sampler or construction of slots or pit and trough samplers in the bed of the river to collect the passing sediment. This method is found to be very efficient especially in coarse sediment beds (Dingman, 2009). In this study, the US BL-84 sampler is used to measure bedload due to its availability and ability to sample in both shallow and deep water.

2.6.4 Depth measurement in rivers

The estimation of river bed profiles, also termed as bathymetry is key in many applications including flood risk management, land subsidence, inland navigation, bank erosion prediction as well as understanding fluvial processes dynamics (Arseni et al., 2019; Forghani et al., 2022; Kim et al., 2019; Merwade, 2009; Panhalkar & Jarag, 2015).

Conventional measurement of bathymetry mapping has been done through the use of total stations (Panhalkar & Jarag, 2015), RTK GPS, wading (Legleiter & Overstreet, 2012), single beam echosounders (which is applied in this study) (Arseni et al., 2016; El-Hattab, 2014; Legleiter & Overstreet, 2012) and the recently introduced multi-beam echosounders (Gouda et al., 2019; Le Deunf et al., 2020); single and multi-beam Acoustic Doppler Current Profilers (ADCP) (Legleiter & Overstreet, 2012; Okada et al., 2017). Single beam echosounders propagate sound waves through the water columns to determine their depths. Most hydrographic echosounders are made with dual frequency for

45

low (~24 kHz) and high (~200 kHz) pulsation. Low frequency pulses are suitable for use in deep water depths, while the high frequency is appropriate for shallow waters since high frequencies tend to attenuate faster (Forghani et al., 2022; Parente & Vallario, 2019). Parente and Vallario (2019) explained that it is advantageous to combine these two, due to their discrete frequencies.

Although Parente and Vallario (2019) found bathymetry survey (especially, in situ measurement) to be very common elsewhere, it is not common in the West Africa sub-region. For instance, in Ghana, only a few studies have explored single beam echo sounding techniques (Angnuureng et al., 2022b; Boakye et al., 2021) and ADCPs (Boakye et al., 2021) in their studies. For instance, Boakye et al. (2021) used an ADCP and a single beam echosounder to measure cross-section of some tributaries of the Pra River, however the focus of the study was to obtain river depth to estimate the river discharge as well as suspended sediment yield of the rivers. Forghani et al. (2022) asserts that direct measurement of riverine bathymetry is costly and involves complex logistics; therefore, this may account for the low riverine bathymetry surveys in Ghana despite the importance of this parameter in river hydrological and morphological studies.

In relation to the challenges associated with conventional measurement of river bathymetry, indirect means are being explored (Forghani et al., 2022). These include remote sensing – satellite and UAV- assisted bathymetry (Conner & Tonina, 2013; Kim et al., 2019; Legleiter & Overstreet, 2012); Light Detection and Ranging (LiDAR) (Conner & Tonina, 2013) and surface flow velocities (Forghani et al., 2022). Curtarelli et al. (2015) suggests that the use of remote sensing-based methods is advantageous due to wide coverage and

46

ability to cover areas with limited access. It is noted however, that this method is limited by depth and transparency of the water body under study (Curtarelli et al., 2015).

Low coverage and point measurements associated with conventional bathymetry survey require the need to estimate depths for unmeasured areas. Different interpolation methods have been applied in this regard. The interpolation methods were established on the principle of "autocorrelation" (Forghani et al., 2022). Basically, interpolation methods are of two categories. (1) Global – which implies that individual interpolated data value is influenced by every data value used. (2) Local – implying that individual interpolated data value is only influenced by the neighbouring point values in the dataset, this is mainly done with specified points in a designated radius (Forghani et al., 2022).

Interpolation methods could also be classified by distinguishing as exact or approximate methods. That is, their ability to preserve original data points to the inferred surfaces (Forghani et al., 2022). Examples are the inverse distance weighting (IDW), radial basis function (RBF), global polynomial interpolation, local polynomial interpolation, kriging (ordinary kriging, simple kriging and universal kriging), Triangulated Irregular Network (TIN), Topo to Raster (Al-Ansari et al., 2015; Panhalkar & Jarag, 2015). Detailed explanation of their usage is available in (EL-Hattab, 2014; Forghani et al., 2022). Aside Al-Ansari et al. (2015) who used the TIN interpolation method to estimate the bed levels of the Tigris River (Iraq) in 2012-2013 and compared with that of 1976 for changes due to anthropogenic impacts, most of the studies (example, El-Hattab, 2014; Forghani et al., 2022; Parente & Vallerio, 2019) explored the above listed interpolation techniques and more to determine the most effective and reliable

47

model based on the Mean Error, Root Mean Square Error, Standard Error, Minimum and Maximum values. This therefore gives an indication that most bathymetry studies are usually done to explore the best models for interpolation and not to report the measured depths for comparisons with others. Although exploring interpolation methods is important, reporting measured depths is also key for understanding the temporal changes of river depths for decision making regarding factors that influence the changes. This study will therefore include both purposes listed above.

2.6.5 Beach profiling and sediment volume

The interlinking effects of beach/shoreline orientation, short and long-term wave characteristics, nearshore bathymetry, winds systems, riverine systems as well as anthropogenic influences affect beach dynamics (Hentry et al., 2012). Determination of the impact of these factors on the beach is through the estimation of the beach sediment budget by studying both short and long-term beach profile variations (Jayson-Quashigah et al., 2019).

Beach morphological dynamics have been monitored using various conventional approaches with varying degrees of resolution (Abdul-Kareem et al., 2022; Brempong et al., 2021; Hentry et al., 2012; Jayson-Quashigah et al., 2019). They include LiDAR technology, satellite imagery, aerial photographs, GPS, dumpy level and a graduated staff (Hentry et al., 2014). These approaches are associated with at least one of these challenges: low spatial and temporal resolution of data collected, labour-intensive, high cost of operation (Klemas, 2015). For instance, based on good spatial coverage of aerial photographs, Jayson-Quashigah et al. (2019) stated that the process involved in obtaining

48

near-vertical aerial photographs could be quite costly due to the strenuous field preparation involved. Also, obtaining highly accurate GPS for monitoring beaches is said to be expensive. Satellite imagery is found to have wide spatial coverage, hence providing detailed spectral information, however it is affected by operational cost, the interference by dust and clouds which impedes pixel resolution and subsequent underestimation of sediment budget (Jayson-Quashigah et al., 2019; Whitehead et al., 2014). Furthermore, Boak and Turner (2005) indicated that LiDAR technology provides highly accurate and very dense elevation measurements but due to its costly nature, the availability is limited spatio-temporally.

Based on these challenges associated with conventional methods, routine monitoring of coastal systems in developing countries like Ghana is hindered (Appeaning Addo et al., 2018; Jayson-Quashigah et al., 2019). Overcoming these hindrances has brought about the profiling of beaches as well as 2D shoreline analysis, which are used for analysing the morphological dynamics of beaches as well as their sediment volume. Yoo and Oh (2016), suggests that beach volumes variability is not fully explained with the two approaches and could cause underestimation of volume changes, because areas between profiles are not accounted for.

In recent years, the Unmanned Aerial Vehicle – drone has become an alternative method for monitoring beaches (Adade et al., 2021; Appeaning Addo et al., 2018). This method is quite cheaper with high precision and accuracy in addition to providing high resolution images spatio-temporarily for generating DEMs (Appeaning Addo et al., 2018). Resolution of drone imagery could be as high as less than 10 cm, supporting detailed analysis of

49

morphological changes of beaches (Jayson-Quashigah et al., 2019). For instance, Abdul-Kareem et al. (2022) and Brempong et al. (2021) used the UAV to create DEMs for analysing sediment volume changes along selected communities on the eastern and western coastlines of Ghana. These DEMs were developed using the Agisoft Metashape software and analysed with ArcGIS and the Geomorphic Change Detection software (Wheaton et al., 2010). To sum up, several methods are available and more high precision methods for obtaining beach profiles and sediment volumes at lower cost are being made. UAV is a quite novel approach which is being adopted for use in Ghana due to the affordability and high precision results obtained from its usage, hence would be used in the present study.

2.7 Summary

This chapter provided reviews of information on climate, river processes, coastal processes, their interactions and how these processes are measured by the various authors.

50

CHAPTER THREE

MATERIALS AND METHODS

3.1 Overview

This chapter begins with a brief description of the coast of Ghana, including the major rivers flowing directly into the sea. It also describes the Pra River and delimits the study area (Anlo Beach). Additionally, the techniques for the collection, processing and analysis of data including sediment samples, river discharges, nearshore aerial photographs of the Anlo Beach, bathymetry and water levels obtained from the field surveys are explained below.

3.2 Study Area

3.2.1 Location and physical characteristics

The coastline of Ghana (Figure 3.1) is about 550 km long, having a series of large and small river basins discharging their water and sediment into the sea. It is divided into the western, central, and eastern zones (Boye et al., 2019), with each of them containing, at least, one of the largest rivers in Ghana – Ankobra (western), Pra (central) and Volta (eastern), which discharge into the Gulf of Guinea. In this study, the estuarine and adjacent coastlines of the Pra River (located within 5°00′N 1°37′W to 5°01′N 1°35′W) is of interest. This river was chosen because it is among the rivers in Ghana with the highest quantity of sediment discharge (Boye et al., 2019; Darby et al., 2020) into the Gulf of Guinea annually, making this river's contribution to coastline stability very significant.

51
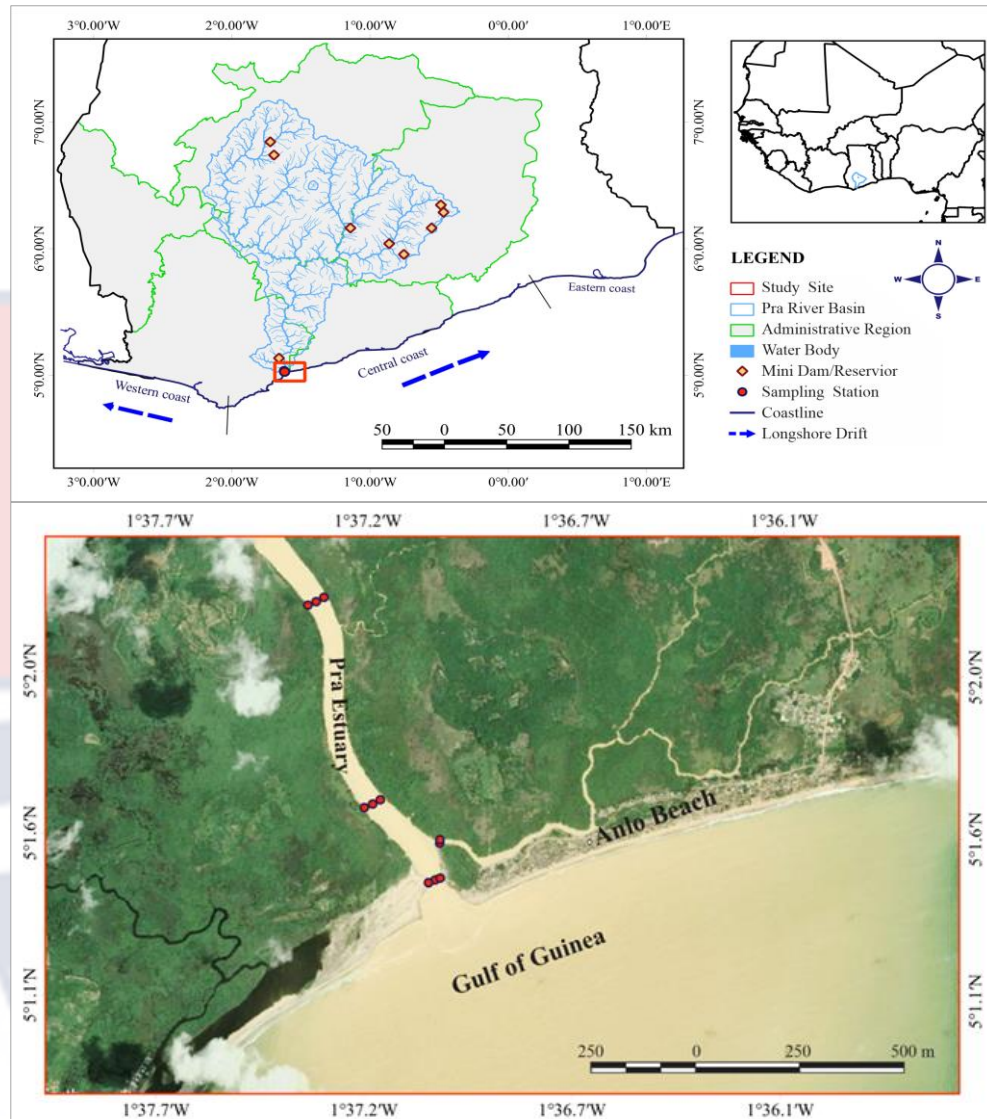
Figure 3.1: Study Area

The Pra River has a total catchment area of 23,200 km^2 with the Birim, Offin, Anum, and Oda rivers as its main tributaries (Awotwi et al., 2021; Kankam-Yeboah et al., 2013; Osei et al., 2021). Being the second largest river basin in Ghana, it takes its source of water from the Mampong-Kwahu plateau, flows downstream for approximately 240 km and discharge into the sea at Anlo Beach, close to Shama, in the Western region of Ghana (Awotwi et al., 2017; Awotwi et al., 2021; Boakye et al., 2021; Osei et al., 2021). It spans five

52

administrative regions in Ghana: North West, Western, Central, Ashanti and Eastern region (Figure 3.1). The catchment has a mean annual flow rate of about 214 m^3/s (Akrasi & Ansa-Asare, 2008). It has elevations ranging from -2 to 842 m, with the northern to the mid portion characterised by a few hills with wide river valleys while the southern is relatively flat (Awotwi et al., 2017). The catchment also contains the only natural meteorite lake called Bosomtwe (Bessah et al., 2020; Osei et al., 2021). The soil type of the Pra River catchment is predominantly alkaline Forest Ochrosols, formed from weathered Birrimian and Tarkwaian geological formations of schists, phyllites, granite and sandstone (Kusimi et al., 2014). Generally, the soils in the catchment are mostly clayey in nature and poorly leached, therefore, they are highly cohesive and are able to retain a lot of moisture (Kusimi et al., 2014). The forest type is moist semi-deciduous.

3.2.2 Climatic conditions

The catchment of the Pra River is within the sub-tropical wet climatic zone, where two rainfall seasons (May to July and September to November) occur and a dry season (between November and March) (Kusimi et al., 2016; Gyamfi et al., 2021). There is high relative humidity (about 70 % to 80 % on average) throughout the year and the mean temperature ranges between 26°C (August) and 30°C (March) (Boakye et al., 2021; Dorleku et al., 2019; Kusimi et al., 2014). Spatially, the pattern of precipitation rises from north to south of the catchment, having a mean precipitation of 1550 mm, and varying between 1200 mm to 1700 mm annually (Osei et al., 2021). Also, the air temperature reduces towards the southern portion of the catchment (Awotwi et al., 2021). At

53

the coastal side of the catchment, tidal pattern is semi-diurnal, having a mean range of ~0.96 m (Boateng, 2012). The longshore sediment drift on this coast is from west to east (Figure 3.1).

3.2.3 Socio-economic characteristics

The Pra River catchment has been severely altered because of agriculture, urbanisation, logging and mining due to its richness in economic tree species as well as minerals, respectively. This catchment has the highest density of both urban and rural settlement in Ghana (Awotwi et al., 2014; Gyamfi et al., 2021; Water Resources Commission, 2012). Nine reservoirs/ mini dams including the Brimsu Dam, Owabi Dam and the Barekese Dam have been built on rivers in the catchment for industrial as well as domestic purposes (Awotwi et al., 2021; Boakye et al., 2021; Gyamfi et al., 2021; Kusimi et al., 2016; Water Resources Commission, 2012).

Most parts of the catchment, especially the mid to southern parts are heavily exploited by large-scale gold mining companies such as Perseus Mining (Ghana) Limited, Newmont Ghana Gold Limited, AngloGold Ashanti (Ghana) Limited, among many others (Water Resources Commission, 2012). Aside these large-scale mining companies, there are thousands of small-scale miners who operate illegally in the catchment. The mid to the southern section has wider channels which is mainly occupied by alluvial gold miners who mine either in the river banks or within the bed of the river. At the northern portion of the catchment, these illegal miners are restricted to the banks of the rivers as a result of the smaller width of the river (Kusimi et al., 2014).

Due to its favourable environment for agricultural activities, over 63 % of the inhabitants in the catchment engage in farming as their main occupation on a small or large scale (Water Resources Commission, 2012). Growing of cocoa on large scale is a characteristic of the farmers in this basin, accounting for more than 70 % of household income through exportation as an agricultural product. This catchment alone contributed about 8.2 % to the Agriculture GDP of Ghana in the year 2010 (Water Resources Commission, 2012). On a smaller scale, farmers in the catchment engage in the cultivation of food crops such as plantain, maize, cassava and other tuber crops (Awotwi et al., 2021; Bessah et al., 2020).

At the south-eastern side of mouth of the Pra River is situated the Anlo Beach community in the Western Region of Ghana. It has a population of 4500 and forms part of the Shama District (Dada et al., 2022). This community is bordered to the north by a small tributary of the Pra River and a mangrove wetland and to the south by the Atlantic Ocean. Common economic activities in this area include fishing (31%) and trading (Asiedu, 2019; Dada et al., 2022).

3.3 Data Collection

A reconnaissance survey was undertaken in April 2022 to obtain a general knowledge of the study area. The data for this study were taken bi-monthly over a period of five (5) months, specifically in May, July and September, 2022, with the exception of shoreline data which included October, 2022, making six months for the shoreline study. This period was used for data collection because of the high amount of rainfall and its associated increase in sediment-filled runoffs which end up in rivers, and subsequently into the coastal

55

area (Kusimi et al., 2016). The data gathered for this work include suspended sediment load, bedload, flow velocity, estuarine bathymetry, water levels, and aerial photographs of the shoreline.

3.3.1 Sediment sampling

The sediment sampling was primarily undertaken to quantify how much sediment are being transported to the Anlo Beach. It was also to identify the bedload characteristics in order to assess their relevance for building up the beach. The bedload and suspended load samples were taken approximately 100 m way from the mouth to about 1.6 km inland. Three cross-sections were created: 100 m, 600 m and 1.6 km inland (Figure 3.1), using a systematic sampling approach. These cross-sections were then divided into three stations (Boakye et al., 2021) each, where both suspended and bedload were sampled from. In addition, a nearby tributary located approximately 250 m from the river's mouth was sampled – one cross-section with two stations, about 50 metres off the confluence of the tributary. In total, eleven (11) stations were sampled for both the bedload and suspended load. The cross-sectional profile and the sample stations help in accounting for the variation in sediment concentration across the various sections (areas closer to the banks and the middle portion) of the estuary (Boakye et al., 2021). The samples from the tributary were to determine the quantity of sediment which is transported into the main Pra River.

3.3.2 Suspended load sampling

To obtain the suspended sediment concentration at each cross-section, a Depth-integrated sampler (US DH-48) which has been designed by the USGS Federal Interagency Sedimentation Project (FISP) (Davis, 2005) to sample suspended sediment at a rate proportional to the velocity of the river flow was used to sample the sediment in suspension (Figure 3.2, Figure 3.3) (Boakye et al., 2021; Cantalice et al., 2015; Kusimi et al., 2014; Logah et al., 2017; Ofori et al., 2016). The depth-integrated sampler consists of moulded aluminium metal of about 2.04 kg, with a handle attached to it, and a sampling bottle (pint glass milk bottle) with an orifice, which is calibrated with a nozzle of 6.35 mm in diameter (Edwards & Glysson, 1999).

Figure 3.2: Suspended sediment sampling with a depth-integrated sampler

The sampler was slowly dipped into the bottom of the water column, and then raised to ensure that the water fetched constitutes samples from all layers of the water column (Leeks, 2005; Sulaiman et al., 2021). An up and down motion at a constant speed was ensued until the sampler was about 90 % full. The 90 % capacity was to ensure that there was no biasness while lifting

57

the sampler from the water column, since there will be no sampling if the bottle is full before pulled out (Ongley, 1996). The samples were then transferred into transparent plastic containers, labelled and transported to the lab for processing and analysis.

3.3.1.2 Bedload sampling

The bedload was sampled using the US BH-84 bedload sampler. This sampler has been designed by the USGS Federal Interagency Sedimentation Project (FISP) (Davis, 2005) for sampling sediment that is transported by the river on or immediately above its bed. This sampler is made up of a metal orifice (760 mm), with a sampling mesh (size: 0.2 mm) attached to it (Gray et al., 2010). The sampler was gently placed on the bed of the river at each sampling station for a period of 1 minute. The direction of the orifice was placed against the moving current and moving bedload was trapped into the net. The sampled sediments were then transferred into labelled plastic containers, sealed and transported to the lab for processing and analysis (Cantalice et al., 2015). Figure 3.3 gives a pictorial view of the sampling of bedload and suspended load.
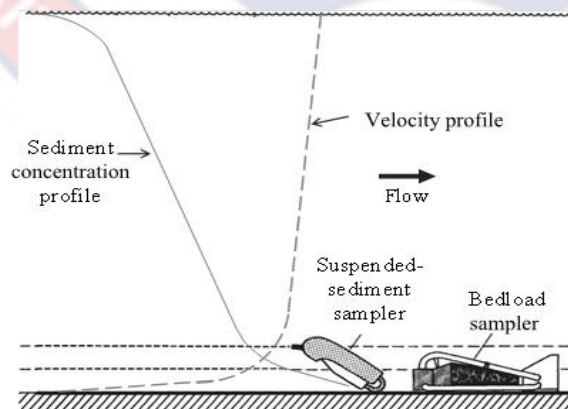
Figure 3.3: A schematic diagram of bedload and suspended load measurement
Source: Dingman (2009)

58

3.3.2 Flow velocity

The flow velocity of a river is used in addition to the river depth and width to calculate the river discharge. To achieve this measurement, flow meter, which is made up of an electronic device, connected to a propeller (mounted on a pole), and a heavy-weight metal called Messenger for keeping the bottom of the propeller stable in the water column was used. This device measures the frequency with which the propeller rotates in the water column (Cantalice et al., 2015). The Valeport current meter was gently dropped into the water column for a period of one 30 s. On each cross-section (as used for sediment sampling), the Equal-Width-Increment method was adopted to measure the flow velocities at each point, sampling between four (4) and seven (7) stations (Ofori et al., 2016). The number of velocities taken varied based on the width of each river cross-section (Boakye et al., 2021).

3.3.3 River depth

The measurements of river depth were to aid in computing river discharges and obtain the bathymetry of the riverbed. The resultant bathymetry would then provide the rate of sedimentation/deposition and erosion of the channel. To achieve this, the MIDAS Surveyor GPS Echosounder was used to randomly sample various portions of the riverbed for depth acquisition. The echosounder is a specialised device with inbuilt GPS for measuring the depth of a water column, while taking the coordinates. It also provides the date and time of data collection. This device records depths by sending a pulse through the water column and measures the elapsed time for the signal generated from the

59

transducer to hit the bottom and reflect back (Figure 3.4). The depth (D) is then mathematically expressed as:

$$D = \frac{1}{2}(v * t) + k + d_r \qquad\qquad (1)$$

Where v is the mean velocity of the sound in water; t is the time from the transducer to the bottom of the water column and back; k is the system index constant and d_r is the distance from the reference water surface to transducer (Arseni et al., 2016). The echosounder was mounted on a boat and the transducer was placed 0.5 m (d_r) below the water surface. Traverse on the river was in a jag form with a longitudinal since the width of the river is not large (Figure 3.5).
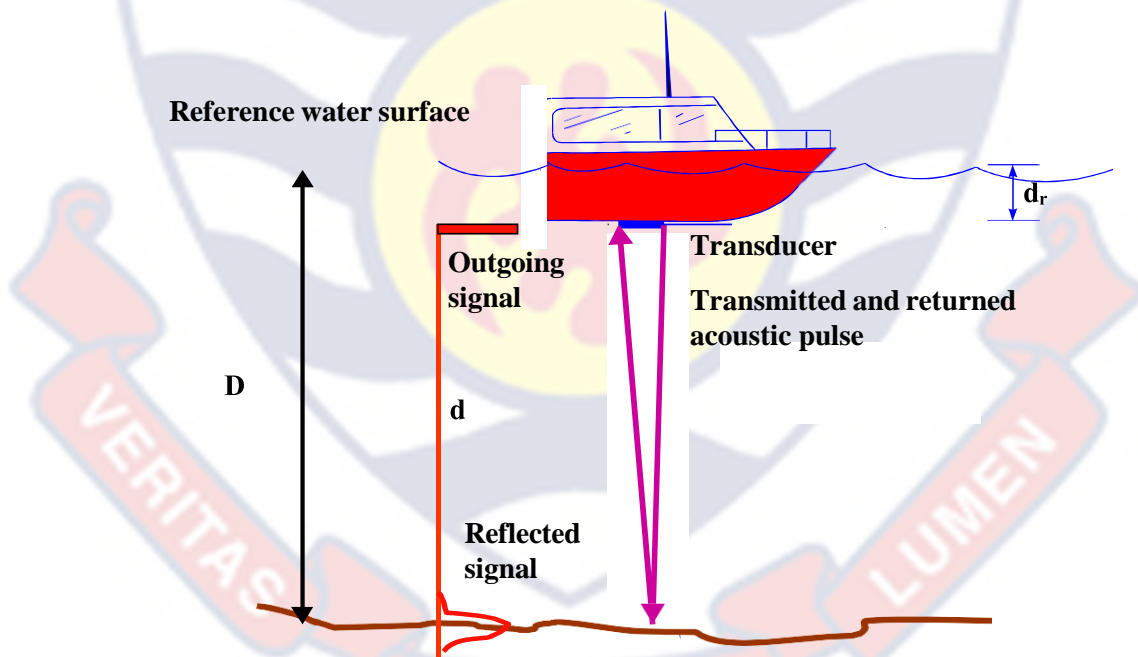
Figure 3.4: Mechanism for obtaining depth measurement from a single beam echo sounder, mounted on a moving boat. Source: Bergen (2002)

Figure 3.5: Depth measurement across the Pra Estuary

3.3.4 Water levels

A pressure sensor was logged at a frequency of 10 minutes to measure the water temperature, pressure, the water level, date and time using the HOBOware Pro software. The 10 minutes frequency was used because the recording was for a short period, therefore high temporal resolution was key. The water level checker was attached to a rope and tied to a heavy stationary object to prevent the device from floating away. The device was then gently placed inside the water column in the morning, before the collection of other parameters began and removed after completing the collection of all datasets for that particular day.

3.3.5 Shoreline data acquisition

Aerial photographs of the Anlo Beach and the nearshore were taken to process and obtain shoreline position of the various months for the study period. These images were acquired using a UAV – DJI Phantom 4 Pro drone. This

61

UAV contains an in-built camera with a high resolution of 12.4 Megapixel and a smart battery power of 6000 mAh to allow for a flight of not less than 20 minutes. The images from the UAV were as much as possible, captured to coincide with low tide for the entire study period to reduce the influence of tide on shoreline positions (Angnuureng et al., 2019; Angnuureng et al., 2020a; Angnuureng et al., 2022; Jayson-Quashigah et al., 2019).

To ensure precise georeferencing of aerial images, the establishment of GCPs are important (Angnuureng et al., 2019). Therefore, fourteen (14) clearly marked concrete pillars were mounted permanently on the Anlo Beach. These pillars were randomly distributed on the beach due to limited open space availability and to avoid washing away of the pillars if mounted close to the shore (Figure 3.7). Although at least four GCPs are needed for georeferencing (Crowell et al., 1991), the fourteen pillars were installed to ensure high precision. These pillars were coordinated to the national grid (Ghana Meter Grid) using a static Differential GPS (D-GPS) (Figure 3.6) (Angnuureng et al., 2022; Jayson-Quashigah et al., 2019). Each GCP was observed for 40 minutes on the average to lessen the Root Mean Square Error (RMSE) (Figure 3.6). The Topcon post-processing software was used in processing the data from the D-GPS (Jayson-Quashigah et al., 2019).

Figure 3.6: GCPs establishment at Anlo Beach
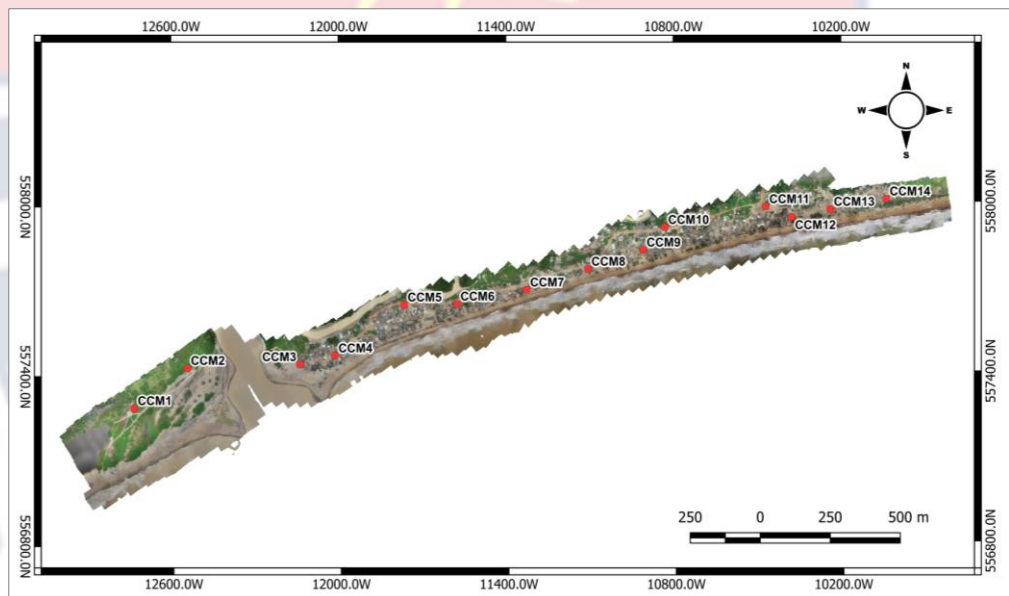
Figure 3.7: GCPs location on Anlo Beach

The Drone Deploy software was used to pre plan flight missions (Figure 3.8), while ensuring that images to be captured by the drone overlap. Hence, the flight path was set to lateral and longitudinal, allowing for 3D reconstruction of the terrain. The drone images were taken at a height of 70 m to ensure that a wider area is captured while taking into consideration the image resolution for sediment budget estimation to reduce associated errors (Abdul-Kareem et al.,

63

2022; Angnuureng et al., 2022b; Brempong et al., 2021; Jayson-Quashigah et al., 2019).
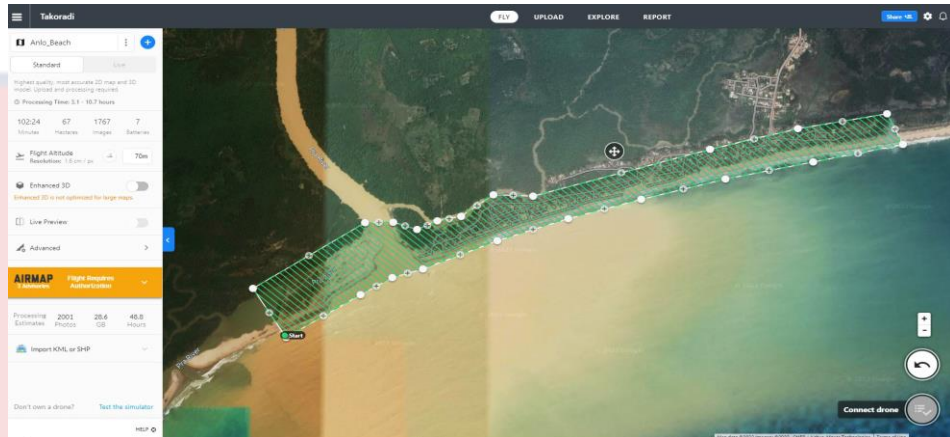
Figure 3.8: Flight plan of the drone

3.4 Data Processing and Analysis

3.4.1 Aerial photographs processing

On the average, 1150 images were captured along the ~3.5 km of beach during each flight time. These images were filtered manually in order to avoid error in the point cloud due to the processing of blurred or overexposed ones (Angnuureng et al., 2020a; Jayson-Quashigah et al., 2019). The Agisoft Metashape software was used to post-process the images (Agisoft, 2019). This software was used because of its user-friendly interface (straightforward) as well as the ultra-modern procedures involved, making it the best option for a quick and very effective tool for remotely sensed data processing (Mancini et al., 2013). In the Agisoft Metashape software, a 3D surface was reconstructed using the Structure from Motion (SfM) and Multi-View Stereo (MVS) algorithms (Snavely, 2011; Westoby, 2012) implemented. Basically, the processing of the images involves four stages, namely: 1. Alignment of images;

64

2. Pixel-based dense stereo reconstruction with the GCPs and the aligned images; 3. DEM building; 4. Orthomosaic building projected on the built DEM surface (Agisoft, 2019). The Orthophotos and DEMs built were exported in GeoTIFF format and transferred to the ArcGIS, QGIS and GCD software, for further processing. Before exporting the DEMs, areas of the beach with fishing boats, coconut trees and other objects which may exaggerate topographic heights were as much as possible, eliminated (Angnuureng et al., 2022a). All images had approximately 1.87 cm/pix average spatial resolution.

3.4.2 Shoreline change analysis

To obtain the shoreline position for each month, the water-land boundary from the orthophotos were identified and manually digitised in the ArcMap software using the High Water line (HWL) as the proxy (Boak & Turner, 2005; Crowell et al., 1991). This proxy was used to ensure a consistency with what has often been used in Ghana (Abdul-Kareem et al., 2022; Angnuureng et al., 2020a; Angnuureng et al., 2022a; Angnuureng et al., 2022b; Appeaning Addo et al., 2008; Jayson-Quashigah et al., 2019; Jonah et al., 2016; Wiafe et al., 2013).

DSAS 5.0, an extension of ArcMAP was used to compute shoreline changes. The software was used because it contains several statistical approaches for shoreline change estimation. The shorelines were imported using a defined features class into a personal geodatabase as a DSAS requirement. In addition, a baseline was constructed about 30 m onshore off the closest shoreline through manual digitisation (Himmelstoss et al., 2009). Object ID, SHAPE_Length (alias: Shape_Length), SHAPE (alias: Shape) were attributed

65

to the baseline automatically, while the DSAS_ID column was indicated with 9. A total of 1636 transects were casted with 2 m intervals (to ensure that small-scale spatial changes are captured) at simple right angles from the baseline to the farthest shoreline position. This was done by setting transects to clip the farthest shoreline position.

For this study, the Net Shoreline Movement (NSM) was used for shoreline change analysis. The NSM was used to determine the net extent of shoreline location between the oldest and current shoreline, since this study is short-term (Abdul-Kareem et al., 2022). A summary of the drone workflow has been presented in (Figure 3.9).
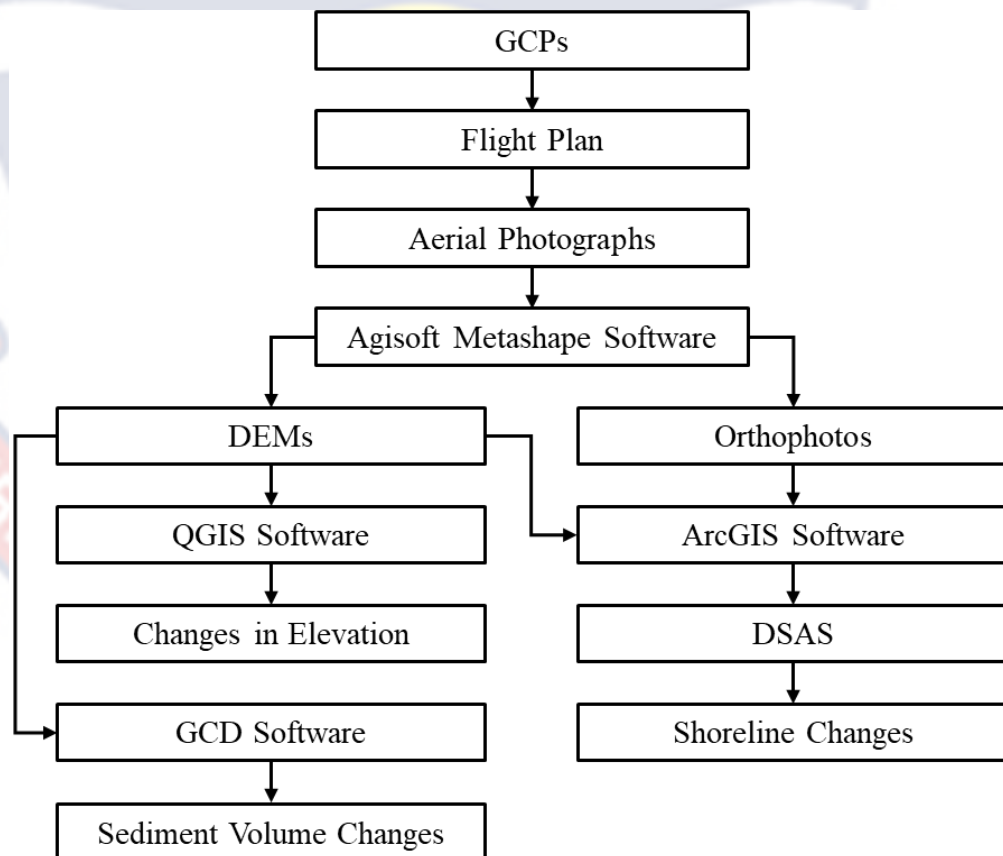
Figure 3.9: Summary of drone workflow

3.4.3 Quantification of uncertainty for shoreline data analysis

In this study, uncertainties associated with the shoreline change estimation were quantified based on Crowell et al. (1991), Hapke et al. (2011) and Moore (2000). Other errors related to the UAV imagery were included in the study. The principal sources of error were digitisation of the HWL position, resolution variations in imagery used and the tidal range. The total shoreline positional error for each epoch (Ex) was then computed with the formula:

$$E_X = \sqrt{E_d^2 + E_p^2 + E_t^2} \qquad (2)$$

where E_d is the digitising error E_p is the photogrammetric error and E_t is the tidal error. This method assumes the individual errors to be normally distributed (Dar and Dar, 2009). The total uncertainties were subsequently included in the shoreline change computation as weights for error estimation of shoreline change at any given transect. This was expressed as:

$$E_a = \sqrt{E_m^2 + E_j^2 + E_s^2 + E_o^2} \qquad (3)$$

where E_m, E_j, E_s and E_o are the total shoreline positional error for the various months – May, July, September and October 2022, respectively.

3.4.4 Geomorphic change detection

In order to identify the extent of sediment lost or gained for the study period, the GCD standalone software was used to investigate the beach budget estimation and morphological changes using a standard DEM of difference (DoD) (Wheaton et al., 2010). The DEM of difference (ΔDEM) was computed by subtracting the older DEM from the new DEM: this is given by the formula:

$$\Delta\text{DEM} = Z_2 - Z_1 \qquad (4)$$

67

where Z_2 is the new DEM and Z_1 is the old DEM. The individual total RSME obtained through the processsing of the image was used for uncertainty of each DEM. Hence, the total RMSEs for the DEMs was computed with the formula:

$$\delta u = \sqrt{\delta z_1^2 + \delta z_2^2} \qquad\qquad (5)$$

where δu is the propagated error, δz_1 and δz_2 are the errors from the deicidal DEMs. The error propagated was used as the minimum level of detection threshold to ensure that the actual surface changes is differentiated from the intrinsic noise associated with the DEM (Wheaton et al., 2010).

3.4.5 Tide level estimation from pressure sensor

After retrieval of the pressure sensor from the water, the HOBOware Pro software was used to extract the data in a spreadsheet form. In Microsoft Excel, an average of the water levels was obtained by dividing the data points by the total number of water levels recorded. This was used as a reference surface for the bathymetry mapping (Blair, 1983). The water level was used as surface reference because the estuarine region is influenced by the fluctuating water levels due to tidal changes.

3.4.6 River bathymetry

The depth recorded by the echosounder was displayed on the SurveyLog software and extracted in ASCII format (Valeport, 2020). The data was subsequently converted to CSV file in Microsoft Excel 2016, cleaned by manually removing outliers. In addition, the data was corrected by adding the draft value of 0.5 m and imported to ArcMap 10.5. In ArcMap, the CSV file

was converted to a vector Shapefile for further processing (Parente & Vallario, 2019).

First, the natural neighbour interpolation (NTN) method available in "Spatial Analyst" extension was applied to the data to obtain the Digital Elevation Model (DEM). The NTN algorithm uses a weighted average of the nearby data points with the weights being proportional to the points used for the interpolated area (Parente & Vallario, 2019). According to EL-Hattab (2014), no extrapolation is done for areas beyond the convex hull of the neighbouring points when the NTN is applied. Therefore, the Ordinary Kriging (OK) and IDW interpolation methods under the Geospatial Analyst extension was applied after the NTN to cover (extrapolate) areas farther from the data points' threshold (Batista et al., 2017; Parente & Vallario, 2019). These interpolation methods were selected for analysis due to the usage by several authors as well as the high performance associated with them (Batista et al., 2017; Curtarelli et al., 2015; EL-Hattab, 2014; Parente & Vallario, 2019).

To access the performance of the OK and IDW for the interpolated areas, a cross-validation of the predicted values was done to obtain the RMSE, absolute mean, mean, maximum and minimum errors. The RMSE explains the extent of deviation of interpolated values from the actual ones. The underlying assumption is that the errors occurring in the data are random, having a mean of 0 and distributed normally about the mean. Mathematically, the RMSE was expressed as

$$RMSE = \sqrt{\frac{\sum_{i=1}^{N}(Z_i(x,y) - Z\prime_i(x,y))^2}{N}} \qquad (6)$$

69

Where: N is the number of the depth points; Z_i (x,y) is the measured depth at the location i(x,y); Z'_i (x,y) is the interpolated depth at the same location i(x,y) (EL-Hattab, 2014; Parente & Vallario, 2019).

To obtain the changes in river depth for the various months, the older DEM was subtracted from the newer DEM. A mathematical expression is given at Equation (4).

3.4.7 River flow rate

After obtaining the river velocities, the formula, $Q = VA_t$ (7) was used to compute the river flow rate/discharge, where Q is the river discharge in m^3/s, V is the river mean velocity and A_t is the cross-sectional area. The total cross-sectional area was computed by first obtaining the area between two sampling points (A_1). This is given by the formula:

$$A_1 = \frac{1}{2}(d_0 + d_1)w_1 \tag{8}$$

where d_0 and d_1 are the depth values of cross-section; w is the distance between the d_0 and d_1. The total cross-sectional area was then calculated by summing all the area between sampling points (Boakye et al., 2021).

3.4.8 Sediment discharge

The sediment samples (Figure 3.10) were kept undisturbed for at least two weeks to ensure settling and coagulation of sediment at the bottom of the containers. The samples were weighed using an electronic scale, the water on top of the samples was poured off, and the sediment was transferred into aluminium foil containers (pre-weighed). The evaporation method (Boakye et al. 2021; Kusimi, 2014; Kusimi et al., 2014; Ofori et al., 2016) was adopted by

drying the sediment samples in an oven at a temperature of 105 °C for 72 hours to ensure that samples got fully dried within these hours, since the samples contained large quantities of water. The samples were allowed to cool down in a desiccator, and the dry mass was obtained. The weight of the containers used for both the water-sediment mixture and the dry mass were deducted to obtain the actual weight of each sample, before and after drying.

To obtain the suspended sediment discharge, the suspended sediment concentration was first obtained by dividing the mass of samples after drying by the mass before drying and this was multiplied by one million (1,000,000) to convert it to parts per million (PPM), thereby obtaining the milligram per litre of (mg/l) of each sample. The suspended sediment discharge in tons/day (SSQ) was then computed using the instantaneous concentration and flow equation:

$$SSQ = 0.0864 \sum SSC_i\, Q \qquad\qquad (9)$$

where, SSC_i: suspended sediment concentration in each vertical of a cross-section; Q is the flow rate/discharge; and 0.0864 is a constant for unit adjustment (Cantalice et al., 2015; Boakye et al., 2021).

The bedload discharge in tons/day (QB) was computed using the equation:

$$QB = 0.0864 \sum \frac{m}{wt_2} L_x \qquad\qquad (10)$$

where, m: mass of sediment from bedload transport; w: width of sampler's orifice 0.075 m; t_2: sampling time of bedload transport, and L_x: distance between sampling points (m) (Cantalice et al., 2015). The total sediment discharge in tons/day was obtained by summing up the suspended load and bedload discharge.

Figure 3.10: Some sediment samples obtained from the Pra Estuary

3.4.9 Sediment particle size analysis

To determine the type of sediment that is being transported by the Pra River, the dry sieving method of analysis was used to group the sediment into various sizes. The ADAM tabletop scale (HCB602H) was used to weigh 100 g each of the dried bedload samples. These were sieved through the US-Tyler sieves 4000, 2000, 1000, 500, 250, 125, 63 μm and a base pan (Faseyi, 2022) (Figure 3.11) for 5 minutes. In cases where the dried bedload was less than 100 g, the total mass of the sample was used for the analysis. The weight of particles retained on each sieve was recorded and expressed in percentage of the gross weight measured (Boye, 2015). The percentage of particles, which passed a particular sieve, was expressed as:

$$P\% = \frac{m_i}{m_t} \tag{11}$$

Where, m_i is the weight of particles passing through a sieve size and m_t is the gross weight of sample sieved. The percentage of particles passing through each sieve was plotted against a log-transformed gradation curve (Al-Ansari, 2015; Boye, 2015; Diplas et al., 2008). The particle sizes were then classified using

72

Blott and Pye (2012) classification system. The statistical analysis was done by computing the mean and median grain sizes using the weight of particles and the particle sizes.

Figure 3.11: Sieving of sediment samples for particle size analysis

3.5 Summary

The Pra River Catchment with focus on the coastal frontage (~3.5 km alongshore) and 1.6 km inland of the estuarine region was selected for the study. A period of six months was used to collect data (May – October, 2022). Variables such as river depths, water levels, suspended sediment, bedload, river velocities, and aerials photographs were collected for each survey. After obtaining the data, these variables were processed and analysed using software like Microsoft Excel and ArcMap to obtain results, including river bathymetry and shoreline changes, bathymetry maps, river discharges, bedload, suspended load discharges and particle size distribution.

73

CHAPTER FOUR

RESULTS

4.1 Overview

This chapter provides results obtained from the analysis of river velocities, river depths, bedload, suspended load, water levels, aerial photographs. The results presented here include riverine sediment load and water discharges, particle size distribution of the Pra Estuary, shoreline changes, beach sediment volume dynamics, and bathymetry changes of the Pra Estuary.

4.2 Riverine Sediment Load and Water Discharges

Results observed from suspended sediment concentration (Figure 4.1) shows that averagely, the SSC of May was 1374.66 mg/L, in July it was 1628.91 mg/L and in September it increased further to 2367.58 mg/L. The highest average SSC recorded for this study occurred ~ 600 m from the river mouth in September (2728.52 mg/L), at a discharge of 138.19 m^3/s. The lowest SSC was also recorded ~ 100 m from the river mouth in May (1060.07 mg/L) of a discharge of 15.96 m^3/s (Figure 4.1). It is interesting to note that the smaller tributary, recorded relatively high SSC for all months, although all corresponding discharges were less than 4 m^3/s. A Spearman correlation (r_s = 0.32, p = 0.613) revealed a very weak and non-significant relationship between river discharge and suspended sediment concentrations in the Pra estuary. This means that these high suspended sediment concentrations are not influenced by the discharges. Overall, the average SSC for the Pra estuary was 1757.18 mg/L.

74
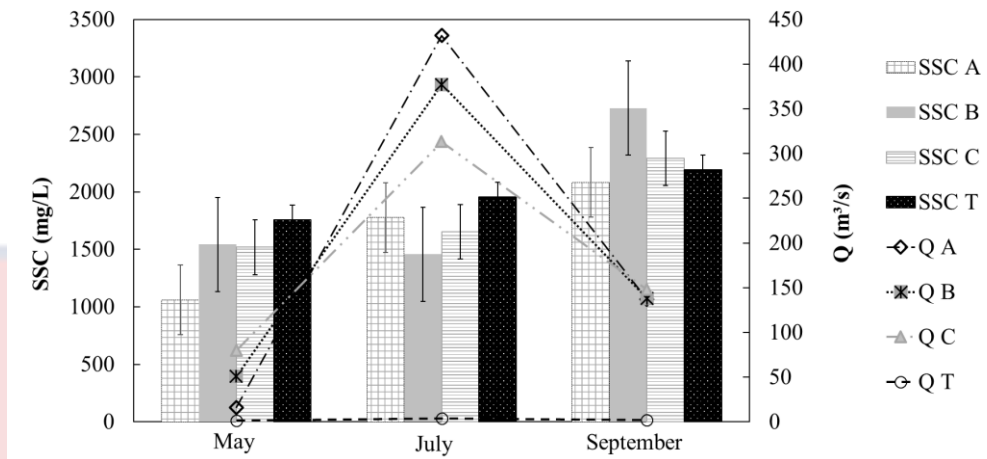
Figure 4.1: Suspended sediment concentrations (SSC) and river discharges (Q) of the various cross-sections
(A: 100 m from river mouth; B 600 m from river mouth; C: 1.6 km from river mouth; T: Tributary, 250 m from river mouth)

After obtaining the results for the three (3) cross-sections, an average for each month was computed to represent the river sediment and water discharge to the sea. The result (Figure 4.2) shows that July recorded the highest discharge of 374.20 m^3/s and sediment discharge of 9235.33 tons/day from the Pra River to the sea. May recorded the least water and sediment discharge of 48.83 m^3/s and 1148.65 tons/day, respectively. In addition, the average daily discharge for the Pra River was computed to be 188 m^3/s and the average total sediment discharge was 4537.03 tons/day.
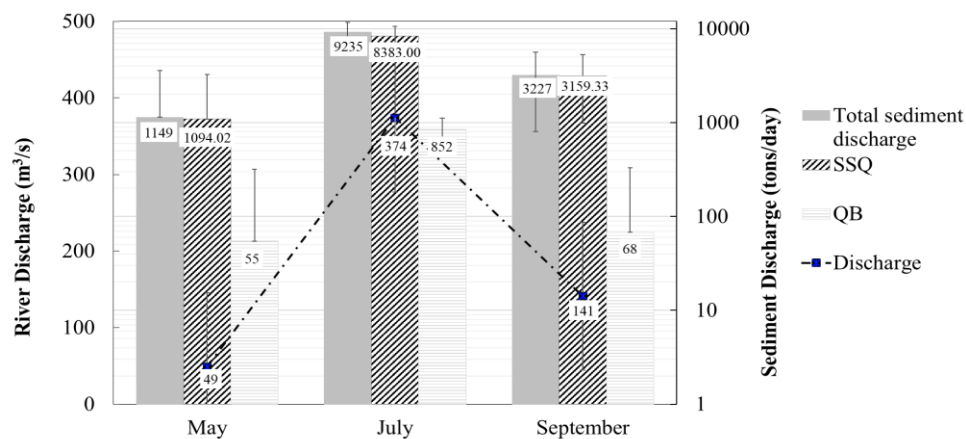
Figure 4.2: Average monthly dynamics of the river discharges and total sediment discharges

Regarding the ratio of suspended sediment to bedload discharged in the Pra Estuary, the highest average percentage of bedload for each month was 6.66 % in May, 8.68 % in July, and 2.12 % in September. However, on a cross-sectional basis, areas which were ~100 m from the river mouth obtain the highest average percentage of bedload discharge (9.27 %), followed by areas ~ 600 m from the mouth (5.16 %) and lastly, those which are 1.6 km from the mouth (3.03 %). It was also noted that the tributary which is ~ 250 m from the mouth of the river recorded 10.38 % of bedload discharge. In general, the average percentage of bedload discharged was 5.82 %.

4.3 Sediment Particle Size Distribution

Figure 4.3 (A) shows that bedload materials transported in May and July were ≥ 0.25 mm in size. However, in September, they were much finer, with about 40 % and 10 % being finer than 0.25 and 0.125 mm, respectively. The tributary (Figure 4.3 T) had similar patterns of particle sizes in May and July, with about ~75 % being 0.25 mm in size. Yet, this pattern changed in September, resembling areas which are ~ 600 m and ~ 1.6 km from the river

mouth (Figure 4.3 B; C). For areas which are ~ 600 m and ~ 1.6 km from the river mouth about 70 % of the sediments were finer than 0.063 mm in May. In July, coarser particles of 0.5 mm occurred in these same areas; nonetheless, more particles (80 %) were finer than 0.063 mm.

In general, particles were coarser in areas close to the mouth (Figure 4.3 A; T), and decrease in sizes farther inland (Figure 4.3 B; C). Overall, sediment particle sizes were observed to be finer for September. The mean and median particle of each area is presented in Table 4.1.
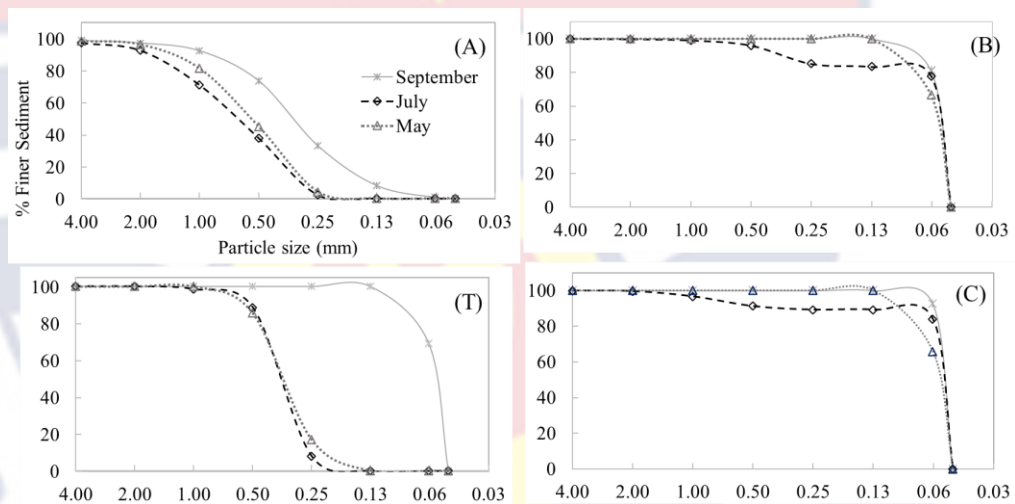
Figure 4.3: Sediment particle size distribution of the sampled cross-sections

Table 4.1: Mean and median particle sizes of bed sediment transported in the various sampled cross-sections

Section	Mean (mm)	Median (mm)
A	0.302	0.487
B	0.054	0.063
C	0.054	0.058
A to C	0.100	0.062
T	0.182	0.292

The median particle size obtained for the Pra Estuary (Table 4.1), implies that 50 % of the sediments were less than 0.062 mm. Upon classifying the particle sizes based on the Blott and Pye (2012), it was revealed that about 52.1 % were silt (< 0.063 mm), 47.3 % were sand (< 4 mm ≥ 0.063 mm) and only 0.6 % were gravels (≥ 4 mm) (Figure 4.4).

Based on the observation that the percentage of bedload transport to sea was very small for Sections father than 600 m from the mouth but relatively higher for areas 100 m from the mouth and the tributary, it was necessary to assess its relationship with the associated mean particle sizes. Both variables were not normally distributed after testing for normality with Q-Q Plot, therefore the Spearman correlation was used. Spearman correlation (r_s = 0.76, p = 0.004) suggests a very strong significant positive correlation between the percentage of bedload discharged and the mean particle size of the sediment.
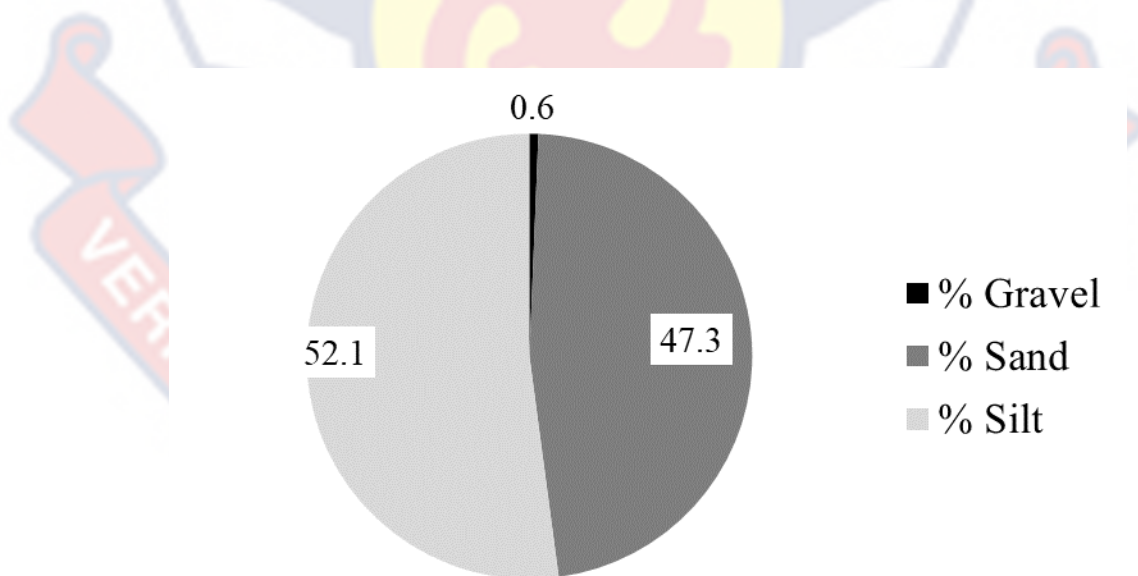
Figure 4.4: Classification of bedload material based on Blott and Pye (2012)

4.4 Beach Topography Dynamics

The resolution of DEMs obtained from the drone data processing was quite high, ranging between 0.037 m and 0.076 m. Six transects, namely I, II, III, IV, V, VI were casted from the back beach to the foreshore to obtain the profiles of the beach (Figure 4.5).
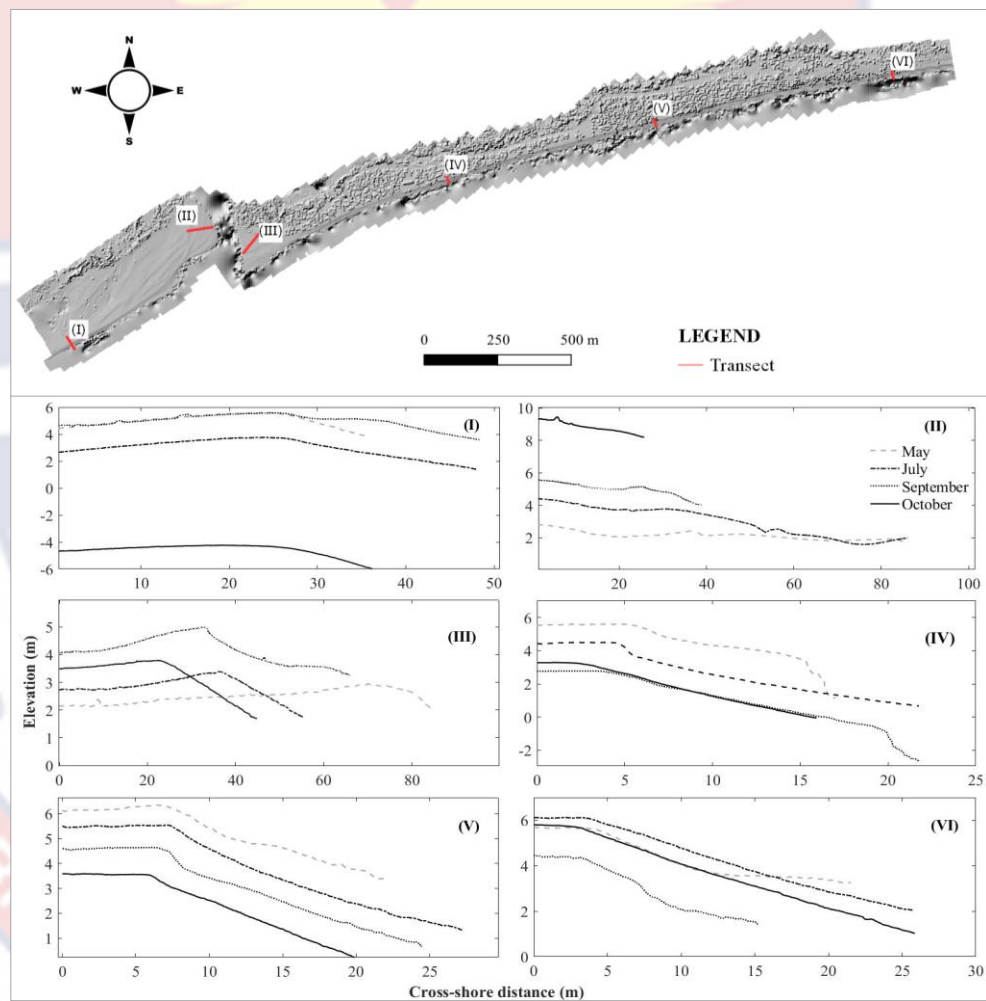
Figure 4.5: Beach profiles variations on six selected transects on Anlo Beach

The average beach slope for entire study period was 0.13 signifying a steep slope. The mean beach slope for the individual months were 0.11 (May), 0.12 (July), 0.16 (September) and 0.14 (October). All the beach profiles depict

79

that the Anlo Beach is a low-lying area with even the peak elevation being 8 m high and it occurred at the river mouth in October. Most of the areas are less than 6 m high. In addition, trend in the beach profiles shows that erosion and accretion on the beach occurs at both the foreshore and backshore. It could be seen from Figure 4.5 that cross-shore distances of the Anlo Beach, aside the mouth is generally less than 50 m, signifying a very narrow beach. Shorter cross-shore distances represent areas covered by sea water at the time of image capture.

The profiles I and II located on the western side of the river mouth is generally gently sloping while profiles III, IV, V and VI on the eastern side are relatively steeper. On profile I, beach height loss of about 2 m in July was built back in September. However, in October, a larger margin of beach height (9 m) loss occurred. On profile II, there was a continuous increase in the height of the back beach, however, the beach face reduced in width from about 86 m in May and July to 26 m in October, suggesting a widening of the river mouth. On profile III, about 30 m of the beach width was lost in July while the back beach accreted from 2.2 m to 4 m in September, however 0.6 m of beach height got eroded in October. Generally, shorter cross-shore distances occurred on profiles IV, V and VI, having the longest width of 27 m, occurring in July on profile V and the shortest width (15 m) occurring on profile VI in September (Figure 4.5).

4.5 Beach Sediment Volume Dynamics

The computed sediment budget of the Anlo Beach shows that sediment loss is dominant over the six months period, with a net sediment loss of approximately -105,695.72 m^3 from May to October 2022 and -25 % imbalance

in erosion-accretion equilibrium (Table 4.2). The ratio of area erosion to accretion (Figure 4.6) shows that between May and July 60 % of the beach lost sediments. However, 61 % of the area accreted between July and September, to augment the deficit. Yet, from September to October, 69 % of the beach experienced sediment loss. Overall, 75 % of the beach eroded between May to October. This is portrayed by Figure 4.7 which shows the altimetric changes of the Anlo Beach. It could also be realised that the spatial distribution of sediment dynamics depicts an eastward drift (Figure 4.7).

Table 4.2: Sediment volume changes on the Anlo Beach

Attribute	2022			
	May to July	**July to September**	**September to October**	**May to October**
Erosion (m³)	-41,964	-119,282.01	- 277,359	-160,639.10
	(± 3,497)	(± 1,325.58)	(± 1,112.29)	(± 221.55)
Average depth of erosion (m)	1.27 (± 0.11)	7.46 (± 0.08)	6.28 (± 0.08)	3.60 (± 0.11)
Deposition (m³)	26,758	180,431.35	125,322.61	54,943.390
	(± 2,775)	(± 3,766.88)	(± 1,509)	(± 1,787.43)
Average depth of deposition (m)	1.02 (± 0.11)	3.97 (± 0.08)	6.95 (±0.08)	3.28 (± 0.11)
Net volume change (m³)	-15,309	61,149.34	- 152,036.17	-105,695.72
	(± 4,465)	(± 3,993.32)	(±1,122.37)	(± 5,086.24)
% Imbalance	-11 %	10 %	-19 %	-25 %
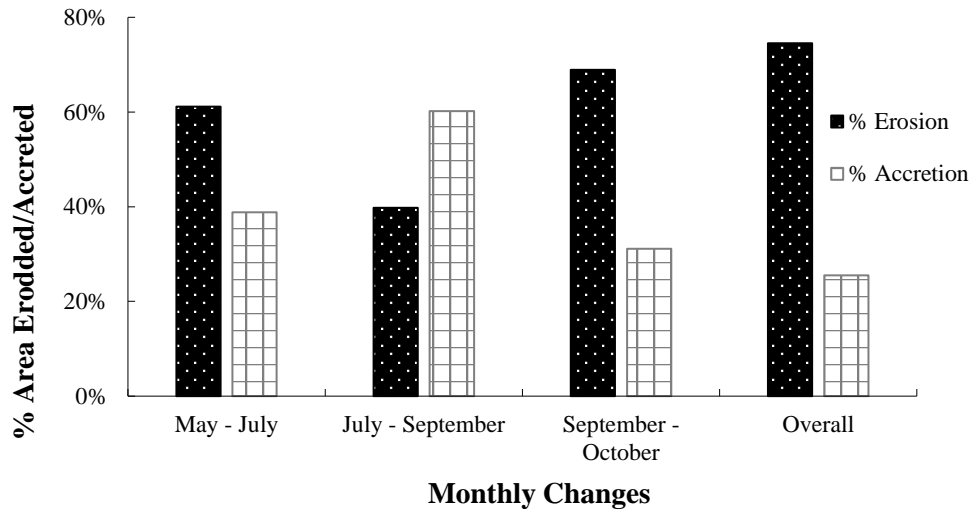
Figure 4.6: Ratio of beach sediment erosion and accretion in the various months studied
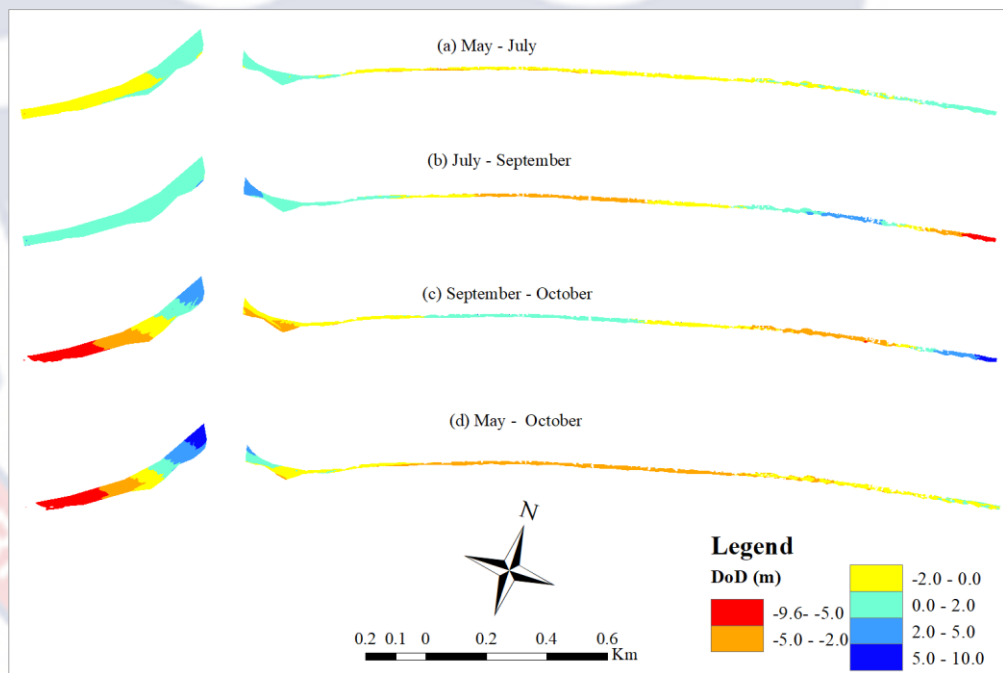
Figure 4.7: Altimetry changes of Anlo Beach from May to October 2022

4.6 Alongshore Changes in Shoreline

In total, the positional uncertainties of the shorelines were estimated to be ± 0.46 m. Based on the HWL proxy, the four shoreline positions spanning a

period of six months (May, July, September and October, 2022) were digitised (Figure 4.8). To compare the dynamics of shorelines close to the river mouth and those farther from it, the shorelines were divided into two sections: A and B. Section A, has a total length of ~1.4 km, with ~600 m each of shorelines located west and east of the river mouth. Section B, is ~ 2 km east of section A (Figure 4.8). A summary of the net shoreline movement has been provided in Table 4.3

From May to July, the average shoreline change at sections A and B was -6.54 m and 0.26 m respectively. This indicates a general landward retreat of shoreline in areas close to the river mouth, while the farther east shows a very little advances seaward (Figure 4.8). However, the overall shoreline changes of -2.57 implies a general erosion of the beach.
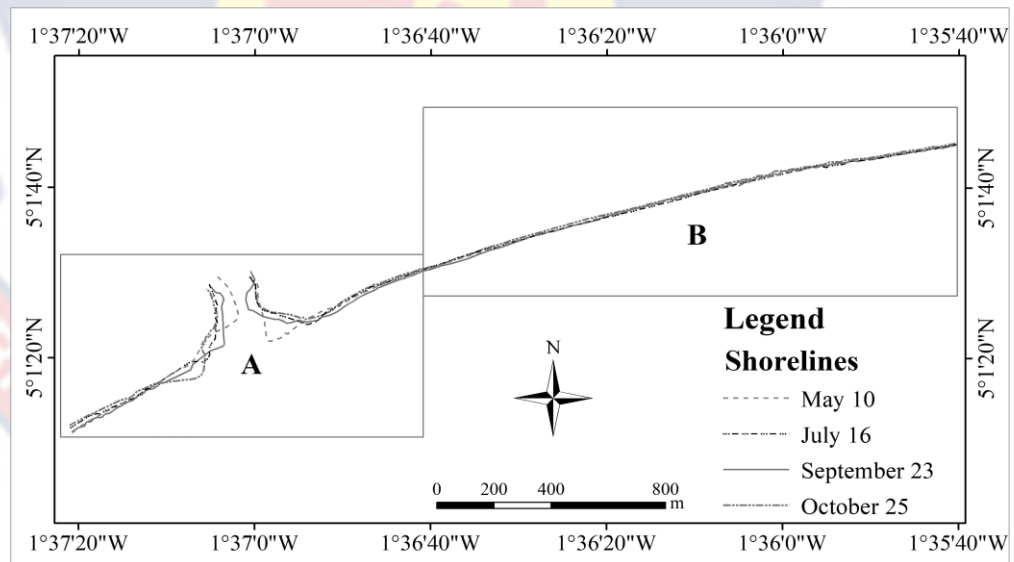
Figure 4.8: Shoreline positions of Anlo Beach from May to October 2022

From July to September, the average shoreline changes at sections A and B were 12.25 m and -0.58 m respectively. This indicates a general seaward

83

advancement of shoreline at areas immediately adjacent the river mouth, while the beach farther east lost the accreted beach which occurred in July. The 4.74 m positive change in the overall shoreline position indicates a general accretion of the beach. From September to October, both sections of the shoreline (A and B) retreated landwards by 14.55 m and 9.58 m, respectively. The whole shoreline also retreated averagely by 9.85 m landwards, within one month, indicating a very high shoreline recession in such a short period of time.

Overall, the results depict an average beach erosion of 8.22 m from May to October, 2022 (Figure 4.9). It was also observed that the maximum erosion and accretion values were found in section A (Table 4.3), an indication of a highly dynamic river mouth.
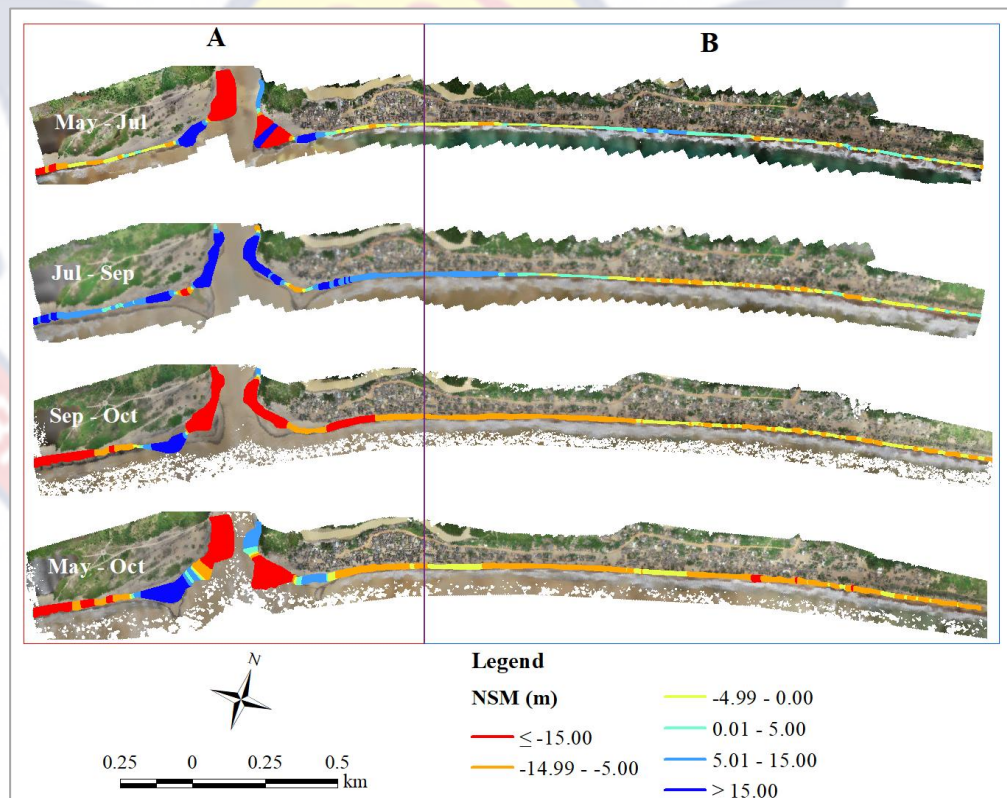
Figure 4.9: Net shoreline movement of Anlo Beach for the study period

84

Table 4.3: Summary statistics of the temporal shoreline movement dynamics of Anlo Beach

Period	Section	Net Shoreline Movement Statistics				
		Total Transects	Min (m)	Max (m)	Mean (m)	SD (m)
May - Jul	A	684	-89.26	99.76	-6.54	25.24
	B	959	-8.23	7.19	0.26	3.10
	A-B	1643	-89.26	99.76	-2.57	16.80
Jul - Sep	A	6.84	-17.05	38.70	12.25	10.29
	B	960	-9.64	13.92	-0.58	5.33
	A-B	1645	-17.07	38.70	4.74	10.02
Sep – Oct	A	684	-68.76	48.06	-14.55	18.16
	B	987	-12.85	0.51	-6.59	3.04
	A-B	1671	-68.76	48.06	-9.85	12.48
May - Oct	A	678	-109.4	55.46	-10.06	29.46
	B	959	-18.88	-0.44	-6.94	3.04
	A-B	1638	-109.4	55.46	-8.22	19.16

4.7 Bathymetric Changes in the Pra Estuary

For each of the three bathymetry maps created using the ordinary kriging (OK) and inverse distance weighting (IDW) interpolation methods in ArcMap, the cross-validation for each of them revealed that both could provide good results. However, based on the root mean square errors (RMSE) and mean errors (ME), OK could make better predictions of the river depths, therefore it was selected for this study. It is also noted that based on the ME for each of the

85

months, both OK and IDW slightly overestimate the river depths. The individual MEs and RMSEs are provided in Table 4.4.

Table 4.4: Comparison of interpolation models' performance in the prediction of river depths

Month	OK		IDW	
	ME (m)	RMSE (m)	ME (m)	RMSE (m)
May	0.000069	0.04048	0.000490	0.05012
July	0.000009	0.06181	0.000042	0.07718
September	0.000040	0.02126	0.000379	0.03405

For the bathymetry of the various months studied, July recorded the deepest depth of 9.18 m while the shallowest depth of 0.56 m occurred in September. On the individual months' basis, depth distribution of May was more uniform, with most parts of the estuary falling within 4.5 to 6 m. However, the areas closer to the mouth seemed shallower than other parts of the estuary. The mean depth of May was 4.41 m with minimum and maximum depths of 1.25 m and a 7.59 m respectively, at a mean water level of 0.29 m. In July, the middle portion of the river was much deeper, reaching a maximum depth of 9.18 m, and minimum depth of 1.49 m, and a mean depth of 4.88 m at a mean water level of 0.13 m implying the occurrence of general erosion in the estuary (Figure 4.10). In September, the maximum and minimum depths obtained were 7.47 m and 0.56 m respectively, with an average depth of 4.61 m at a mean water level of 0.09 m.
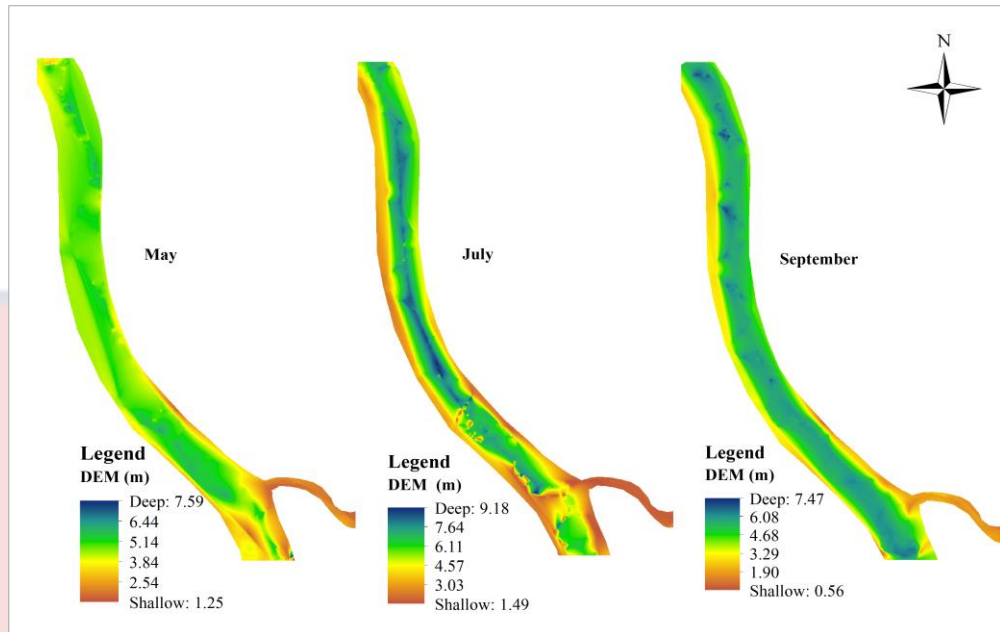
Figure 4.10: Bathymetry of the Pra Estuary for the sampled months

In order to assess the temporal bathymetric dynamics of the Pra Estuary, the difference between the older and newer DEMs were computed (Figure 4.11). The largest change occurred between May and July, obtaining a maximum sediment deposition of 4.25 m and maximum erosion of -5.90 m. A mean depth change of -0.65 m indicates a general erosion of the river bed in July. Between July and September, the maximum depth of sediment deposition was 3.41 m; the maximum depth of erosion was -4.33 m and a mean depth change of 0.48 m, implying a dominance of sedimentation in September. Overall, the maximum depths of accretion and erosion from May to September were 2.30 m and -4.65 m respectively. The mean change in depth was -0.17 m which indicates that river bed erosion is predominant in the Pra Estuary.

87
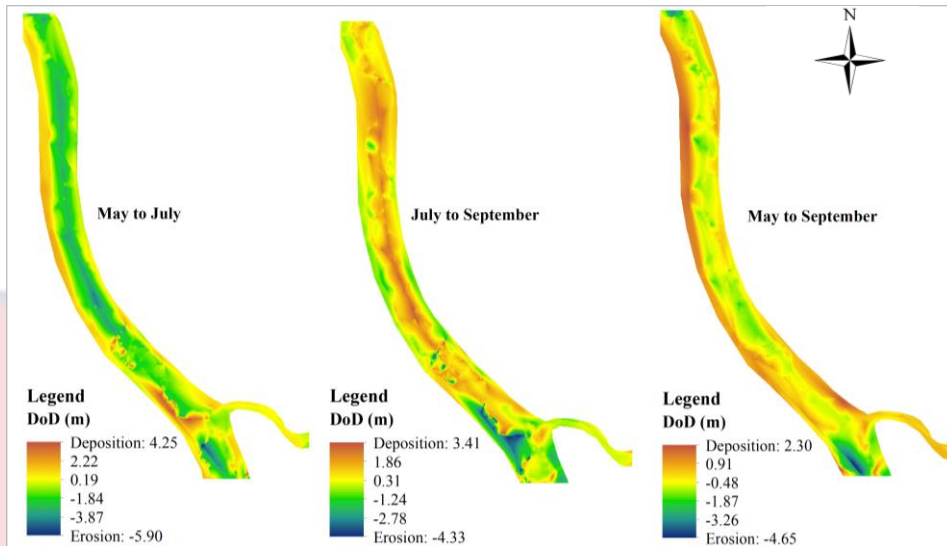
Figure 4.11: Bathymetric changes of the Pra Estuary for the study period

An average of the bathymetry for the various months was computed to obtain the general bathymetry of the Pra Estuary (Figure 4.12). The results show that deeper depths ~ 7.05 m occur in the middle portion of the river and reduce to ~ 2 m at the west side. It could be realised that the tributary has a much shallower depth of ~ 1.37 m. For the whole estuary, the mean depth was 4.62 m, meaning that the Pra Estuary is relatively shallow.
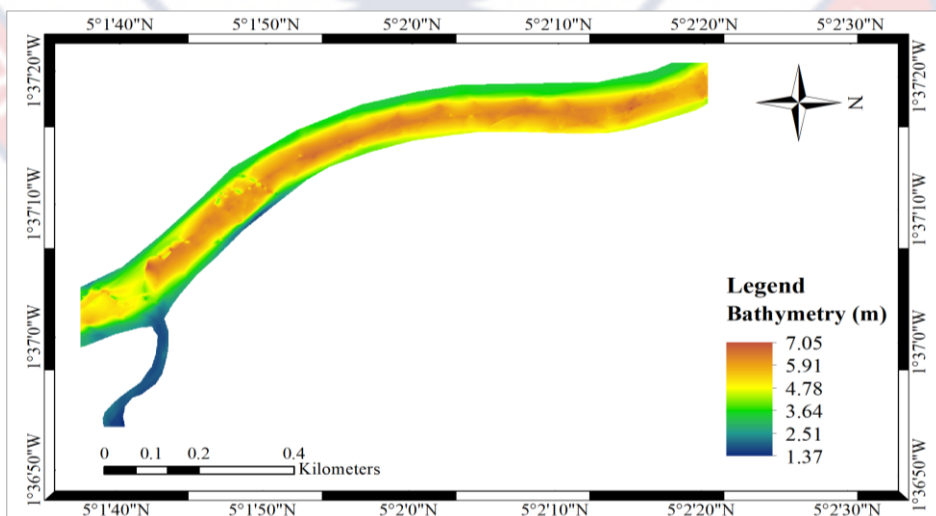
Figure 4.12: Bathymetry of the Pra Estuary

4.8 Summary

Results from the study were presented in the paragraphs above. The average SSC for the Pra estuary was 1757.18 mg/L; average total sediment discharge was 4537 tons/day at an average discharge of 188 m^3/s, and particle sizes containing 52% silt. The beach was found to be generally steep, with an average slope of 0.13, however, areas closer to the mouth were gentler. The beach sediment and shoreline erosion were -105,695.72 m^3 and -8.22 m, respectively between May and October, 2022.

89
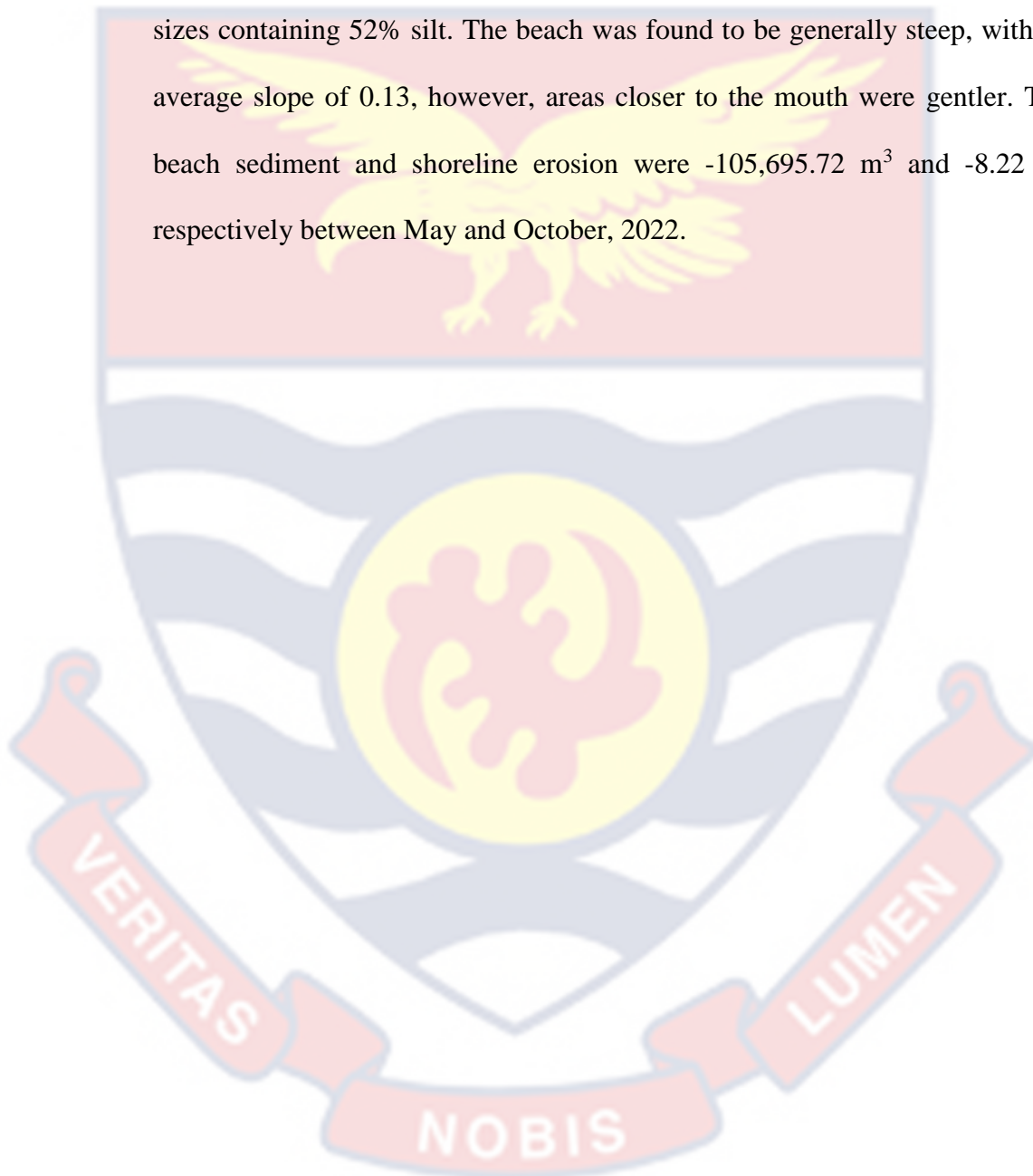
CHAPTER FIVE

DISCUSSION

5.1 Overview

This chapter entails a detailed discussion on the results presented in Chapter 4. The discussion has been done under the following topics: Water and sediment transport in the lower reaches of the Pra River; Sediment particle size distribution and bedload discharge to the sea; Factors responsible for the short-term evolution of the Anlo Beach; Beach sediment dynamics; Impact of estuarine bathymetry and beach morphology on coastal inundation.

5.2 Water and Sediment Transport in the Lower Reaches of the Pra River

The obtained river discharges implied that the average flow rate for the lower reaches of the Pra River was ~188 m^3/s. This result is close to 214 m^3/s and 215 m^3/s reported in the Pra River by Akrasi and Ansa-Asare (2008) and Kankam-Yeboah et al. (2013), respectively. The highest discharge of 374.20 m^3/s occurring in July is similar to Kankam-Yeboah et al. (2013). In Kankam-Yeboah et al. (2013), the highest average monthly river discharge from 1954 to 1997 was ~ 380 m^3/s, occurring in July. Boakye et al. (2021) also measured an instantaneous discharge of 650 m^3/s at Beposo for July in 2018, however this result is quite higher compared to the present study. Zeiringer et al. (2018) explained that river discharges at a specific location is influenced by precipitation type – the quantity, intensity, extent as well as how the rainfall is distributed over the entire catchment; soil moisture that occurred due to previous rainfall, and meteorological factors affecting infiltration and evapotranspiration. Therefore, the basic reason for this disparity may be

90

localised rainfall patterns which could impact river discharges and the decreasing rainfall levels in the catchment.

It is clear from the results that river discharges follow the rainfall pattern in the catchment (Kusimi, 2014). For instance, Bekoe et al. (2012) observed that the Ayensu River, which forms part of the South-western River systems in Ghana, has a seasonal discharge pattern which is similar to the Pra River and may be as a result of the bi-modal rainfall pattern in the middle to the southern parts of Ghana. Furthermore, Kankam-Yeboah et al. (2013), Nsiah et al. (2022) and Obuobie et al. (2012) all agree that rainfall levels are decreasing in the Pra River basin, hence, could be a reason for the lower discharges observed in the present study since discharges depend highly on rainfall and its associated surface runoffs.

On account of the measured SSC, it could be realised that concentrations of suspended sediment obtained for the entire period of study was quite high. For instance, the highest average concentration of suspended sediments reached 2376.58 mg/L in September and the least of 1374.46 mg/L in May. It is noted that these concentrations are lower than Boakye et al. (2021) at Beposo and Kusimi (2014) at Sekyere Hemang, both of which are farther upstream of the area sampled for the present study. Perhaps, sedimentation along the river course might have caused it as Walling (1983) maintained that only a portion of eroded sediment from the upper and middle course of river basins reach the lower course, and consequently, the outlet. Nevertheless, it is an undeniable fact that these sediment loads, especially the suspended sediment concentrations are extremely high, when compared with other rivers like the lower Volta (4.5 mg/l – 20 mg/L) (Logah et al., 2017), Densu (Ofori et al., 2016), the White Volta

91

(375 mg/L) (Mawuli & Amisigo, 2016), Yangtze (1,100 mg/L) (Wei, 2011), Amazon – Obidos (176 mg/L) (Martinelli et al., 1989), Mahanadi (110 mg/L) (Bastia & Equeenuddin, 2016) Capibaribe (662.05 mg/L) (Cantalice et al., 2015).

There exists virtually no correlation between SSC and river flow rate as in the case of Boakye et al. (2021) in the Pra River catchment as well as Syvitski and Milliman (2007) on a global scale. This gives the indication of other factors being responsible for the higher concentrations observed in the study. Studies like Boakye et al. (2021), Boye et al. (2019) and Kusimi et al. (2014) point towards the clearing of forested and perennial crop farmlands like cocoa for alluvial gold mining as the main cause of high suspended sediment concentrations in the Pra River. Illegal gold mining along the banks and alluvial mining within the river have been the most destructive activities on water quality and sediment injection into the rivers. Citing from Kusimi (2014) the (illegal) alluvial mining occurs along the main tributaries Pra River catchment and also found in most communities in the catchment, causing the discharge of huge quantities of sediment in suspension. Other reasons include logging, biennial crop production, urbanisation which exposes the catchment to erosion from the relatively high rainfall in the catchment.

Furthermore, the highest mean monthly total sediment discharge of the Pra River was 9235.33 tons/day in July 2022 and the average total sediment discharge was 4537.03 tons/day, indicating very large quantities of sediment being transported to the sea on a daily basis. These values concur with Akrasi (2011) who estimated 3089.801 tons/day as the total sediment discharged by the Pra River. On the suspended sediment discharged by the Pra River, an average

92

of 4212 tons/day obtained for this study higher than the other rivers in Ghana like the Densu River (15 tons/day) (Ofori et al., 2016) but close to Akrasi (2011); Akrasi and Ansa-Asare (2008); Milliman and Farnsworth (2011). However, based on more recent studies by Boakye et al. (2021) and Kusimi et al. (2014), the present study recorded lower SSQ. This is expected for two reasons: 1. single data point used in the present study gives a snapshot of the whole event and may underestimate the average daily sediment discharge; 2. Boakye et al. (2021) confirmed that sediment load in the Pra River catchment is on the decline due to the ban imposed on illegal small-scale mining activities (Galamsey) in Ghana.

5.3 Sediment Particle Size Distribution and Bedload Discharge to the Sea

Throughout the study, silt particles dominated the Pra Estuary with an overall median and mean of 0.062 mm and 0.100. This is explained clearer by the overall ratio of 52 % silt (< 0.063 mm) dominating the study area, with <1 % being gravels. The overall mean and median particle sizes are lower than the observation of Al-Ansari et al. (2015) for the Tigris River in Iraq (0.18, 0.15 mm). The silt particles observed is a fairly higher than both Logah et al. (2017) in the Lower Volta River (30 %) and Faseyi (2022) who observed that between 2020 and 2021, about 34 % of bed materials were silt and about 1 % were gravels in the Pra and Ankobra River estuaries. The percentage of silt is also lower than Akita et al. (2020) who obtained 38 % silt/clay in the Densu Estuary in 2017. This suggests that bedload particle sizes in the Pra Estuary is getting finer.

The dominance of silt particles may be due to the geology of the catchment which is mainly the naturally soluble forest Ochrosols and precambraim rocks weathered from the Tarkwaian and Birimian formations (Awotwi et al., 2018; Boakye et al., 2021). Kusimi et al. (2016) described the forest Ochrosols as "clayey and not well leached" therefore the incessant surface mining activities in the catchment expose these soils to be eroded and transported as very fine particles downstream of the catchment. Studies by Boakye et al. (2020) on the spatial distribution of erosion in the Pra River catchment revealed soil erosion rate in the catchment is $\sim 1.28 \times 10^6$ tons/year. It was also identified that about 21.3 % of the catchment is prone to high and very high erosion, especially the Lower Offin River sub-catchment, principally from the intense alluvial mining and small-scale mining, urbanisation rate (32 %) (Awotwi et al., 2018) and farmlands on or along steep slopes.

It has been noted that coarser bedload is very predominant in areas close to the river mouth, similar to sediment particles on the Anlo Beach (from field observation, since beach sediment particle size was not captured in this study). This may be the effect of turbulence from the interaction of the sea and river, causing finer particles to stay in suspension.

Furthermore, the percentage of bedload discharged ranged between 0.6 % and 21 %, and an average of 6.96 % which is very indicative of low bedload transport (Cantalice et al., 2015). It was then relatable when the percentage of bedload discharged correlated well with the mean particle size. This gives an indication that since most of the sediment is very fine, less would be transported on the river bed due to their low densities, except during a period of low turbulence. In the few studies (Akrasi, 2011; Boateng et al., 2012; Boye et al.,

94

2019) conducted on the Pra River that included Bedload, 10 % was used as the correction factor for bedload discharge. However, this study has demonstrated that bedload discharge depends more on the particle size distribution. This is agreed by Boateng et al. (2012) that giving a correction factor to bedload discharge should be based on the particle size distribution and the river hydraulics. Boateng et al. (2012) further found out that the use of 10 % as a correction factor may be wrongly estimated since their studies found the percentage of bedload of rivers in Ghana to range between 10 % and 56 % in sediment discharge datasets between 1974 and 1963. Cantalice et al. (2015) also found bedload percentage in the Capibaribe River (Brazil) to vary between 0.12 % to 27.3 %.

Riverine sediment impact on beach building has been noted to be dependent on particle size of sediment discharged. For instance, Boateng (2012) and Boye et al. (2019) referred to Ayibotele and Tuffour-Darko (1979) and used 50 % as portion of suspended sediment that is relevant for beach building. This is because, Ayibotele and Tuffour-Darko (1979) found 50 % of suspended sediment in Ghanaian rivers to be less than 0.063 mm in size, and would be disturbed by the slightest turbulence and would not stay on the beaches. Jayson-Quashigah et al. (2019) further maintained that even sediment particles which are less than 0.15 mm could easily suspend and get transported offshore, thereby contributing less to beach sediment budget. It could therefore be inferred from these instances that only 48 % of bedload in the Pra River would be relevant for beach building and reduction of coastal erosion at the Anlo Beach.

95

5.4 Factors responsible for the short-term evolution of the Anlo Beach

The alongshore movement of the shoreline on Anlo Beach depicts overall net shoreline movement of -8.22 m within a period of six months. This exhibits the occurrence of severe coastal erosion within a short period of time. The result is relatively higher than Boye et al. (2019) who estimated -1.62 m mean shoreline change between 1974 and 2005 on the coastline of Western Region – Ghana. This is acceptable because Boye et al. (2019) did a long-term study which covers a large area spatially Also, the time range between the current study and Boye et al. (2019) as well as other factors affecting the Anlo Beach coastline could be responsible for the large disparity between the current results and Boye et al. (2019). A number of studies on other parts of Ghana coastline have reported shoreline retreat (Angnuureng et al., 2019; Angnuureng et al., 2020a; Appeaning Addo et al., 2008; Boateng, 2012; Boye et al., 2019; Brempong et al., 2021; Dadson, 2015; Jayson-Quashigah et al., 2013; Jayson-Quashigah et al., 2019; Ly, 1980; Otoo, 2018), however, Abdul-Kareem et al. (2022) recorded shoreline advancement of 6.45 m from January to May 2021 at the Apam Beach. In this study, areas close to the mouth (Figure 4.9 A) and those farther away (Figure 4.9 B) experienced varying levels of erosion and accretion in the various months, yet, erosion was significant in both areas (A: -10.06 m; B: -6.94 m) for the overall change (Table 4.3). It has been established by Anim (2012), Boye et al. (2019), Li et al. (2014) and Walling (1983), that essentially beaches mostly depend on the supply of sufficient sediment from inland water bodies to offset sediment loss from beach face and establish equilibrium. Therefore, inadequate coarser bedload (< 156 tons/day) from the Pra River to nourish the mouth and adjacent beaches (Jayson-Quashigah et al., 2019) in

96

addition to the reworking of sediments by waves, river discharge and currents would cause beach front erosion (Anim, 2012; Li et al., 2014).

Sandy beach shorelines are naturally exposed to high impact of waves and currents. However, the natural impact of these coastal hydrodynamics on shorelines is often exacerbated by human influences. Boateng (2012) and Boye et al. (2019) demonstrated a minimal erosion at the Anlo Beach. Yet, during the present study the results depicted a high level of erosion on the whole stretch of the Anlo Beach. Satellite images from Google Earth Pro (2022) revealed a shift of the Pra River mouth from Shama to the Anlo Beach (Figure 4.13). Upon further investigations, it was made known by some community members of the community that the changes in river mouth location was an intervention made by some of the community members to ease flooding in the community. The source of this flooding was the small tributary (Figure 4.13 – areas shaded red) of the river Pra which borders the northern part of the community. This river was often overtopping its banks and flooding most parts of the community during high rainfall, hence their decision to re-channel the mouth eastward in 2017 for easy outflow of the discharges. However, such an unaided decision exposed the community to interactions of river discharges with tidal currents and waves especially during high tides at the river mouth and extending to areas father away. It is clear from the 2015 satellite image (Figure 5.1) that the river mouth would have eroded after a period of time due to high oceanic forcing, just like Abdul-Kareem et al. (2022). Yet, human interventions shortened this process culminating in a rapid loss of the landmass at a very short period of time.

97
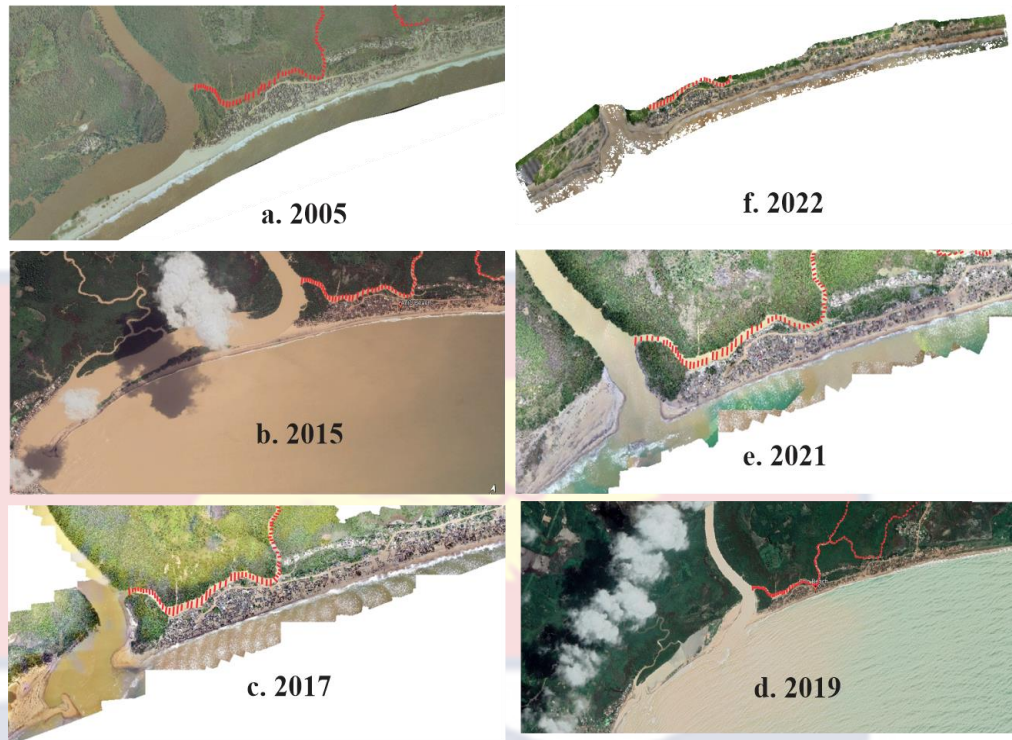
Figure 5.1: Evolution of the Pra River mouth

Sources: Adade (2022); Author: field data collection (2022); Google Earth Pro, (2022)

Another factor which could be responsible for the erosion of the Anlo Beach coastline is the "knock-on effects" of sea defence structures updrift of this coast (Figure 5.2) as explained by Angnuureng et al. (2013); Angnuureng et al. (2019); Angnuureng et al. (2022a); Boateng (2012) and Jayson-Quashigah et al. (2019). Longshore drift on this section of the coastline is from west to east, and naturally sediment is supposed to be transported to nourish the coast. Yet, the construction of the Takoradi Harbour and Sekondi Port has intercepted the longshore sediment transport at the coast, depriving the adjacent beaches of sediment as explained by Boateng (2012) and Li et al. (2014). For this reason, downdrift coasts depend solely on riverine sediments to stabilise the beaches.

The "knock on effect" has probably caused the erosion of the coastal frontage of the Aboadze community, hence, the construction of new jetties and revetments (began in 2021, based on Google Earth Pro satellite image) to prevent the bypassing of the already "insufficient sediment". This may have heightened erosion at the adjacent Anlo Beach coastline.
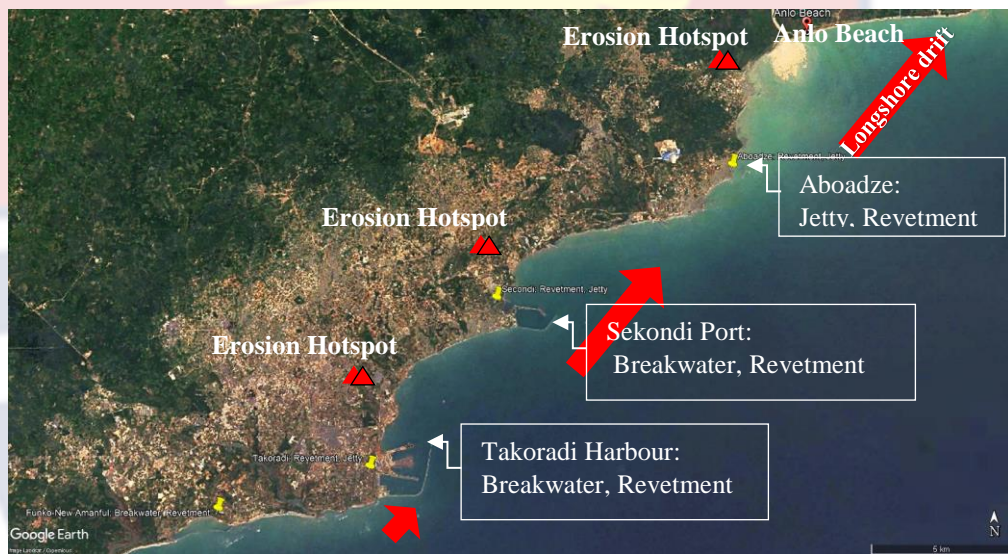
Figure 5.2: Anthropogenic impact on longshore drift

5.5 Beach Sediment Dynamics

Over the entire period of study, the Anlo Beach experienced varying levels of sediment loss and gains with sediment gains occurring between July and September. However, between May and July as well as September and October, more sediment losses were recorded (Table 4.2). Based on Tran and Barthélemy (2020), erosion and accretion cycles can occur within short time scales, even in a few days to several weeks. Nonetheless, the overall net sediment loss of 105,695.72 m^3 from the Anlo Beach between May and October, point toward a severe loss of sediment over the six months study period. The

99

sediment loss on the Anlo Beach is also higher than losses observed on the eastern coast of Ghana (Angnuureng et al., 2019; Jayson-Quashigah et al., 2019). This is in contrast to Abdul-Kareem et al. (2022) who observed 3725.22 m^3 of sediment gains on the Apam Beach (also contains a river supplying sediment to the beach). This disparity might be due to seasonality differences, that is, the present study was conducted in the wet season while the work of Abdul-Kareem et al. (2022) was conducted in the dry season. Abdul-Kareem et al. (2022) agrees with Quartel et al. (2008) that seasonal patterns influence beach dynamics. This is because more erosive processes occur in the wet season leading to the narrowing and loss of beaches (Anim, 2012).

Aside the immediate mouth of the river, almost every portion of the beach has experienced some level of sediment loss from May to October 2022, and this was estimated to be 75 % of the beach. A worse case was recorded by Brempong et al. (2021), who observed that 97 % of the Dzita Beach experienced some level of sediment loss between May and December, 2018. On the eastern portion of the mouth, beach sediment loss was more pronounced at the middle section (-5 to -2 m), this is consistent with the beach profiles IV and V. Observations of the sediment distribution for the overall study shows that sediments on the beach drifted more to the eastern portion of the beach, implying that it follows the longshore drift pattern of the central and eastern coast of Ghana. Just like Appeaning Addo (2010, 2015), longshore current of 0.5 m/s - 1.5 m/s is very strong on the surf zone of Accra and might be similar to Anlo Beach (Xorse, 2013). Therefore, together with waves, the prevailing winds, and spring tides, a lot of havoc could occur (Anim, 2012). Report presented by Anane-Amponsah and Ahiabor (2017) indicated that for the past

30 years, over 1000 houses along the beach has been destroyed due to the effects of tidal waves from the sea. Appiah (2022) also reported the displacement of about 50 % of the population and the collapse of the only school in the community. It could be seen from Figure 5.3 that the uprooted coconut trees, and destroyed houses is very overwhelming to the Anlo Beach community.

Figure 5.3: The dire state of Anlo Beach: (a) collapsed bathhouse (b) eroded beach face, causing the uprooting of coconut trees (c) some collapsed houses due to storm surges (d) eroded beach face

The beach profiles show that sediment loss occurs from the back beach to the foreshore. The actual cause of sediment loss is not certain, however, based on the findings of Angnuureng et al. (2022a, b) on the Elmina beach (~ 33 km to Anlo Beach), it could be deduced that uninterrupted swells originating from the south of the Atlantic Ocean hits the Anlo Beach to cause rapid erosion

101

through the process of backwash. Angnuureng et al. (2022b) found that the nearshore bathymetry of Elmina up to 1 km offshore increased from 0.6 to 10.2 m. This implies that deeper depths exist and more sediment could be trapped offshore. Conceivably, offshore bathymetry may account for the loss of sediment on the Anlo Beach after backwash transports the sediment further offshore and deposit them in canyons, just like Anim (2012). However, this is not fully conclusive since bathymetry of the nearshore was difficult to measure, and was not included in the present study.

Furthermore, sediment loss from the beach could also be from anthropogenic influences. Faseyi (2022) observed very rare cases of sand mining on the beach. However, a further interview by Faseyi (2022) with some community members revealed that sand mining was undertaken by the government for construction of roads and the Essipong Sports Stadium in Sekondi, leading to the loss of large volumes of sediment on the Anlo Beach. Dada et al. (2022) also confirmed that out of 156 respondents interviewed in the Anlo Beach community, about 113 engage in moderate to high usage of the beach sand. The type of usage was however not explained further. Jonah et al. (2017) clarified that beach sediment on four coastal districts in the Central Region are mined on commercial and non-commercial scales and transported manually or by the use of trucks. Yet, like Faseyi (2022), during the present study period, no sand mining activity was observed on the Anlo Beach. Hence, although sand mining could influence sediment volume reduction, it is not fully conclusive that sand mining is a principal cause of sediment loss on the beach.

5.6 Impact of Estuarine Bathymetry and Beach Morphology on Coastal Inundation

River bathymetry is key in many applications including flood risk management, land subsidence, inland navigation, bank erosion prediction as well as understanding fluvial processes dynamics (Arseni et al., 2019; Forghani et al., 2022; Kim et al., 2019; Merwade, 2009; Panhalkar & Jarag, 2015). The result has provided an overview of the bathymetry of the Pra Estuary and its temporal dynamics. The temporal bathymetry changes for the entire period exhibited that more erosion occurs in areas closer to the river mouth and in the middle section of the river, while sediment deposition occurred along the banks. Between May and July, erosion of the middle portion of the river was more prevalent while between July and September, sediment deposited at the eroded areas, leading to a positive mean depth change of 0.48 m. In this study, high percentages of bedload discharges are associated with relatively coarser sediment particles which are found closer to the river mouth. This makes it conceivable to infer that high erosion would occur with increasing percentage of bedload discharges.

The dominance of erosion in July coincides with the rainfall pattern of the basin (Kankam-Yeboah et al., 2013) as well as the high river discharges obtained at this period of data collection. This agrees with Anim (2012) and Quartel et al. (2008) that high erosion occurs in the rainfall season. For the five months period, the overall mean changes in river depth depicted very mild erosion (-0.17 m). There are good chances that sedimentation would be high in the subsequent months, following the dry season in the catchment – November to April. Boakye et al. (2021) agrees that the sedimentation of the Pra estuary is

103

a factor of seasonality. Currently, the average depth of the Pra Estuary is 4.6 m, which is similar to other world rivers like the Tigris (Al-Ansari et al., 2015). Due to the low availability of river bathymetry information in Ghana and other African countries, it is difficult to make comparisons (Komi et al., 2017).

The tributary bordering the Anlo Beach had an average depth of 1.37 m, however, depths measurements were not taken in farther inside the community due to the shallow bathymetry ($\leq$ 0.5 m). Combining factors like the sea level rise, relatively shallow river bathymetry, the steep beach slope, the low elevation as obtained from beach profiles, and the sandwich of the community between the sea and a wetland, it is plausible to conclude that Anlo Beach is highly susceptible to inundation from both the river (during very high discharges) as well as from the sea, especially, during spring tides (Appeaning Addo et al., 2011; Mutimukuru-Maravanyika et al., 2017). This is demonstrated by the findings of Boateng et al. (2017), which indicates that Anlo Beach is highly vulnerable and Asiedu (2019) which found the Anlo Beach to be located in a very high flood risk zone in the lower parts of the Pra River basin. The findings therefore affirm that Anlo Beach is highly exposed and vulnerable to coastal inundation.

5.7 Summary

The study suggests a decreasing trend of average daily river discharges (188 m³/s), sediment load (4537 tons/day) and particle sizes (52% silt). They were however larger than other rivers in Ghana and elsewhere due to the intense illegal small-scale mining and decreasing trend of rainfall in the catchment. Beach sediment and shoreline erosion were -105,695.72 m³ and -8.22 m,

respectively between May and October, 2022. This was due to smaller sediment particles, and blockage of longshore sediment transport by sea defence structures west of this beach. Also, shallow bathymetry was observed at the Pra Estuary, which could lead to flooding during rainfall and high discharges.

105

CHAPTER SIX

SUMMARY, CONCLUSIONS AND RECOMMENDATIONS

6.1 Overview

In this chapter, the summary of the thesis, conclusions made from the study as well as some recommendations which are linked to the major findings in the study are presented. Furthermore, the conclusions have been structured based on the objectives set for this study.

6.2 Summary

The transport of sediment to coastal areas is important due to the impact they make on the coastal and marine environment. In addition, they play a very major role in future trends of shoreline positions forecasting for proper coastal management decisions. In spite of the substantial role they play in ensuring coastal stability, incessant human interventions are affecting sediment discharges from rivers, leading to land loss to the sea.

Due to the knowledge gap in the link between the high sediment discharged by the Pra River to adjacent beaches on the coastal frontage and the high rate of erosion occurring in the area, this study was set principally to assess the contribution of riverine sediment discharge from the Pra River to the short-term evolution of the Anlo Beach. Specifically, the study assessed: 1. the quantity of sediment discharge by the Pra River into the sea; 2. the short-term changes in shoreline along the Anlo Beach; 3. the bathymetric changes of the Pra Estuary. This study has been justified as important due to the impact riverine sediment has on beach dynamics; many investments put into the investigation of coastal morphodynamics as a result of erosion prevalence in Ghana and

finally, the categorisation of this study under the Coastal Geomorphology and Engineering – ACECoR thematic area, to provide relevant information for addressing riverine systems and coastal area management issues.

The Pra River catchment with focus on the coastal frontage (~3.5 km alongshore) and 1.6 km inland of the estuarine region was studied, with field surveys spanning a period of six months – May to October, 2022. Variables including river depths, water levels, suspended sediment, bedload, river velocities, and aerials photographs were collected for each survey, and subsequently processed and analysed using established protocols to produced river bathymetry and shoreline changes, bathymetry maps, river discharges, river sediment discharges and particle size distribution of sediment discharged.

Results from the study suggests a decreasing trend of average daily river discharge (188 m^3/s), average total sediment transport (4537.03 tons/day), average daily bedload transport (324.92 tons/day), average suspended sediment transport (4212.12 tons/day), average daily suspended sediment concentration (1757.18 mg/L), as well as particle size distribution (52 % silt). They were however larger than other rivers in Ghana and elsewhere primarily due to the intense illegal small-scale mining and decreasing trend of rainfall in the catchment.

Moreover, for the six months period shoreline changes (-8.22 m) and beach sediment volumes (-105,695.72 m^3) showed an overall erosion which were attributed to low supply of coarse sediment, uninformed channelisation of river mouth eastward, "knock-on effects" due to the interruption of longshore sediment transport with hard-engineered sea defence structures, local long-shore drift, waves, spring high tides, deep offshore bathymetry and sand mining.

107

Lastly, the mean depth of the Pra Estuary (4.6 m) was found to be relatively shallow, and based on the temporal dynamics that occurred bi-monthly, mild erosion was more dominant. This was attributed mainly to precipitation pattern; therefore, more sedimentation of the Pra Estuary is expected from October to April since precipitation to cause erosion is less. In sum, the relatively shallow bathymetry, sea level rise, gentle beach slope, and the sandwiched Anlo Beach community between the sea and the mangrove wetland, makes the community very susceptible to coastal flooding, especially during spring high tides.

6.3 Conclusions

The Pra River catchment with focus on the coastal frontage (~3.5 km alongshore) and 1.6 km inland of the estuarine region was studied, with field surveys spanning a period of six months – May to October, 2022. Variables including river depths, water levels, suspended sediment, bedload, river velocities, and aerials photographs were collected for each survey, and subsequently processed and analysed using established protocols to produce river parameters (flow rate, sediment discharges, particle size distribution and bathymetry maps) and beach parameters (sediment volumes/budget, profiles and shoreline changes).

The sediment discharge trends and particles size distribution does not fully support beach stability. The dominance of suspended sediment which is 100 % very fine and the 52 % very fine bedload makes it plausible to infer that the Pra River would not be able to fully support beach building since only 48% of bedload discharged or 32 % of the total sediment discharged is coarse enough

108

to support the beach building. Total daily river sediment and bedload discharge showed a decreasing trend compared with previous studies in the upstream of the catchment. However, values measured are higher than most rivers in Ghana. The decrease may be due to the anti-galamsey operations, low rainfall and upstream sedimentation. Sediment sizes also showed an increasing trend of finer particles from May to September. This is attributed to the continuous exposure of the dominant clayey-like soil – forest Ochrosols in the catchment to erosion due to alluvial mining, urbanisation and farming along steep slopes.

The shoreline changes and sediment volume on the Anlo Beach portrayed a very high erosion of the beach. Reasons for the changes are the interlinking impact of anthropogenic activities and natural causes. These include the inadequate coarse sediment discharge from the Pra River, uninformed rechanneling of river mouth eastward by community members, sediment starvation from the interruption of longshore sediment transport with hard-engineered sea defence structures, eastward drift of sediment from the Anlo Beach, waves, spring high tides, deep offshore bathymetry and sand mining.

The mean depth of the Pra Estuary was found to be relatively shallow, and based on the temporal bathymetric changes that occurred on bi-monthly basis, mild erosion was predominant. The cause is attributed mainly to precipitation pattern, hence more sedimentation of the Pra Estuary is expected from October to April since precipitation to cause erosion is less in this period. In sum, the Anlo Beach community is very susceptible to coastal flooding, especially during spring high tides.

It is important to note that due to the high cost involved in collection of data used for this study, field surveys were limited to once bi-monthly sampling (in May, July and September), particularly for the sediment, bathymetry, water levels and river discharges. An additional shoreline data was also collected on the sixth month (October). Presently, the river mouth and the beach are in a disequilibrium state due to the recent rechanneling of the river mouth from Shama to Anlo Beach. In addition to this, the smaller number of data points makes it difficult to give very firm conclusions for this study.

6.4 Recommendations

This study recommends that more strict laws must be enforced to ensure less illegal mining activities in the catchment. This is by forming task forces from stake holders like District Assemblies, the security agencies, the Minerals Commission, Water Resource Commission, the Environmental Protection Agency, assembly members, community leaders and indigenes to ensure efficient surveillance. This is because fine sediment particles are less useful for establishing balance of the beach system. Mercury used in the extraction of the gold poses severe health risk to users of the Pra River as well as the coastal ecosystem. Urbanisation and agriculture are important for nation building; however, measures must be put in place at the district level to ensure efficient and sustainable use of lands to reduce the exposure of land surfaces to erosion.

To ensure the stability of shorelines, it is recommended that communities are well educated and government should establish a comprehensive policy for dealing with coastal erosion. Environmental impact assessment is highly recommended before any coastal defence structure is built.

Also, beach sand mining should be completely stopped by adopting local bye-laws to enhancing coastal protection. The neglect of vulnerable coastal communities which lead to the uptake of unaided decisions for mitigating coastal erosion and inundation be avoided due to high negative impacts associated with it.

Furthermore, dredging of shallow rivers at the beginning of the rainfall season should be implemented in District Assemblies to reduce the impact of floods on the community. Also, due to the low terrain and the high susceptibility to tidal waves, storm surges and flooding, it is recommended that community members are relocated and an approach be implemented by studying the area.

As stated in the conclusions, this study was a short-term, hence, more studies on riverine sediment discharges characteristics, river bathymetry and shoreline monitoring must be undertaken on long-term basis to have a better picture of the Anlo Beach. Undertaking studies on wave parameters and localised longshore drift to better understand the direction of sediment movement is recommended. Also, the nearshore and offshore bathymetry should be explored to provide a clearer picture of the direction of movement of sediment from the Pra River. This would aid in providing sustainable solutions to the management of the Anlo Beach coastline and other adjacent coasts. In addition, shoreline modelling of the effects of the human interventions on the mouth of the Pra River is recommended to predict the future of the Anlo Beach.

REFERENCES

Abdul-Kareem, R., Asare, N. K., Angnuureng, D. B., & Brempong, E. K. (2022). Shoreline variability of a bay beach: The case of Apam Beach, Ghana. *Estuaries and Coasts*, *45*, 2373–2386. https://doi.org/10.1007/s12237-022-01110-9

Achite, M., & Ouillon, S. (2007). Suspended sediment transport in a semiarid watershed, Wadi Abd, Algeria (1973-1995). *Journal of Hydrology*, *343*, 187–202. https://doi.org/10.1016/j.jhydrol.2007.06.026

Adade, R. (2022). *Orthophotos of Anlo Beach* (pp. 1–5). Centre for Coastal Management, University of Cape Coast.

Adade, R., Aibinu, A. M., Ekumah, B., & Asaana, J. (2021). Unmanned Aerial Vehicle (UAV) applications in coastal zone management—a review. *Environmental Monitoring and Assessment,* 193(154), 1–12. https://doi.org/10.1007/s10661-021-08949-8

Agisoft LLC. (2019). *Agisoft Metashape user manual professional edition* Retrieved from https://www.academia.edu/41606940/Agisoft_Metashape_User_Manual_Professional_Edition_Version_1_5

Akita, L. G., Laudien, J., & Nyarko, E. (2020). Geochemical contamination in the Densu Estuary, Gulf of Guinea, Ghana. *Environmental Science and Pollution Research*. https://doi.org/10.1007/s11356-020-10035-4

Akrasi, S. A. (2005). The assessment of suspended sediment inputs to Volta Lake. *Lakes & Reservoirs: Research and Management*, *10*(3), 179–186. http://dx.doi.org/10.1111/j.1440-1770.2005.00272.x

Akrasi, S. A. (2011). Sediment discharges from Ghanaian rivers into the sea. *West African Journal of Applied Ecology*, *18*, 1–13. https://doi.org/10.431

112

4/wajae.v18i1.70320

Akrasi, S. A., & Ansa-Asare, O. D. (2008). Assessing sediment and nutrient transport in the Pra Basin of Ghana. *West African Journal of Applied Ecology*, *13*, 45–54. Retrieved from https://www.semanticscholar.org/paper/Assessing-Sediment-and-Nutrient-Transport-in-the-of-Akrasi-AnsaAsare/970724e4 c81545ed1039d445ba8041863967e2b5

Al-Ansari, N., Ali, A. A., Al-Suhail, Q., & Knutsson, S. (2015). Flow of River Tigris and its effect on the bed sediment within Baghdad, Iraq. *Open Engineering*, *5*(1), 465–477. https://doi.org/10.1515/eng-2015-0054

Alexandrov, Y., Balaban, N., Bergman, N., Chocron, M., Laronne, J., Powell, D., Reid, I., Tagger, S., & Wener-Franka, I. (2008). Differentiated suspended sediment transport in headwater basins of the Besor catchment, northern Negev. *Israel Journal of Earth Sciences*, *57*(3-4), 177–188. https://doi.org/10.1560/IJES.57.3-4.177

Alexandrov, Y., Cohen, H., Laronne, J. B., & Reid, I. (2009). Suspended sediment load, bed load, and dissolved load yields from a semiarid drainage basin: A 15-year study. *Water Resources Research*, *45*(8), 1–13. https://doi.org/10.1029/2008WR007314

Allersma, E., & Tilmans, W. M. K. (1993). Coastal conditions in west africa: A review. *Ocean & Coastal Management*, *19*(3), 199–240. https://doi.org/10.1016/0964-5691(93)90043-x

Alves, B., Angnuureng, D. B., Morand, P., & Almar, R. (2020). A review on coastal erosion and flooding risks and best management practices in West Africa: what has been done and should be done. *Journal of Coastal Conservation*, *24*(38), 1–22. https://doi.org/10.1007/s11852-020-00755-7

113

Amegashie, B. K., Quansah, C., Agyare, W. A., Tamene, L., & Vlek, P. L. (2011). Sediment-bound nutrient export from five small reservoir catchments and its implications for the Sudan savanna zone of Ghana. *Lakes & Reservoirs: Research and Management*, *16*(1), 61–76. http://dx.doi.org/10.1111/j.1440-1770.2011.00459.x

Amenuvor, M., Gao, W., Li, D., & Shao, D. (2020). Effects of dam regulation on the hydrological alteration and morphological evolution of the Volta River Delta. *Water*, *12*(646). https://doi.org/10.3390/w12030646

Amlalo, D. S. (2005). *The Protection, Management and Development of the Marine and Coastal Environment of Ghana*. Retrieved from http://www.fig.net/pub/figpub/pub36/chapters/chapter_10.pdf#search=%22causes%20of%20shoreline%20erosion%20in%20ghana%22

Ampadu, B. (2021). Overview of hydrological and climatic studies in Africa: The case of Ghana. *Cogent Engineering*, *8*, 1914288, 4–10. https://doi.org/10.1080/23311916.2021.1914288

Anane-Amponsah, M., & Ahiabor, G. (2017). *Anlo Beach to be wiped out in a year*. Graphics Online. Retrieved from https://www.graphic.com.gh/news/general-news/anlo-beach-to-be-wiped-out-in-a-year.html

Angnuureng, D. B., Almar, R., Senechal, N., Castelle, B., Addo, K. A., Marieu, V., & Ranasinghe, R. (2017). Shoreline resilience to individual storms and storm clusters on a meso-macrotidal barred beach. *Geomorphology*, *290*, 265–276. https://doi.org/10.1016/j.geomorph.2017.04.007

Angnuureng, D. B., Amankona, G., Brempong, E. K., & Attipoe, E. (2022b). Short-term effect of sea defense on shoreline and wave variability in Elmina Bay, Ghana. *Journal of Coastal Conservation*, *26*(57), 1–12.

114

https://doi.org/10.1007/s11852-022-00906-y

Angnuureng, D. B., Appeaning Addo, K., & Wiafe, G. (2013). Impact of sea defense structures on downdrift coasts: The case of Keta in Ghana. *Academia Journal of Environmental Sciences*, *1*(6), 104–119. https://doi.org/10.15413/ajes.2013.0102

Angnuureng, D. B., Brempong, K. E., Jayson-Quashigah, P. N., Dada, O. A., Akuoko, S. G. I., Frimpomaa, J., Mattah, P. A., & Almar, R. (2022a). Satellite, drone and video camera multi-platform monitoring of coastal erosion at an engineered pocket beach: A showcase for coastal management at Elmina Bay, Ghana (West Africa). *Regional Studies in Marine Science*, *53*(102437). https://doi.org/10.1016/j.rsma.2022.102437

Angnuureng, D. B., Jayson-Quashigah, P. N., Almar, R., Stieglitz, T. C., Anthony, E. J., Aheto, D. W., & Addo, K. A. (2020b). Application of shore-based video and unmanned aerial vehicles (Drones): Complementary tools for beach studies. *Remote Sensing*, *12*(394). https://doi.org/10.3390/rs12030394

Angnuureng, D. B., Jayson-Quashigah, P.-N., Appeaning Addo, K., Aheto, D. W., Almar, R., Bonou, F., & Brempong, E. K. (2019). Quantification of the shoreline evolution of an open beach between coastal defenses. *Coastal Sediments,* 1562–1576. https://doi.org/10.1142/9789811204487_0135

Angnuureng, D., Frimpomaa, J., Anim, M., Akuoko, I., Alves, B., & Addison, N. (2020a). Assessing the challenges of beach quality: the perception of a beach user in Ghana. *Journal of Fisheries and Coastal Management*, *2*, 41–55. https://doi.org/10.5455/jfcom.20200423042514

Anim, M. (2012). *lithological responses to sea erosion along the coastline from*

Gold Hill (Komenda) to Amissano (Saltpond). (Master's thesis, University of Cape Coast, Ghana). Retrieved from http://hdl.handle.net/12345678 9/2725

Appeaning Addo, K. (2010). Changing morphology of Ghana's Accra coast. *Journal of Coastal Conservation*, *15*(4), 433–443. https://doi.org/10.1007 /s11852-010-0134-z

Appeaning Addo, K. (2015). Monitoring sea level rise-induced hazards along the coast of Accra in Ghana. *Natural Hazards*, *78*(2), 1293–1307. https://doi.org/10.1007/s11069-015-1771-1

Appeaning Addo, K., Jayson-Quashigah, P. N., Codjoe, S. N. A., & Martey, F. (2018). Drone as a tool for coastal flood monitoring in the Volta Delta, Ghana. *Geoenvironmental Disasters*, *5*(17), 2–13. https://doi.org/10.1186/ s40677-018-0108-2

Appeaning Addo, K., Larbi, L., Amisigo, B., & Ofori-Danson. (2011). Impacts of coastal inundation due to climate change in a CLUSTER of urban coastal communities in Ghana, West Africa. *Remote Sensing*, *3*, 2029–2050. https://doi.org/10.3390/rs3092029

Appeaning Addo, K., Walkden, M., & Mills, J. P. (2008). Detection, measurement and prediction of shoreline recession in Accra, Ghana. *ISPRS Journal of Photogrammetry and Remote Sensing*, *63*(5), 543–558. https://d oi.org/10.1016/j.isprsjprs.2008.04.001

Appiah, S. J. (2022). *Tidal waves at Anlo Beach*. Retrieved from https://sha madistrict.gov.gh/tidal-waves-at-anlo-beach

Arseni, M., Ro, A., Georgescu, L. P., & Murariu, G. (2016). Single beam acoustic depth measurement techniques and bathymetric mapping for

116

catusa lakegalati. *Annals Of "Dunarea De Jos"*, *2*, 281–288.

Arseni, M., Voiculescu, M., Georgescu, L. P., Iticescu, C., & Rosu, A. (2019). Testing different interpolation methods based on single beam echosounder river surveying. Case study: Siret River. *International Journal of Geo-Information*, *8*(507), 3–10. https://doi.org/10.3390/ijgi8110507

Asiedu, E. (2019). *Impact of Flooding and Bank Erosion on Livelihoods.* (Master's thesis, University of Ghana). Retrieved from http://localhost:80 80/handle/1234567/38327

Awotwi, A., Anornu, G. K., Quaye-ballard, J. A., & Annor, T. (2018). *Monitoring land-use / land-cover changes due to extensive gold mining, urban expansion and agriculture in the Pra River Basin of Ghana , 1986-2025*. *29*(10). https://doi.org/10.1002/ldr.3093

Awotwi, A., Anornu, G. K., Quaye-Ballard, J. A., Annor, T., Forkuo, E. K., Harris, E., Agyekum, J., & Terlabie, J. L. (2019). Water balance responses to land-use/land-cover changes in the Pra River Basin of Ghana, 1986–2025. *Catena, 182,* 104129. https://doi.org/10.1016/j.catena.2019.104129

Awotwi, A., Anornu, G. K., Quaye-Ballard, J. A., Annor, T., Nti, I. K., Odai, S. N., Arhin, E., & Gyamfi, C. (2021). Impact of post- reclamation of soil by large-scale, small-scale and illegal mining on water balance components and sediment yield: Pra River Basin case study. *Soil and Tillage Research*, *211*, 105026. https://doi.org/10.1016/j.still.2021.105026

Awotwi, A., Kwame Anornu, G., Quaye-Ballard, J., Annor, T., & Kwabena Forkuo, E. (2017). Analysis of climate and anthropogenic impacts on runoff in the Lower Pra River Basin of Ghana. *Heliyon*, *12*(e00477), 477. http://dx.doi.org/10.1016/j.heliyon.2017.e00477

Ayadi, I., Abida, H., Djebbar, Y., & Mahjoub, M. R. (2010). Variabilité de l'exportation sédimentaire en Tunisie Centrale: Analyse quantitative des déterminants. *Hydrological Sciences Journal*, *55*(3), 446–458. https://doi.org/10.1080/02626661003741526

Ayibotele, N. B., & Tuffour-Darko, T. (1979). *Sediment loads in the southern rivers of Ghana*.

Babiński, Z. (2005). The relationship between suspended and bed load transport in river channels. *Sediment Budgets 1*, *291*, 182–188. Retrieved from https://www.semanticscholar.org/paper

Bastia, F., & Equeenuddin, S. M. (2016). Spatio-temporal variation of water flow and sediment discharge in the Mahanadi River, India. *Global and Planetary Change*, *144*, 51–66. https://doi.org/10.1016/j.gloplacha.2016.07.004

Bekoe, E. O., Logah, F. Y., Kankam-Yeboah, K., & Amisigo, B. (2012). Low flow characterization of a coastal river in Ghana. *International Journal of Modern Engineering Research*, *2* (5), 3210 – 3219.

Bessah, E., Raji, A. O., Taiwo, O. J., Agodzo, S. K., & Ololade, O. O. (2020). The impact of varying spatial resolution of climate models on future rainfall simulations in the pra river basin (Ghana). *Journal of Water and Climate Change*, *11*(4), 1263–1283. https://doi.org/10.2166/wcc.2019.258

Bini, M., Casarosa, N., & Luppichini, M. (2021). Exploring the relationship between river discharge and coastal erosion: An integrated approach applied to the Pisa Coastal Plain (Italy). *Remote Sensing*, *13*(226), 1–22. https://doi.org/10.3390/rs13020226

Blair, C. (1983). Tidal Corrections In Hydrographic Surveying. *Journal of*

118

Waterway, Port, Coastal, and Ocean Engineering, 109(1), 31–40. https://doi.org/10.1061/(asce)0733-950x(1983)109:1(31)

Blott, S. J., & Pye, K. (2012). Particle size scales and classification of sediment types based on particle size distributions: Review and recommended procedures. *Sedimentology*, *59*(7), 2071–2096. https://doi.org/10.1111/j.1365-3091.2012.01335.x

Boak, E. H., & Turner, I. L. (2005). Shoreline definition and detection: A review. *Journal of Coastal Research,* 21, 688–703. https://doi.org/10.2112/03-0071.1

Boakye, E., Anornu, G. K., Quaye-Ballard, J., & Donkor E. A. (2018). Land use change and sediment yield studies in Ghana: review. *Journal of Geography and Regional Planning*, *11*(9), 122–133. http://doi.org/10.5897/jgrp2018.0707

Boakye, E., Anyemedu, F. O. K., Donkor, E. A., & Quaye-Ballard, J. A. (2020). Spatial distribution of soil erosion and sediment yield in the Pra River Basin. *SN Applied Sciences*, *2*(320). https://doi.org/10.1007/s42452-020-2129-1

Boakye, E., Anyemedu, F. O. K., Donkor, E. A., & Quaye-ballard, J. A. (2021). Variability of suspended sediment yield in the Pra River. *Environment, Development and Sustainability*, *24*, 1241–1258. https://doi.org/10.1007/s10668-021-01494-x

Boateng, I. (2009*).* Development of integrated shoreline management planning: a case study of Keta, Ghana. *Proceedings of the Federation of International Surveyors Working Week 2009 - Surveyors Key Role in Accelerated Development, TS 4E, Eilat*. Eilat, Israel.

Boateng, I. (2012). An application of GIS and coastal geomorphology for large scale assessment of coastal erosion and management: A case study of Ghana. *Journal of Coastal Conservation, 16*, 383–397. https://doi.org/10.1007/s11852-012-0209-0

Boateng, I. (2012). Policy process in coastal and marine resource management in Ghana. *Proceedings from Shaping the Change XXIII FIG Congress.* Munich, Germany.

Boateng, I., Bray, M., & Hooke, J. (2012). Geomorphology Estimating the fluvial sediment input to the coastal sediment budget : A case study of Ghana. *Geomorphology*, *138*(1), 100–110. https://doi.org/10.1016/j.geomorph.2011.08.028

Boateng, I., Wiafe, G., & Jayson-Quashigah, P. N. (2017). Mapping vulnerability and risk of Ghana's coastline to sea level rise. *Marine Geodesy*, *40*(1), 23–39. https://doi.org/10.1080/01490419.2016.1261745

Boye, B. C. (2015). *Causes and trends in shoreline change in the western region of Ghana.* (Doctoral thesis, University of Ghana). Retrieved from https://ugspace.ug.edu.gh/handle/123456789/8444

Boye, B. C., Boateng, I., Appeaning, A. K., & Wiafe, G. (2019). An assessment of the contribution of fluvial sediment discharge to coastal stability: A case study of Western Region of Ghana. *African Journal of Environmental Science and Technology*, *13*(5), 191–200. https://doi.org/10.5897/ajest2017.2387

Brempong, E. K., Angnuureng, D. B., Addo, K. A., & Jayson-Quashigah, P.-N. (2021). Short-term seasonal changes of the Dzita Beach of Ghana using geographic information system and photogrammetry. *Interpretation*, *9*(4),

1–11. http://dx.doi.org/10.1190/INT-2021-0027.1

Bunte, K., Abt, S. R., Potyondy, J. P., & Swingle, K. W. (2008). A comparison of coarse bedload transport measured with bedload traps and helley-smith samplers. *Geodinamica Acta*, *21*(1 –2), 53–66. https://doi.org/0.3166/ga.21.43-66

Cantalice, J. R. B., Souza, W. L. da S., & Silva, Y. J. A. B. (2015). Bedload and suspended sediment of a watershed impacted by dams. In V. Hrissanthou (Ed.). *Effects of sediment transport on hydraulic structures.* Volume 11 (pp. 20–36). IntechOpen. http://dx.doi.org/10.5772/61478

Chakrapani, G. J. (2005). Factors controlling variations in river sediment loads. *Current Science*, *88*(4), 569–575. Retrieved from http://www.jstor.org/stable/24110256

Chen, Y., Chen, N., Li, Y., & Hong, H. (2018). Multi-timescale sediment responses across a human impacted river-estuary system. *Journal of Hydrology*, *560*, 160–172. https://doi.org/10.1016/j.jhydrol.2018.02.075

Chen, Y., Takeuchi, K., Xu, C., Chen, Y., & Xu, Z. (2006). Regional climate change and its effects on river runoff in the Tarim Basin, China. *Hydrological Processes*, *20*, 2207–2216. https://doi.org/10.1002/hyp.6200

Conner, J. T., & Tonina, D. (2013). Effect of cross-section interpolated bathymetry on 2D hydrodynamic model results in a large river. *Earth Surface Processes and Landforms*, *39*(4), 463–475. https://doi.org/10.1002/esp.3458

Croslinig, R. (2011). *Rob's geoblog Cavs Geography homework: 7.3*. Retrieved from http://2.bp.blogspot.com/-Any3YjfZEmU/TqZrjD5Y8SI/AAAAAA AAA Dw/Pl5bPmJ6Bj4/s1600/longshore+drift.PNG

Crowell, M., Leatherman, S. P., & Buckley, M. K. (1991). Historical shoreline change: Error analysis and mapping accuracy. *Journal of Coastal Research*, *7*(3), 839–852. Retrieved from https://www.semanticscholar.or g/paper/Historical-Shoreline-Change:-Error-Analysis-and-Crowell-Leath erman/c952be 21bc5862269d48239a00fda7fad078c995

Curtarelli, M., Leão, J., Ogashawara, I., Lorenzzetti, J., & Stech, J. (2015). Assessment of spatial interpolation methods to map the bathymetry of an Amazonian Hydroelectric Reservoir. *International Journal of Geo-Information*, *4*, 220–235. https://doi.org/10.3390/ijgi4010220

Dada, O. A., Angnuureng, D. B., Almar, R., Dzantor, S., & Morand, P. (2022). Social perceptions of coastal hazards in the Anlo Beach community in the Western Region of Ghana. *Journal of Coastal Conservation*, *26*(63), 12–13. https://doi.org/10.1007/s11852-022-00909-9

Dadson, I. Y. (2015). *Coastal erosion dynamics and landmass change along Cape Coast-Sekondi coastline in Ghana*. (Doctoral thesis, University of Cape Coast, Ghana). Retrieved from http://hdl.handle.net/123456789/64 35

Dar, I. A., Dar, M. A., Dar, I. A., & Dar, M. A. (2009). Prediction of shoreline recession using geospatial technology: A case study of Chennai Coast, Tamil Nadu, India. *Journal of Coastal Research*, *25*(6), 1276–1286. https://doi.org/10.2112/JCOASTRES-D-09-00051.1

Darby, S. E., Appeaning Addo, K., Hazra, S., Rahman, M. M., & Nicholls, R. J. (2020). Deltas in the Anthropocene. In R. J. Nicholls (Ed.), *Deltas in the Anthropocene* (pp. 103–126). Springer International Publishing. https://doi.org/10.1007/978-3-030-23517-8_5

Das, S. (2019). Four decades of water and sediment discharge records in Subarnarekha and Burhabalang basins: an approach towards trend analysis and abrupt change detection. *Sustainable Water Resources Management*, *5*(4), 1665–1676. https://doi.org/10.1007/s40899-019-00326-1

Das, S., & Banerjee, S. (2021). Investigation of changes in seasonal streamflow and sediment load in the Subarnarekha-Burhabalang basins using Mann-Kendall and Pettitt tests. *Arabian Journal of Geosciences*, *14*(946). https://doi.org/10.1007/s12517-021-07313-x

Das, S., Sangode, S. J., & Kandekar, A. M. (2021). Recent decline in streamflow and sediment discharge in the Godavari Basin, India (1965–2015). *Catena*, *206,* 105537. https://doi.org/10.1016/j.catena.2021.105537

Davidson-Arnott, R. (2010). *Introduction to coastal processes and geomorphology*. Cambridge, England: Cambridge University Press. Retrieved from https://www.academia.edu/65497185/Introduction_to_Coastal_Processes_and_Geomorphology

Davis, B. E. (2005). *A guide to the proper selection and use of federally approved sediment and water-quality samplers.* (Open-File Report 2005-1087). Reston, USA: U.S. Geological Survey. Retrieved from http://fisp.wes.army.mil/Report%20QQ-Users%20Guide.pdf>(Aug.12, 2005)

Dean, R. G., & Darlrymple, R. A. (2004). *Coastal processes with engineering applications*. Cambridge: Cambridge, University Press. Retrieved from https://books.google.com.gh/books/about/Coastal_Processes_with_Engineering_Appli.html?id=XlDmIdpqMFYC&redir_esc=y

Dingman, S. L. (2009). *Fluvial hydraulics*. Oxford: Oxford, University Press Inc. Retrieved from https://global.oup.com/us/companion.websites/97801

95172867/

Diplas, P., Kuhnle, R., Gray, J., Glysson, D., Edwards, T., & Diplas, G. P. (2008). *Sediment transport measurements* (pp. 305–347). Retrieved from https://www.semanticscholar.org/paper/Sediment-transport-measurements:-Chapter-5-Diplas-Kuhnle/053604d11cb86f55846efe7d0629b3f2a077367a

Dorleku, M. K., Affum, A. O., Tay, C. K., & Nukpezah, D. (2019). Assessment of Nutrients Levels in Groundwater within the Lower Pra Basin of Ghana. *Ghana Journal of Science*, *60*(1), 24–36. http://dx.doi.org/10.4314/gjs.v60i1.3

Duru, U., Wohl, E., & Ahmadi, M. (2017). Factors controlling sediment load in the Central Anatolia Region of Turkey: Ankara River Basin. *Environmental Management*, *59*(5), 826–841. https://doi.org/10.1007/s00267-016-0818-8

Edwards, T. K., & Glysson, G. D. (1999). Field methods for measurement of fluvial sediment. In H. P. Guy, & V. W. Norman (Eds), *U. S Geological Survey* (pp. 2–51). Retrieved from https://www.semanticscholar.org/paper/Sediment-transport-measurements:-Chapter-5-iplasKuhnle/053604d11cb86f55846efe7d0629b3f2a077367a

El-Hattab, A. I. (2014). Single beam bathymetric data modelling techniques for accurate maintenance dredging. *Egyptian Journal of Remote Sensing and Space Science*, *17*(2), 189–195. https://doi.org/10.1016/j.ejrs.2014.05.003

Ergenzinger, P. (1992). River bed adjustment in a step-pool system: Lainbach. Upper Bavaria. In P. Billi, R. D. Hey, C. R. Thorne, & P. Tacconi (Eds.), *Dynamics of gravel-bed rivers* (pp. 415–430). Chichester, West Sussex,

England: Wiley.

Esteves, M., Legout, C., Navratil, O., & Evrard, O. (2019). Medium term high frequency observation of discharges and suspended sediment in a Mediterranean mountainous catchment. *Journal of Hydrology*, *568*, 562–574. https://doi.org/10.1016/j.jhydrol.2018.10.066

Faseyi, C. A. (2022). *Assessment of ecological health status and socio-economic drivers of pollution in the southwestern estuarine system of Ghana*. Unpublished doctoral thesis, University of Cape Coast.

Flores, J. A., Wu, J. Q., Stöckle, C. O., Ewing, R. P., & Yang, X. (2020). Estimating river sediment discharge in the Upper Mississippi River using landsat imagery. *Remote Sensing*, *12*(2370), 1–22. https://doi.org/10. 3390/rs12152370

Forghani, M., Qian, Y., Lee, J., Farthing, M., Hesser, T., Kitanidis, P. K., & Darve, E. F. (2022). Variational encoder geostatistical analysis (VEGAS) with an application to large scale riverine bathymetry. *Advances in Water Resources*, *170*(104323), 1–24. https://doi.org/10.1016/j.advwatres.2022. 104323

Frihy, O. E. (2001). The necessity of environmental impact assessment (EIA) in implementing coastal projects: lessons learned from the Egyptian Mediterranean Coast. *Ocean & Coastal Management*, *44*, 489–516. https://doi.org/10.1016/S0964-5691(01)00062-X

Gallay, M., Martinez, J. M., Allo, S., Mora, A., Cochonneau, G., Gardel, A., Doudou, J. C., Sarrazin, M., Chow-Toun, F., & Laraque, A. (2018). Impact of land degradation from mining activities on the sediment fluxes in two large rivers of French Guiana. *Land Degradation and Development*,

29(12), 4323–4336. https://doi.org/10.1002/ldr.3150

Geography Revision. (2022). *Coastal Processes*. Retrieved from https://geogra

phy-revision.co.uk/gcse/coastal-landscapes/coastal-processes/

Gitto, A. B., Venditti, J. G., Kostaschuk, R., & Church, M. (2017).

Representative point-integrated suspended sediment sampling in rivers.

Water Resources Research, *53*(4), 2956–2971. https://doi.org/10.1002/20

16WR019187

Gomez, B. (1991). Bedload transport. *Earth-Science Reviews*, *31*, 89–132.

https://doi.org/10.1016/0012-8252(91)90017-A

Google Earth Pro. (2022). *Aerial photographs of the middle to southern portion*

of Ghana (No. 7.3.6).

Gooley, T. (2016). *How to read water: clues and patterns from puddles to the*

sea. New York, NY: The Experiment, LLC. pp. 142–167.

Gouda, E., Mesbah Abdelrahman, S., & Mohasseb, M. (2019). *Multi-beam*

echosounder data uncertainty relative to single-beam echo sounder data

in depth determination. Retrieved from https://www.academia.edu/44834

054/Multi_beam_Echosounder_Data_Uncertainty_Relative_to_Single_B

eam_Echo_Sounder_Data_in_Depth_Determination

Gray, J. R., & Simões, F. J. M. (2008). *Estimating Sediment Discharge* (pp.

1065–1086). Retrieved from https://www.usgs.gov/publications/estimatin

g-sediment-disc harge-appendix-d

Guo, L., Su, N., Zhu, C., & He, Q. (2018). How have the river discharges and

sediment loads changed in the Changjiang River basin downstream of the

Three Gorges Dam? *Journal of Hydrology*, *560*, 259–274. https://doi.org/

10.1016/j.jhydrol.2018.03.035

Gyamfi, C., Tindan, J. Z., & Edgar, G. (2021). Regional studies evaluation of CORDEX Africa multi-model precipitation simulations over the Pra River basin, Ghana. *Journal of Hydrology: Regional Studies*, *35*(100815). https://doi.org/10.1016/j.ejrh.2021.100815

Habersack, H., Seitz, H., & Leidermann, M. (2010). *Integrated automatic bedload transport monitoring*. Retrieved from https://pubs.usgs.gov/sir/2010/5091/papers/Habersack.pdf

Haider, G., Othayq, M., Zhang, J., Vieira, R.E., & Shirazi, S.A. (2021). Effect of particle size on erosion measurements and predictions in annular flow for an elbow. *Wear, 476*(20357). https://doi.org/10.1016/j.wear.2020.203579

Hapke, C. J., Himmelstoss, E. A., Kratzman, M. G., List, J. H., & Thieler, E. R. (2011). *National assessment of shoreline change: Historical shoreline change along the New England and Mid-Atlantic coasts.* https://doi.org/10.3133/ofr20101118

Hentry, C., Chandrasekar, N., & Saravanan, S. (2012). Beach dynamics of Colachel open coast , Kanyakumari District (SW India). *Zeitschrift Für Geomorphologie*, *57*(1), 75–95. https://doi.org/10.1127/0372-8854/2012/0077

Hicks, D. M., Duncan, M. J., & Duncan, M. J. (1997). The efficiency of depth-integrating samplers in sampling the suspended sand load in gravel bed rivers. *Journal of Hydrology,* 201, 138-160. https://doi.org/10.1016/S0022-1694(97)00040-1.

Hopsch, S. B., Thorncroft, C. D., Hodges, K., & Aiyyer, A. (2007). West African storm tracks and their relationship to Atlantic tropical cyclones.

Journal of Climate, *20*(11), 2468–2483. https://doi.org/10.1175/JCLI413
9.1

Huo, Z., Feng, S., Kang, S., Li, W., & Chen, S. (2008). Effect of climate changes
and water-related human activities on annual stream flows of the Shiyang
river basin in arid north-west China. *Hydrological Processes*, *22*, 3155–
3167. https://doi.org/10.1002/hyp6900

Jayson-Quashigah, P.-N., Appeaning Addo, K., Amisigo, B., & Wiafe, G.
(2019). Assessment of short-term beach sediment change in the Volta
Delta coast in Ghana using data from Unmanned Aerial Vehicles (Drone).
Ocean and Coastal Management, *182*(104952). https://doi.org/10.1016/j.
ocecoaman.2019.104952

Jonah, F. E. (2015). Managing coastal erosion hotspots along the Elmina, Cape
Coast and Moree area of Ghana. *Journal of Ocean and Coastal
Management*, *109*, 9–16. http://dx.doi.org/10.1016/j.ocecoaman.2015.02.
007

Jonah, F. E., Adams, O., Aheto, D. W., Jonah, R. E., & Mensah, E. A. (2017).
Coastal zone management challenges in Ghana: Issues associated with
coastal sediment mining. *Journal of Coastal Conservation*, *21*(3), 343–
353. https://doi.org/10.1007/s11852-017-0511-y

Jonah, F. E., Mensah, E. A., Edziyie, R. E., Agbo, N. W., & Adjei-Boateng, D.
(2016). Coastal erosion in Ghana: causes, policies, and management.
Coastal Management, *44*(2), 116–130. https://doi.org/10.1080/08920753.
2016.1135273

Joshi, S., & Xu, Y. J. (2017). Bedload and suspended load transport in the 140-
km reach downstream of the Mississippi River avulsion to the Atchafalaya

River. *Water*, *9*(9), 1–28. https://doi.org/10.3390/w9090716

Kankam-Yeboah, K., Obuobie, E., Amisigo, B., & Opoku-Ankomah, Y. (2013). Impact of climate change on streamflow in selected river basins in Ghana. *Hydrological Sciences Journal*, *58*(4), 773–788. https://doi.org/10.1080/0 2626667.2013.782101

Kim, J. S., Baek, D., Seo, I. W., & Shin, J. (2019). Retrieving shallow stream bathymetry from UAV-assisted RGB imagery using a geospatial regression method. *Geomorphology*, *341*, 102–114. https://doi.org/10.101 6/j.geomorph.2019.05.016

Klemas, V. V. (2015). Coastal and environmental remote sensing from unmanned aerial vehicles: An overview. *Journal of Coastal Research*, *31*(5), 1260–1267. https://doi.org/10.2112/JCOASTRES-D-15-00005.1

Komi, K., Neal, J., Trigg, M. A., & Diekkrüger, B. (2017). Modelling of flood hazard extent in data sparse areas : a case study of the Oti River basin, West Africa. *Journal of Hydrology: Regional Studies*, *10*, 122–132. https://doi. org/10.1016/j.ejrh.2017.03.001

Kuhnle, R. (2008). *Sediment transport measurements*. USGS Publications Warehouse, (pp. 337–351). https://doi.org/10.1061/9780784408148.ch05

Kusimi, J. M. (2014). *Sediment yield and bank erosion assessment of Pra River basin.* (Doctoral Thesis, University of Ghana). Retrieved from http://197.255.68.203/handle/123 456789/5467

Kusimi, J. M., Amisigo, B. A., & Banoeng-Yakubo, B. K. (2014). Sediment yield of a forest river basin in Ghana. *Catena*, *123*, 225–235. https://doi.org/10.1016/j.catena.2014.08.001

Kusimi, J. M., Yiran, G. A. B., & Attua, E. M. (2016). Soil erosion and sediment

129

yield modelling in the Pra River basin of Ghana using the revised universal soil loss equation (RUSLE). *Ghana Journal of Geography*, *7*(2), 38–57. Retrieved from https://www.ajol.info/index.php/gjg/article/view/129216/118774

Latrubesse, E. M., Stevaux, J. C., & Sinha, R. (2005). Tropical rivers. *Geomorphology*, *70*, 187–206. https://doi.org/10.1016/j.geomorph.2005.02.005

Le Deunf, J., Debese, N., Schmitt, T., & Billot, R. (2020). A review of data cleaning approaches in a hydrographic framework with a focus on bathymetric multibeam echosounder datasets. *Geosciences 10*(7), 1–29. https://doi.org/10.3390/geosciences10070254

Leeks, G. (2005). Measuring sediment loads, yields and source tracing. *Encyclopedia of Hydrological Sciences*. New York, NY: John Wiley and Sons Inc. https://doi.org/10.1002/0470848944.hsa088

Legleiter, C. J., & Overstreet, B. T. (2012). Mapping gravel bed river bathymetry from space. *Journal of Geophysical Research: Earth Surface*, *117*(F04024), 1–24. https://doi.org/10.1029/2012JF002539

Li, X., Zhou, Y., Zhang, L., & Kuang, R. (2014). Shoreline change of Chongming Dongtan and response to river sediment load : A remote sensing assessment. *Journal of Hydrology*, *511*, 432–442. https://doi.org/10.1016/j.jhydrol.2014.02.013

Liu, C., He, Y., Li, Z., Chen, J., & Li, Z. (2021). Key drivers of changes in the sediment loads of Chinese rivers discharging to the oceans. *International Journal of Sediment Research*, *36*(6), 747–755. https://doi.org/10.1016/j.ijsrc.2020.05.005

Logah, F. Y., Amisigo, A. B., Obuobie, E., & Kankam-Yeboah, K. (2017). Floodplain hydrodynamic modelling of the Lower Volta River in Ghana. *Journal of Hydrology: Regional Studies*, *14*, 1–9. https://doi.org/10.1016 /j.ejrh.2017.09.002

Logah, F. Y., Kankam-Yeboah, K., Ofori, D., & Gyau-Boakye, P. (2014). Flood pulse alterations of some river basins in Ghana. *Ghana Journal of Science*, *54*, 19–32. Retrieved from https://www.ajol.info/index.php/gjs/article/vie w/115824

Ly, C. K. (1980). The role of the Akosombo Dam on the Volta River in causing coastal erosion in central and eastern Ghana (West Africa). *Marine Geology*, *37*, 323–332. https://doi.org/10.1016/0025-3227(80)90108-5

Mancini, F., Dubbini, M., Gattelli, M., Stecchi, F., Fabbri, S., & Gabbianelli, G. (2013). Using unmanned aerial vehicles (UAV) for high-resolution reconstruction of topography: The structure from motion approach on coastal environments. *Remote Sensing*, *5*(12), 6880–6898. https://doi.org/ 10.3390/rs5126880

Martinelli, L. A., Victoria, R. L., Devol, A. H., & Forsberg, B. R. (1989). Suspended sediment load in the Amazon Basin: an overview. *GeoJournal, 19*(4), 381–389. https://doi.org/10.1007/BF00176907

Mawuli, L., & Amisigo, B. (2016). Estimating fluvial sediments loads using surrogate techniques in a data-poor catchment-the case of the White Volta basin. *International Journal of Agriculture and Environmental Research*, *2*(4), 804–823. Retrieved from www.ijaer.in

Merwade, V. (2009). Effect of spatial trends on interpolation of river bathymetry. *Journal of Hydrology*, *371*, 169–181. https://doi.org/doi:10.

1016/j.jhydrol.2009.03.026

Milliman, J. D., & Farnsworth, K. L. (2011). River discharge to the coastal ocean: A global synthesis. In *river discharge to the coastal ocean: A global synthesis*. https://doi.org/10.1017/CBO9780511781247

Mohanty, P. K., Patra, S. K., Bramha, S., Seth, B., Pradhan, U., Behera, B., Mishra, P., & Panda, U. S. (2012). Impact of groins on beach morphology: A case study near Gopalpur Port, east coast of India. *Journal of Coastal Research*, *28*(1), 132–142. https://doi.org/10.2112/JCOASTRES-D-10-00045.1

Moore, L. J. (2000). Shoreline mapping techniques. *Journal of Coastal Research*, *16*(1), 111–124. https://journals.flvc.org/jcr/article/view/80780

Mouyen, M., Longuevergne, L., Steer, P., Crave, A., Lemoine, J. M., Save, H., & Robin, C. (2018). Assessing modern river sediment discharge to the ocean using satellite gravimetry. *Nature Communications*, *9*(3384), 2–6. https://doi.org/10.1038/s41467-018-05921-y

Mutimukuru-maravanyika, T., Mills, D. J., Asare, C., & Asiedu, G. A. (2017). Enhancing women's participation in decision-making in artisanal fisheries in the Anlo Beach fishing community, Ghana. *Water Resources and Rural Development*, *10*, 58–75. https://doi.org/10.1016/j.wrr.2016.04.001

Nguyen, V. B., Nguyen, Q. B., Zhang, Y. W., Lim, C. Y. H., & Khoo, B. C. (2016). Effect of particle size on erosion characteristics. *Wear*, 348-349, *126–137*. https://doi.org/10.1016/j.wear.2015.12.003

Nsiah, J. J., Gyamfi, C., Anornu, G. K., & Odai, S. N. (2021). Estimating the spatial distribution of evapotranspiration within the Pra River basin of Ghana. *Heliyon*, *7*(e06828), 2–8. https://doi.org/10.1016/j.heliyon.2021.e0

6828

Nyarko, E., Klubi, E., Laissaoui, A., & Benmansour, M. (2016). Estimating recent sedimentation rates using lead-210 in tropical estuarine systems: Case study of Volta and Pra estuaries in Ghana, West Africa. *Journal of Oceanography and Marine Research*, *04*(141), 3–5. https://doi.org/10.417 2/2572-3103.1000141

Obuobie, E., Diekkrueger, B., Agyekum, W., & Agodzo, S. (2012). Groundwater level monitoring and recharge estimation in the White Volta River basin of Ghana. *Journal of African Earth Sciences*, *71–72*, 80–86. https://doi.org/10.1016/j.jafrearsci.2012.06.005

Ofori, D., Amisigo, B. A., Logah, Y., & Kankam-Yeboah, K. (2016). Suspended sediment tranSsport into a Water Supply reServoir in Southern Ghana. *Ghana Journal of Science*, *56*, 3–14. Retrieved from https://www. ajol.info/index.php/gjs/article/view/177819/167195

Okada, S., Yorozuya, A., Koseki, H., Kuso, S., & Muraoka, M. (2017). Comprehensive measurement techniques of water flow, bedload and suspended sediment in large river using Acoustic Doppler Current Profiler. In S. Wieprecht, S. Haun, K. Weber, M. Noack, & K. Terheiden (Eds.), *River Sedimentation* (pp. 1274–1280). London: Taylor & Francis Group. https://doi.org/10.1201/9781315623207

Oliveira, M. S. D., Menezes, M. D. D., & Curi, N. (2017). Hybrid kriging methods for interpolating sparse river bathymetry point data. *Ciência E Agrotecnologia*, *41*(4), 402–412. http://dx.doi.org/10.1590/1413-7054201 7414008617

Ongley, E. (1996). Water quality monitoring: a practical guide to the design and

implementation of freshwater quality studies and monitoring programmes. In B. Jamie & R. Ballance (Eds.), *Water quality monitoring - a practical guide to the design and implementation of freshwater quality studies and monitoring programmes*. pp. 383. Retrieved from https://apps.who.int/iris /h andle/10665/41851

Orme, A. R. (2005). Africa, Coastal Geomorphology. In *Encyclopedia of Coastal Science* (1st ed.). pp. 9–20. Retrieved from https://openlibrary .org/books/OL3436421M/Encyclopedia_of_coastal_science

Osadchiev, A., & Korshenko, E. (2017). Small river plumes off the northeastern coast of the Black Sea under average climatic and flooding discharge conditions. *Ocean Science*, *13*(3), 465–482. https://doi.org/10.5194/os-13-465-2017

Osei, M. A., Amekudzi, L. K., & Quansah, E. (2021). Characterisation of wet and dry spells and associated atmospheric dynamics at the Pra River catchment of Ghana, West Africa. *Journal of Hydrology: Regional Studies*, *34*(100801), 6–24. https://doi.org/10.1016/j.ejrh.2021.100801

Otoo, D. A. (2018). *Shoreline change analysis of the coastline of Teshie in Accra.* (PhD Thesis, University of Ghana). Retrieved from https://ugspa ce.ug.edu.gh/handle/123456789/29631

Panhalkar, S. S., & Jarag, A. P. (2015). Assessment of spatial interpolation techniques for river bathymetry generation of panchganga river basin using geoinformatic techniques. *Asian Journal of Geoinformatics*, *15*(3), 10–15. Retrieved from https://www.researchgate.net/publication/291349151_As sessment_of_Spatial_Interpolation_Techniques_for_River_Bathymetry_ Generation_of_Panchganga_River_Basin_Using_Geoinformatic_Techniq

ues#fullTextFileContent

Parente, C., & Vallario, A. (2019). Interpolation of single beam echo sounder data for 3D bathymetric model. *International Journal of Advanced Computer Science and Applications*, *10*(10), 6–13. https://doi.org/10.145 69/ijacsa.2019.0101002

Perks, M. T. (2014). Manual sampling. In *Geomorphological Techniques* (pp. 2–7). British Society for Geomorphology. Retrieved from https://www. researchgate.net/publication/260176439_Suspended_sediment_sampling

Quartel, S., Kroon, A., & Ruessink, B. G. (2008). Seasonal accretion and erosion patterns of a microtidal sandy beach. *Marine Geology*, *250*(1–2), 19–33. https://doi.org/10.1016/j.margeo.2007.11.003

Rajab, P. M., & K., T. (2017). Estimation of longshore sediment transport along Puducherry coast, east coast of India; based on empirical methods and surf zone model. *Indian Journal of Geo Marine Sciences*, *46*(07), 1307–1319. Retrieved from http://nopr.niscair.res.in/bitstream/123456789/42250/1/IJ MS46(7)1307-1319.pdf

Roehl, J. W. (1962). Sediment source areas, delivery ratios, and influencing morphological factors. In I. A. H. . Bari (Ed.), *Symposium on Continental Erosion* (pp. 202–213).

Roest, L. W. M. (2018). *The coastal system of the Volta delta, Ghana: Opportunities and strategies for development*. Retrieved from https://res earch.tudelft.nl/files/37464456/Roest_2018_The_coastal_system_of_the_ Volta_delta.pdf

Selvan, S. C., Kankara, R. S., & Bhoopathy, R. (2014). Assessment of shoreline changes along Karnataka coast, India using GIS & Remote Sensing

techniques. *Indian Journal of Marine Sciences*, *43*(7), 3–5. Retrieved from

http://www.niscair.res.in/jinfo/ijms/ijms-forthcoming-articles/BKP-IJM

S-PR-July 2014/MS 27 Edited.pdf

Sequoia. (2017). *LISST-SL2 streamlined isokinetic sediment flux sensor*.

Retrieved from https://www.sequoiasci.com/product/lisst-sl/

StudySmarter. (2022). *River processes*. Retrieved from https://www.studysm

arter.us/explanations/geography/river-landscapes/river-processes/

Sulaiman, S. O., Al-Ansari, N., Shahadha, A., Ismaeel, R., & Mohammad, S.

(2021). Evaluation of sediment transport empirical equations: case study

of the Euphrates River West Iraq. *Arabian Journal of Geosciences*,

14(825), 2–10. https://doi.org/10.1007/s12517-021-07177-1/Published

Syvitski, J. P. M. (2003). Supply and flux of sediment along hydrological

pathways: Research for the 21st century. *Global and Planetary Change*,

39(1-2), 1–11. https://doi.org/10.1016/S0921-8181(03)00008-0

Syvitski, J. P. M., & Milliman, J. (2007). No Geology, geography, and human's

battle for dominance over the delivery of fuvial sediment to the coastal

ocean. *The Journal of Geology*, *115*(1), 1–19. https://doi.org/10.1086/

509246

Syvitski, J. P. M., Vörösmarty, C. J., Kettner, A. J., & Green, P. (2005). Impact

of Humans on the flux of terrestrial sediment to the global coastal ocean.

Science, *308*(5720), 376–380. https://doi.org/10.1126/science.1109454

Tamene, L., Park, S. J., Dikau, R., & Vlek, P. L. G. (2006). Analysis of factors

determining sediment yield variability in the highlands of northern

Ethiopia. *Geomorphology*, *76*, 76–91. https://doi.org/10.1016/j.geomorph.

2005.10.007

136

Tran, Y. H., & Barthélemy, E. (2020). Combined longshore and cross-shore shoreline model for closed embayed beaches. *Coastal Engineering*, *158*, 1–12. https://doi.org/10.1016/j.coastaleng.2020.103692

Valeport. (2020). *Datasheet reference: MIDAS surveyor – echo sounder*. Retrieved from https://www.bing.com/search?q=Datasheet+reference%3A+MIDAS+surveyor+%E2%80%93+echo+sounder&cvid=a59e1d712c8 64fafb824300adf490b1d&aqs=edge..69i57.320j0j4&FORM=ANAB01& PC=LCTS

Walling, D. E. (1984). The sediment delivery problem. *Journal of Hydrology*, *65*(1-3), 209–237. https://doi.org/10.1016/0022-1694(83)90217-2

Walling, D. E. (2006). Human impact on land-ocean sediment transfer by the world's rivers. *Geomorphology*, *79*(3-4), 192–216. https://doi.org/10.101 6/j.geomorph.2006.06.019

Wang, C., Chen, M., Qi, H., Intasen, W., & Kanchanapant, A. (2020). Grain-size distribution of surface sediments in the Chanthaburi Coast, Thailand and implications for the sedimentary dynamic environment. *Journal of Marine Science and Engineering*, *8*(242), 3–10. https://doi.org/10.3390/J MSE8040242

Water Resources Commission. (2012). *Pra River Basin Integrated Water Resources Management Plan*. Retrieved from https://wrc-gh.org/dmsdocu ment/15

Wei, J., He, X., & Bao, Y. (2011). Anthropogenic impacts on suspended sediment load in the Upper Yangtze River. *Regional Environmental Change*, *11*, 857–868. https://doi.org/10.1007/s10113-011-0222-0

Wellens-Mensah, J., Armah, A. K., Amlalo, D. S., & Tetteh, K. (2002). *Ghana*

National Report Phase 1: Integrated problem analysis.

Westoby, M. J., Brasington, J., Glasser, N. F., Hambrey, M. J., & Reynolds, J. M. (2012). *"*Structure-from-Motion" photogrammetry: A low-cost, effective tool for geoscience applications. *Geomorphology, 179*, 300–314. https://doi.org/10.1016/j.geomorph.2012.08.021

Wheaton, J. M., Brasington, J., Darby, S. E., & Sear, D. A. (2010). Accounting for uncertainty in DEMs from repeat topographic surveys: Improved sediment budgets. *Earth Surface Processes and Landforms*, *35*(2), 136–156. https://doi.org/10.1002/esp.1886

Whitehead, K., Hugenholtz, C. H., Myshak, S., Brown, O., LeClair, A., Tamminga, A., Barchyn, T. E., Moorman, B., & Eaton, B. (2014). Remote sensing of the environment with small unmanned aircraft systems (UASs), part 2: scientific and commercial applications. *Journal of Unmanned Vehicle Systems*, *2*, 86–102. https://doi.org/10.1139/juvs-2014- 0006

Wiafe, G., Boateng, I., Appeaning Addo, K., Quashigah, P. N., Ababio, S. D., & Laryea, S. W. (2013). *Handbook of coastal processes and management in Ghana*. The Choir Press, (pp.11).

World Meteorological Organization. (1981). *Measurement of river sediments*. Retrieved from https://openlibrary.org/books/OL3885937M/Measurement _of_river_sediments

WorldAtlas. (2022). *What are the climate change indicators?* Retrieved from https://www.worldatlas.com/articles/what-are-the-climate-change-indicat ors.html

Wu, C., Ji, C., Shi, B., Wang, Y., Gao, J., Yang, Y., & Mu, J. (2019). The impact of climate change and human activities on stream flow and sediment load

in the Pearl River basin. *International Journal of Sediment Research*, *34*(4), 307–321. https://doi.org/10.1016/j.ijsrc.2019.01.002

Xorse, T. M. (2013). *Impact of wave dynamics on the coast of ghana*. (Mphil Thesis, University of Ghana). Retrieved from https://ugspace.ug.edu.gh /bitstream/handle/123456789/8788/10203247_TMSX_DMFS_(Thesis).p df?sequence=1&isAllowed=y

Yang, H. F., Yang, S. L., & Xu, K. H. (2017). River-sea transitions of sediment dynamics : A case study of the tide-impacted Yangtze River estuary. *Estuarine, Coastal and Shelf Science*, *196*, 207–216. https://doi.org/10 .1016/j.ecss.2017.07.005

Yang, S. L., Li, M., Dai, S. B., Liu, Z., Zhang, J., & Ding, P. X. (2006). Drastic decrease in sediment supply from the Yangtze River and its challenge to coastal wetland management. *Geophysical Research Letters*, *33*(L06408), 1–4. https://doi.org/ 10.1029/2005GL025507

Yang, S. L., Zhang, J., Dai, S. B., Li, M., & Xu, J. X. (2007). Effect of deposition and erosion within the main river channel and large lakes on sediment delivery to the estuary of the Yangtze River. *Journal of Geophysical Research: Earth Surface*, *112*(2), 1–13. https://doi.org/10. 1029/2006JF000484

Yoo, C. I., & Oh, T. S. (2016). Beach volume change using UAV photogrammetry Songjung beach, Korea. *International Archives of the Photogrammetry, Remote Sensing and Spatial Information Sciences - ISPRS Archives*, *41*, 1201–1205. https://doi.org/10.5194/isprsarchives-XLI-B8-1201-2016

Zeiringer, B., Seliger, C., Greimel, F., & Schmutz, S. (2018). River hydrology, flow alteration, and environmental flow. In S. Schmutz & J. Sendzimir (Eds.), *Riverine Ecosystem Management, Aquatic Ecology Series 8* (pp. 67–89). Springer International Publishing. https://doi.org/10.1007/978-3-319-73250-3_4

APPENDIX A

Sample of Sediment volume measurement statistics

Attribute	Raw	Threshold DoD Estimate:		
AREAL:				
Total Area of Surface Lowering (m²)	45,420	44,566		
Total Area of Surface Raising (m²)	17,514	16,729		
Total Area of Detectable Change (m²)	NA	61,295		
Total Area of Interest (m²)	62,934	NA		
Percent of Area of Interest with Detectable Change	NA	97%		
VOLUMETRIC:			± Error Volume	% Error
Total Volume of Surface Lowering (m³)	160,685	160,639.10 ±	4,761.82	3%
Total Volume of Surface Raising (m³)	54,985	54,943.39 ±	1,787.43	3%
Total Volume of Difference (m³)	215,670	215,582.49 ±	6,549.25	3%
Total **Net** Volume Difference (m³)	-105,700	-105,695.72 ±	5,086.24	-5%
VERTICAL AVERAGES:			± Error Thickness	% Error
Average Depth of Surface Lowering (m)	3.54	3.60 ±	0.11	3%
Average Depth of Surface Raising (m)	3.14	3.28 ±	0.11	3%
Average Total Thickness of Difference (m) for Area of Interest	3.43	3.43 ±	0.10	3%
Average **Net** Thickness Difference (m) for Area of Interest	-1.68	-1.68 ±	0.08	-5%
Average Total Thickness of Difference (m) for Area With Detectable Change	NA	3.52 ±	0.11	3%
Average **Net** Thickness Difference (m) for Area with Detectable Change	NA	-1.72 ±	0.08	-5%
PERCENTAGES (BY VOLUME)				
Percent Elevation Lowering	75%	75%		
Percent Surface Raising	25%	25%		
Percent Imbalance (departure from equilibrium)	-25%	-25%		
Net to Total Volume Ratio	-49%	-49%		

APPENDIX B

Sample of MATLAB codes for cross-shore profiles graph creation

clear; clc; close all;

Directory ='D:\'; %directory specification

CSP=readtable(".xlsx"); %to read my csv file%%

subplot(6,2,1),% Number of charts = 6, number of columns = 2, position of chart= 1

plot (CSP, "MayXa","MayYa", Color= 'r', marker = 'x',LineWidth= 1.5, ...

   MarkerSize=8, MarkerIndices=[1   57 114 169 225 281 337 393])

hold on

plot (CSP, "JulyXa","JulyYa", Color= 'k', LineStyle='--' , LineWidth=1.5, ...

   marker = 'diamond',MarkerSize=4, ...

   MarkerIndices=[1   57 118 175 235 294 343 401 460 519])

hold on

plot (CSP, "SeptemberXa","SeptemberYa", Color= 'b', LineStyle=':', ...

   LineWidth= 2, marker = '^', MarkerSize=4, ...

   MarkerIndices=[1   57 118 175 235 294 343 401 460 519])

hold on

plot (CSP, "OctoberXa","OctoberYa", Color= 'g', LineStyle='-', ...

   LineWidth= 2, marker = 'o', MarkerSize=4, ...

   MarkerIndices=[1   57 118 175 235 294 343 401 460 519])

title('(a)', FontName= 'Times New Roman')

%%

subplot(6,2,2),% Number of charts = 6, number of columns = 2, position

142